



2009

Role of the F-BAR Protein Hof1 in the Regulation of Chitin Synthesis and Cytokinesis in Yeast

Jennifer Hansen Schreiter
University of Pennsylvania

Follow this and additional works at: <http://repository.upenn.edu/edissertations>

 Part of the [Cell Biology Commons](#), and the [Genetics Commons](#)

Recommended Citation

Schreiter, Jennifer Hansen, "Role of the F-BAR Protein Hof1 in the Regulation of Chitin Synthesis and Cytokinesis in Yeast" (2009).
Publicly Accessible Penn Dissertations. 959.
<http://repository.upenn.edu/edissertations/959>

This paper is posted at ScholarlyCommons. <http://repository.upenn.edu/edissertations/959>
For more information, please contact libraryrepository@pobox.upenn.edu.

Role of the F-BAR Protein Hof1 in the Regulation of Chitin Synthesis and Cytokinesis in Yeast

Abstract

Remodeling of the plasma membrane and extracellular matrix (ECM) at discrete cellular locations plays important roles in various cellular processes including angiogenesis and cytokinesis. In the budding yeast *Saccharomyces cerevisiae*, membrane trafficking delivers enzymes essential for the synthesis of the cell-wall (yeast ECM) component chitin to the bud neck at different phases of the cell cycle. During early stages of budding, a Chs3-synthesized chitin ring is deposited at the base of the new bud that is required for bud-neck integrity and normal cell shape. During cytokinesis, actomyosin ring contraction is linked to the formation of a Chs2-synthesized chitinous disk to divide the mother and daughter cells called the primary septum. Chs3-synthesized chitin also plays an auxiliary role to Chs2 during cytokinesis. Here, I show that the F-BAR protein Hof1 is involved in the endocytic removal of Chs3 from the bud neck alter chitin ring deposition and possibly later after cytokinesis. I also discuss work to show that Hof1 is involved in the localization and function of Inn1, a C2-domain containing protein essential for synthesis of the primary septum during cytokinesis.

Degree Type

Dissertation

Degree Name

Doctor of Philosophy (PhD)

Graduate Group

Cell & Molecular Biology

First Advisor

Erfei Bi

Keywords

biological sciences, Inn1, F-BAR protein, Hof-1, chitin, cytokinesis, budding yeast

Subject Categories

Cell Biology | Genetics

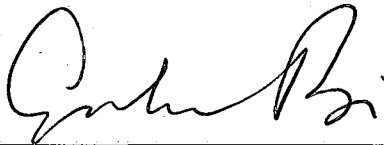
ROLE OF THE F-BAR PROTEIN HOF1 IN THE REGULATION OF CHITIN
SYNTHESIS AND CYTOKINESIS IN YEAST

Jennifer Hansen Schreiter

A DISSERTATION
in
Cell and Molecular Biology

Presented to the Faculties of the University of Pennsylvania in Partial
Fulfillment of the Requirement for the Degree of Doctor of Philosophy

2009



Supervisor of Dissertation



Graduate Group Chairperson

ACKNOWLEDGMENTS

First, I would like to thank all of our collaborators. Liz Vallen and her lab first identified Inn1 in a screen and did much of the work to characterize the protein. Ryuichi Nishihama provided all of the beautiful EM pictures. Katarina Marovcevic in Mark Lemmon's lab performed all the lipid binding assays. Julia Hanna and Masayuki Onishi also performed several experiments and John Pringle provided expert critique of the manuscript.

Here at Penn, I would like to thank the members of my thesis committee: Dr. Chris Burd, Dr. Margaret Chou, Dr. Wei Guo, Dr. Frank Luca, and Dr. Tatiana Svitkina. I really appreciate your guidance, especially in the past year as I have been preparing for graduation.

I would also like to thank past and present members of the Bi lab for helpful advice and discussion: Dr. Xiao-dong Fang, Dr. Xiang-dong Gao, Julia Hanna, Steven Kane, Dr. Jianying Luo, Dr. Younghoon Oh, and Zongtian Tong. Also, I would like to give many thanks to Dr. Andrea Stout for invaluable advice and assistance with most of the microscopy. Most important, I would like to thank my mentor, Dr. Erfei Bi, for his unending support, advice, and enthusiasm.

Last, but not least, I would like to thank my friends and family who have been so supportive of me throughout my graduate career. In particular, I would like to thank my husband Karl for his love, patience, and all the dinners he has cooked, and my two cats, Zabu and Lucy, for keeping me company when I wrote from home and helping me to forget bad days when my experiments didn't work!

ABSTRACT

ROLE OF THE F-BAR PROTEIN HOF1 IN THE REGULATION OF CHITIN SYNTHESIS AND CYTOKINESIS IN YEAST

Jennifer Hansen Schreiter

Dr. Erfei Bi

Remodeling of the plasma membrane and extracellular matrix (ECM) at discrete cellular locations plays important roles in various cellular processes including angiogenesis and cytokinesis. In the budding yeast *Saccharomyces cerevisiae*, membrane trafficking delivers enzymes essential for the synthesis of the cell-wall (yeast ECM) component chitin to the bud neck at different phases of the cell cycle. During early stages of budding, a Chs3-synthesized chitin ring is deposited at the base of the new bud that is required for bud-neck integrity and normal cell shape. During cytokinesis, actomyosin ring contraction is linked to the formation of a Chs2-synthesized chitinous disk to divide the mother and daughter cells called the primary septum. Chs3-synthesized chitin also plays an auxiliary role to Chs2 during cytokinesis. Here, I show that the F-BAR protein Hof1 is involved in the endocytic removal of Chs3 from the bud neck after chitin ring deposition and possibly later after cytokinesis. I also discuss work to show that Hof1 is involved in the localization and function of Inn1, a C2-domain containing protein essential for synthesis of the primary septum during cytokinesis.

TABLE OF CONTENTS

ACKNOWLEDGEMENTS.....	ii
ABSTRACT.....	iii
LIST OF TABLES AND FIGURES.....	v
I. INTRODUCTION	
Extracellular matrix remodeling.....	1
Chitin: function and synthesis.....	3
Chitin ring formation: Chs3 regulation.....	5
Primary septum formation: Chs2 regulation.....	7
Cytokinesis.....	8
Actomyosin ring.....	9
Coordination of actomyosin ring function and septum formation.....	11
Hof1- an F-BAR protein.....	12
F-BAR domain and endocytosis.....	13
Hof1 function.....	15
II. REGULATION OF CHITIN SYNTHESIS BY THE F-BAR PROTEIN HOF1	
Introduction.....	18
Methods.....	20
Results.....	25
Discussion.....	29
III. HOF1 IS INVOLVED IN COUPLING ACTOMYOSIN RING CONTRACTION TO SEPTUM FORMATION	
Introduction.....	39
Methods.....	41
Results.....	48
Discussion.....	58
IV. PERSPECTIVES.....	86
V. APPENDICES	
Appendix 1: Yeast strains used in Chapter II.....	91
Appendix 2: Plasmids used in Chapter II.....	93
Appendix 3: Yeast strains used in Chapter III.....	94
Appendix 4: Plasmids used in Chapter III.....	97
VI. LITERATURE CITED.....	99

LIST OF TABLES

Table 1	Genes identified by screening for synthetic lethality with <i>hof1</i> Δ.....	83
Table 2	Localization of Inn1 GFP in wild-type and cytokinesis-mutant strains	84

LIST OF FIGURES

Figure 1.1	Schematic representation of cell wall components and their linkages.....	3
Figure 1.2	Chs3 movement in budding yeast.....	5
Figure 1.3	View of the primary and secondary septum.....	8
Figure 1.4	Localization of cytokinesis proteins during the cell cycle.....	10
Figure 1.5	Known processes involving PCH proteins.....	14
Figure 1.6	Primary septum formation in <i>hof1</i> Δ cells.....	15
Figure 2.1	Distinct localization pattern of the F-BAR domain and C-terminus of Hof1 in the cell cycle.....	33
Figure 2.2	The C-terminus of Hof1 is important for cytokinesis.....	34
Figure 2.3	The interaction of Hof1 and Chs4 <i>in vitro</i> and in cells.....	36
Figure 2.4	Higher chitin levels in <i>hof1</i> Δ cells.....	37
Figure 2.5	Chs3 localization in wild-type and <i>hof1</i> Δ cells.....	38
Figure 2.6	Model: Hof1 is a direct linker between chitin synthase III and endocytic machinery.....	31
Figure 3.1	Dependence of PS formation on Inn1.....	63
Figure 3.2	Localization of Inn1 to the bud neck at mitotic exit in wild-type and AMR-deficient cells.....	65
Figure 3.3	Dependence of Inn1 localization on the MEN.....	67
Figure 3.4	Inn1-Hof1 interaction and its role in the symmetric localization of Inn1 at the neck.....	68
Figure 3.5	Functional and physical interactions between Inn1 and Cyk3.....	70
Figure 3.6	Mechanisms of Inn1 bud-neck localization.....	72

Figure 3.7	Structure-function analysis of Inn1.....	74
Figure 3.8	Lack of detectable phospholipid binding by the putative C2 domain of Inn1.....	76
Figure 3.9	Evidence that Inn1 functions downstream of Iqg1 and upstream of Chs2 in AMR-independent cytokinesis.....	77
Figure 3.10	A model for the assembly and function of Inn1 in cytokinesis.....	78
Figure 3.11	Sequence features of Inn1.....	79
Figure 3.12	Approximately normal assembly of the actomyosin ring in <i>inn1Δ</i> cells.....	80
Figure 3.13	Dosage-dependent suppression of the growth defect of <i>inn1Δ</i> cells by the putative C2 domain (amino acids 1-134) of Inn1.....	81
Figure 3.14	Apparent lack of binding of phospholipids by the putative C2 domain of Inn1.....	82

CHAPTER I

INTRODUCTION

EXTRACELLULAR MAXTRIX REMODELING

The extracellular matrix (ECM) is structure that surrounds cells and provides structural support, protection from the environment, and helps in relaying extracellular signals to the cell. It is composed of a mixture of proteins and polysaccharides. While it is most common to think of the ECM as helping to construct mammalian tissues, other cell types also contain an ECM including plant, bacterial, and fungal cells. In these cells it is called a cell wall. The bacterial cell wall field is mature, but its uniqueness makes comparisons to eukaryotic cell walls difficult. Even among animal, plant, and fungal eukaryotic cells, the composition of proteins and polysaccharides is very different. However, a common theme is that remodeling of the ECM is important for cell biology. Though the specific cargo differs among different cell types, all eukaryotic ECMs are shaped by a common underlying cytoskeleton that positions a highly conserved secretory machinery to deliver proteins and enzymes which synthesize the ECM (Lesage and Bussey, 2006).

One example of localized ECM remodeling occurs during angiogenesis, the process by which new blood vessels form from the existing vascular bed. Matrix metalloproteinases (MMPs) are a family of proteins that selectively degrade components of the ECM to make space for the migrating endothelial cells which eventually form new blood vessels and ECM (Stetler-Stevenson, 1999). MMPs are regulated on several levels including spatial localization. Of particular interest are MMP-2 and a membrane-type MMP, MT1-MMP (Nguyen et al., 2001). When cells migrate in tissue, degradation of the ECM barrier is essential, but only in the direction of migration, because the ECM is also important scaffolding. Therefore, cells localize MT1-MMP to lamellipodia, the migration front of the cells (Sato et al., 1997; Itoh et al., 2001; Mori et al., 2002), where it can locally

restrict proteolysis by associating with the plasma membrane and catalytically activating a precursor of MMP-2 transported there (Haas et al., 1999).

Localized remodeling of the ECM is also important during cytokinesis, or the cytoplasmic separation of a single cell into two. During this process, an actomyosin ring assembles and contracts and new membrane is inserted at the site of cleavage. Instead of global deposition, new membrane is delivered specifically to the cleavage furrow in sea urchin embryos and *Xenopus* eggs (Shuster and Burgess, 2002; Danilchik et al., 2003). Not only do docking vesicles deliver new membrane for the dividing cell, but endocytic recycling is essential for remodeling the plasma membrane composition and in abscission (Echard, 2008; Montagnac, et al., 2008). In budding yeast, membrane trafficking also plays a critical role in cytokinesis, especially in delivering membrane material and enzymes involved in synthesizing and remodeling the cell wall including those involved in forming the septum (Barr and Gruneberg, 2007). In particular, a large evolutionarily conserved protein complex called the exocyst is required for the fusion of Golgi-derived vesicles to the plasma membrane (Munson and Novick, 2006). Localized Rho activation is also involved in the delivery of vesicles to the bud neck to enable septum formation and cytokinesis (Pruyne and Bretscher, 2000). So while the cargo is different in budding yeast and animal cells, the exocyst and other conserved membrane trafficking machinery are important for cytokinesis in both.

In budding yeast, some of the specific cargos delivered by exocytosis to the division site are enzymes involved in forming a component of the cell wall called chitin. The yeast cell wall is composed of three types of structural polysaccharides: glucans (polymers of glucose), mannans (mannose-rich glycosylated proteins), and chitin (*N*-acetylglucosamine, or GlcNAc, polymers) (Figure 1.1A) (Bulawa, 1993). Glucans comprise 80-90% of the cell wall and consist of glucose residues linked to other glucose molecules through β -1,3 and β -1,6 linkages. Mannans are 10-20% of the cell wall and connect to glucans through either a processed glycosylphosphatidylinositol (GPI) anchor or an alkali-labile bond. Chitin is a minor component of

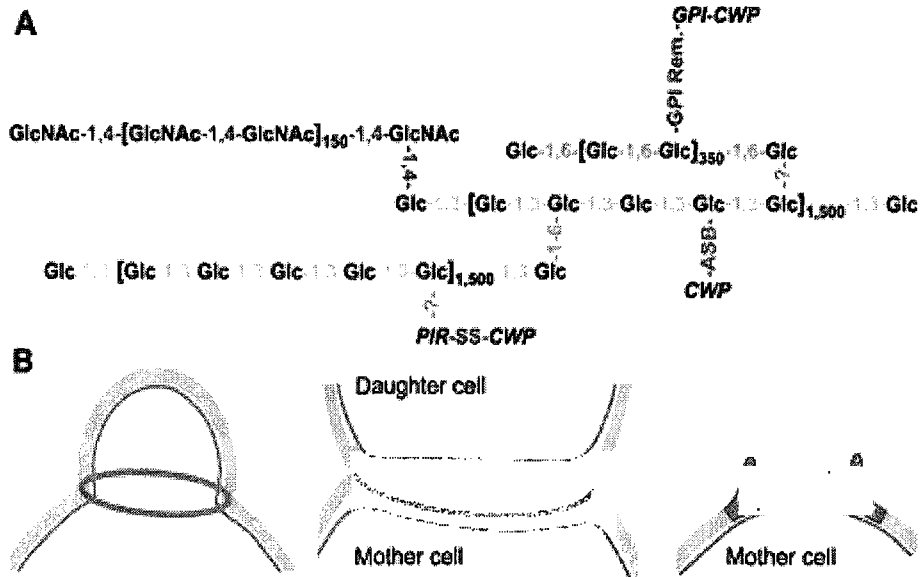


Figure 1.1 **Schematic representation of cell wall components and their linkages** (Lesage and Bussey, 2006)

the cell wall (1-2%) but links to glucans through β -1,4 bonds and is essential for cell wall strength (Lesage and Bussey, 2006)

Chitin: function and synthesis

Chitin is synthesized only during certain portions of the cell cycle and is asymmetrically distributed in the cell wall (Cabib et al., 1982). Most of the cellular chitin (90%) is found in a chitin ring formed at the incipient bud site in late G_1 . It is thought that this chitin ring cooperates with the septin ring that also forms at bud emergence to maintain the integrity of the neck region by controlling growth at the mother-bud neck to maintain a constant neck diameter (Schmidt et al., 2003). A second function of chitin is thought to be a contribution towards the mechanical strength of the cell wall (Hartland et al., 2004). Lastly, about 10% of the cellular chitin is found in an essential structure for cytokinesis, the primary septum (Cabib and Schmidt, 2003). The primary septum is a disk that forms between the dividing cells as the actomyosin ring contracts. A secondary septum composed mainly of glucan and mannan sandwiches and reinforces this

structure and essentially forms the new cell wall for the mother and daughter cells at the division site (Shaw et al., 1991; Cabib et al., 1996). The primary septum is then partially hydrolyzed by a chitinase (Kuranda et al., 1991) and the two cells separate. There are scars left on both cells to mark where division occurred: a bud scar on the mother cells that contains the chitin ring and primary septum, and a birth scar on the daughter cell that does not contain any appreciable level of chitin (Beran et al., 1972; Roncero et al., 1988).

There are three chitin synthases that have the same polymerizing activity, but they produce chitin at different times and at different locations during the cell cycle (Figure 1.1B). All are integral membrane proteins with six or seven putative transmembrane domains (Lesage and Bussey, 2006). Chitin synthase III (Chs3) can generate a small amount of chitin in the lateral cell wall as a reinforcing polymer in certain mutant yeast strains where the cell wall is stressed (Popolo, et al., 1997; Ram et al., 1998). However, as mentioned above, most of the chitin in the cell wall (90%) is found in a Chs3-generated chitin ring formed at the incipient bud site in late G₁. The rest (about 10%) is found in a chitinous disk called the primary septum formed following cytokinesis next to the existing chitin ring by chitin synthase II (Chs2). Individual deletions of *chs2Δ* or *chs3Δ* are not lethal but the double deletion is synthetic lethal with no septa formed. Normally in *chs2Δ* cells, CSIII is capable of producing remedial septa to allow cells to complete cytokinesis (Cabib and Schmidt, 2003). A third enzyme, Chs1, also produces a small amount of chitin in the cell wall, mostly to counteract excessive chitinase activity at acidic pHs (Cabib et al., 1989). While Chs1 and Chs2 are regulated at least in part at a transcriptional level (Choi et al., 1994), Chs3 is stable and levels of the protein remain virtually unaltered during the yeast life cycle. Instead, the localization of Chs3 is regulated post-transcriptionally (Chuang and Schekman, 1996) by targeted secretion and endocytic recycling.

Chitin ring formation: Chs3 regulation

There are several proteins required for chitin synthase III (CSIII) activity with Chs3 being the catalytic subunit (Shaw, et al., 1991). Several other Chs proteins are involved in the intracellular sorting of Chs3 to the plasma membrane where it can generate chitin (Figure 1.2). Chs7 is important for the ER to Golgi movement of Chs3 via COPII vesicles (Trilla et al., 1997; Kota and Ljungdahl, 2005). In the Golgi, Chs5 and Chs6 are required for the exit of Chs3 into specialized vesicles/storage compartments in the trans-Golgi network (TGN) called chitosomes, from where it can be delivered to the plasma membrane in a polarized manner (Ziman et al., 1996; Valdivia and Schekman, 2003). Chs6 is a member of the ChAP family of proteins, which mediate cargo into TGN-derived vesicles and Chs5 is a unique protein that plays a more general role in TGN vesicle formation (Trautwein et al., 2006). Both are part of the exomer, a vesicular coat complex that is required for the capture of select membrane proteins destined for the cell surface (Wang et al., 2006). Chs3 is delivered to the bud neck at two points in the cell cycle, late in G₁ and during telophase/cytokinesis (Chuang and Schekman, 1996; Santos and Snyder,

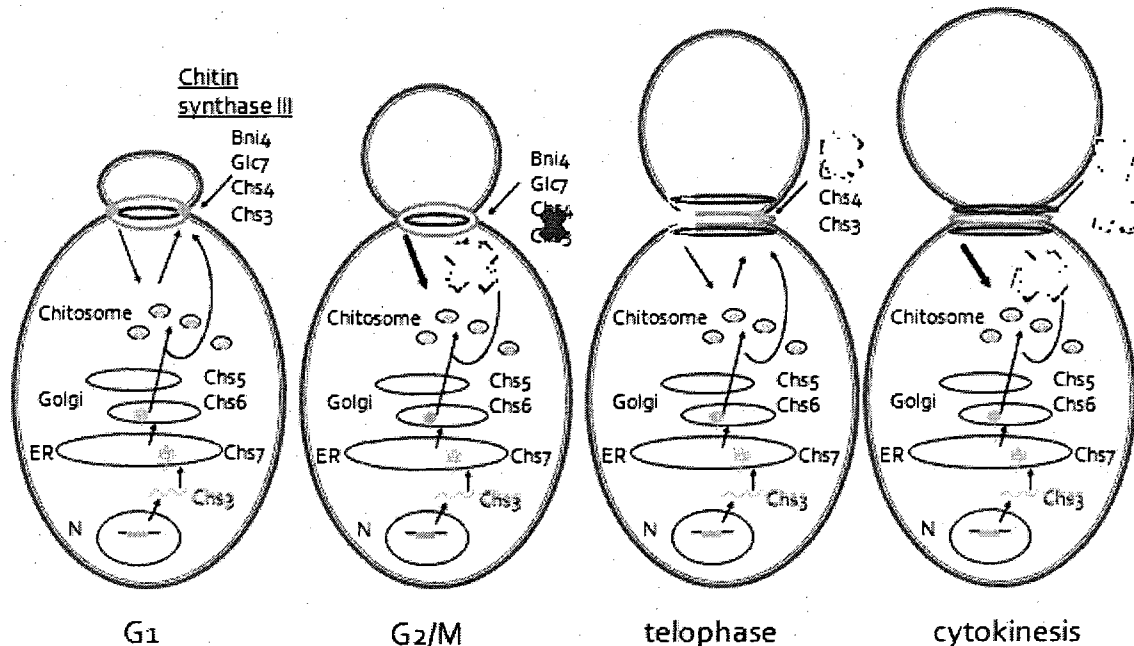


Figure 1.2 **Chs3 movement in budding yeast** (modified from Lesage and Bussey, 2006)

1997), and then endocytosed from the plasma membrane (Holthuis et al., 1998) to populate the chitosome from where it is available to be delivered again to the bud neck (Ziman et al, 1996; Valdivia and Schekman, 2003).

After delivery of Chs3 to the bud neck, at least three other proteins are involved in CSIII activity. Chs4 is the activator and binds directly to Chs3 (DeMarini et al., 1997). Chs4 is delivered to the bud neck independently of Chs3, and its association with membranes depends on prenylation (Grabinska et al., 2007) and also its interaction with other proteins including Chs3 (DeMarini et al., 1997). While Chs3 can be delivered to the bud neck in *chs4*Δ cells, it fails to accumulate there and is instead rapidly endocytosed to the chitosome (Reyes et al., 2007). Through Chs4, Chs3 also interacts with the septin-binding protein Bni4 (DeMarini et al, 1997). The septins are a family of filament forming proteins that act as a scaffold at the bud neck and will be discussed later. Bni4 was thought to only be a linker between Chs4 and the septins, but recently the essential role of Bni4 was discovered to be the targeting of the yeast phosphatase (PP1) catalytic subunit Glc7 to the bud neck and its activation towards substrates necessary to recruit active CSIII (Larson et al., 2008).

The temporal regulation of Chs3, Chs4, and Bni4 localization to the bud neck are different. All three localize as a ring at the incipient bud site to synthesize the chitin ring and remain spatially restricted to the mother side of the bud neck as the bud grows (Shaw et al., 1991; DeMarini et al., 1997; Chuang and Scheckman, 1996). While Bni4 remains, Chs3 and Chs4 disappear from the bud neck around G2/M when the bud is medium-sized. Bni4 levels drop just before cytokinesis but Chs3 and Chs4 re-localize to the bud neck in a Bni4-independent manner during telophase/cytokinesis (Chuang and Scheckman, 1996; DeMarini et al., 1997; Santos and Synder, 1997; Kozubowski et al., 2003). During late G₁, Chs3 cycles between the plasma membrane at the bud neck and the chitosome through endocytosis and exocytosis (Holthuis et al., 1998; Ziman et al, 1996; Valdivia and Schekman, 2003). This recycling continues until G2/M when Chs3 disappears from the bud neck. This same pattern of delivery and endocytosis occurs later in the cell cycle during telophase and ends during cytokinesis. Though

Chs4 shares a similar neck localization pattern with Chs3, it is not present in cytoplasmic punctae with Chs3 (Reyes et al., 2007) to indicate that both have different routes of intracellular trafficking to the cell surface. While many of the proteins involved in delivering Chs3 to the bud neck have been identified, the mechanism responsible for the endocytic removal of Chs3 and presumably Chs4 from the bud neck during both G2/M and cytokinesis is completely unknown.

In Chapter II of this thesis, I will describe recent work to show that the F-BAR protein Hof1 can directly bind to Chs4 and is involved in the removal of Chs3 from the bud neck. Hof1 has been shown to be involved in cytokinesis (Vallen et al., 2000) and is a member of the evolutionarily conserved PCH family of proteins (Chitu and Stanley, 2007). This family of proteins contains the recently described F-BAR domain which is related structurally and functionally to the BAR domain, an important linker between membranes and the cytoskeleton (Itoh et al., 2005; Tsujita et al., 2006; Henne et al., 2007; Shimada et al., 2007). F-BAR domain-containing proteins in mammalian cells have been found to be involved in endocytosis (Itoh et al., 2005; Tsujita et al., 2006; Kamioka et al., 2004; Kessels and Qualmann, 2002; Anggono et al., 2006; Modregger et al., 2000; Schilling et al., 2006; Perez-Otano et al., 2006). I propose that Hof1 is involved in the endocytic removal of CSIII from the bud neck at G2/M and after cytokinesis.

Primary septum formation: Chs2 regulation

The primary septum is a chitin-rich disk centripetally formed as the actinomyosin ring is contracting (Figure 1.3) (Bi et al., 1998; Lippincott and Li, 1998). The secondary septum then forms to sandwich the primary septum and essentially forms the new cell wall for the mother and daughter cells at the division site after cell separation (Shaw et al., 1991; Cabib et al., 1996). Chitin synthase II (CSII), whose catalytic subunit is Chs2, is primarily responsible for primary septum formation. The regulation of Chs2 is somewhat different from Chs3 in that the levels of Chs2 protein peak at the end of mitosis instead of remaining at steady state levels. Chs2 can be found throughout the secretory system in cells that are unbudded or have a small bud, but localize to the bud neck only during telophase in a septin-dependent manner (Chuang and

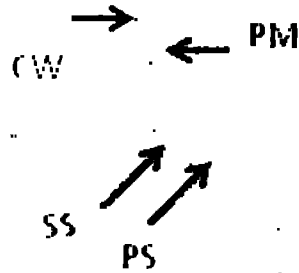


Figure 1.3 **View of the primary and secondary septum.** (EM by R. Nishihama)

Schekman, 1996; DeMarini et al., 1997). Chs2 is then internalized by endocytosis and targeted to the vacuole for degradation (Chuang and Schekman, 1996). Activity of Chs2 can be detected *in vitro* after proteolytic treatment (Sburlati and Cabib, 1986) although whether the protein is synthesized as a precursor and whether or how it is converted into an active form inside a cell is not known.

Depletion of CSII alone is not lethal as CSIII (whose primary function is chitin ring synthesis in G1) presumably can provide an auxiliary septum in its absence (Schmidt et al., 2002), but depletion of both is lethal with cells arresting in chains (Shaw et al., 1991). Therefore, as opposed to the actomyosin ring which is dispensable in budding yeast for cytokinesis, septum formation is essential. In Chapter III, I will describe one potential pathway for how Chs2 activation and primary septum formation might be linked to actomyosin ring contraction during cytokinesis, but first I will discuss cytokinesis in budding yeast.

Cytokinesis

The budding yeast *Saccharomyces cerevisiae* is an ideal model system for studying cytokinesis as it is a well-characterized and genetically tractable organism. Yeast contain many

evolutionarily conserved proteins involved in cytokinesis, including the septins, type II myosin (Myo1p), actin, formins, IQGAP, PCH proteins, and other components of the actomyosin contractile ring and targeted membrane trafficking (Bi, 2001). Another advantage in using budding yeast is that, as opposed to animal cells and fission yeast, the actomyosin ring is not essential for cell survival (Watts et al., 1987; Rodriguez and Paterson, 1990; Bi et al., 1998). Cells lacking the actomyosin ring can still divide, but do so less efficiently, leading to the formation of cell clusters. In contrast, the formation of the septum, which requires targeted exocytosis, is essential for cell survival and cytokinesis (Shaw et al., 1991). The septum is a chitin-rich cell wall structure that allows cells to maintain their osmotic pressure throughout the division process. The formation of the septum must coordinate with the contraction of the actomyosin ring (Bi et al., 1998; Lippincott and Li, 1998). Although the underlying mechanism for this coordination remains unclear, our hypothesis is that the actomyosin ring guides septum formation such that the latter process occurs at the right time and the right place with the highest efficiency.

Actomyosin ring

The formation of the actomyosin ring requires many evolutionarily conserved proteins including septins, type II myosin, F-actin, IQGAP, and the formins (Figure 1.4). At the beginning of the cell cycle, late G1, the septins localize to the bud neck followed closely by the type II myosin (Myo1), its regulatory light chain (Mlc2), and the formin Bnr1. In S phase, the type II myosin essential light chain (Mlc1) localizes, followed by Iqg1 in G2/M, then the formin Bni1, and finally in late anaphase, the actin ring. Therefore, a functional actomyosin ring does not form until late anaphase, although some of the components arrive at the bud neck earlier (Balasubramanian et al., 2004).

The septins are an emerging family of cytoskeletal proteins that bind GTP, form filaments, and play important roles in a variety of cellular processes, with their function during cytokinesis being the best understood (Joo et al., 2005; Longtine et al., 1996; Pan et al., 2007).

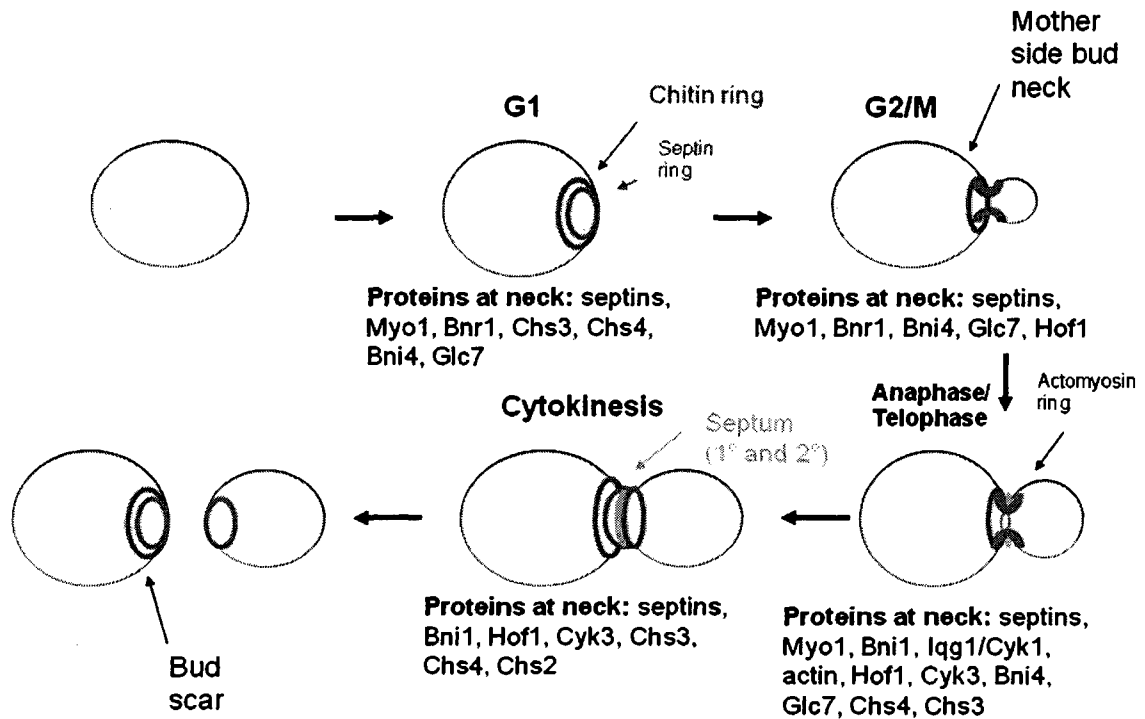


Figure 1.4 Localization of cytokinesis proteins during the cell cycle.

There are five septins expressed vegetatively in budding yeast: Cdc3, Cdc10, Cdc11, Cdc12, and Shs1/Sep7, and two septins that are only expressed during sporulation: Spr3 and Spr28. All five septins localize to the bud neck in vegetatively growing cells, and their localization is mostly interdependent. A defect in septin organization is lethal to the cells and leads to a cytokinesis block. Many of the other proteins involved in forming the actomyosin ring depend on the septins for their localization to suggest that the septins might function as a scaffold at the bud neck (Longtine and Bi, 2003; Gladfelter et al., 2001). However, it is not known how the septins themselves are anchored to the bud neck.

A Myo1 ring forms at the incipient bud site but does not contract until F-actin is recruited to form a functional actomyosin ring in late anaphase (Bi et al., 1998). Like all known type II myosins, Myo1 is regulated by an essential light chain and a regulatory light chain. The regulatory light chain, Mlc2, is not required for actin ring formation but appears to play a role in

the eventual Myo1 ring disassembly (Luo et al., 2004). In contrast to Myo1, which is not essential for cell viability (Bi et al., 1998), the type II myosin essential light chain, Mlc1, is required for cytokinesis and cell viability. This suggests that Mlc1 is involved in the second pathway to cytokinesis in budding yeast, the formation of the septum.

Mlc1 is also the light chain for Iqg1 and its function with this protein appears to be its major role in cytokinesis (Luo et al., 2004). Iqg1 is a member of a family of proteins with multiple domains, including an N-terminal calponin-homology domain (CHD) that binds to F-actin *in vitro* (Shannon and Li, 1999). It is required for the formation of the actomyosin ring and appears to be a component of it, although it does not depend on Myo1 for localization (Shannon and Li, 1999; Epp and Chant, 1997; Lippincott and Li, 1998). Like Mlc1, Iqg1 is essential for cytokinesis and cell viability and therefore is also likely involved in the formation of the septum.

The last proteins involved in actin ring formation are the formins, Bnr1 and Bni1. Bnr1 localizes to the bud neck throughout the cell cycle while Bni1 localizes to the presumptive bud site, the bud tip, and the neck of large-budded cells (Evangelista et al., 1997; Fujiwara et al., 1998; Kamei et al., 1998; Kikyo et al., 1999). Each protein has a different mode of cortical interaction during actin cable assembly, with Bni1 being dynamic in moving between polarized sites and the cytoplasm while Bnr1 is confined to the bud neck (Buttery et al., 2007). Deletion of one gene alone is not lethal, but deleting both causes cell lethality (Kamei et al., 1998; Vallen et al., 2000). These two proteins are required for actin ring formation, likely because they can nucleate actin filaments (Vallen et al., 2000; Pruyne et al., 2002; Sagot et al., 2002).

Coordination of actomyosin ring function and septum formation

In budding yeast, an unknown mechanism ensures that actomyosin ring contraction is followed by the formation of the septum (Bi et al., 1998; Lippincott and Li, 1998). Both processes are important for efficient cytokinesis, with the actomyosin ring possibly providing directionality for normal septum formation (Vallen, et al., 2000) and septum formation being essential for actomyosin ring contraction. There must be a temporal and spatial coordination mechanism

between the actomyosin ring and septum to carry out cytokinesis. This likely involves proteins that are physical components of each pathway or regulatory proteins that link the two pathways together.

As mentioned above, the septins, Mlc1, Iqg1, and the formins are likely involved in the coordination of these two pathways, although their role in septum formation is unclear. Two other proteins that might be involved are Hof1 and Cyk3. Hof1 is an F-BAR domain protein whose deletion causes a temperature-sensitive growth defect with cells arresting in chains. At the permissive temperature, the actomyosin ring can form and contract, while at the non-permissive temperature, the ring can form but fails to contract normally (Vallen et al., 2000). Hof1 localizes to the bud neck starting in G2/M but during anaphase/telophase it appears to 'ride-along' with the actomyosin ring contraction. However, at the end of contraction when the ring disappears, Hof1 lingers as two fuzzy bands on either side of the bud neck during septum formation (Vallen et al., 2000). Cyk3, a SH3 domain protein, shares this same anaphase/telophase localization pattern with Hof1 and deletion of the two is synthetic lethal (Korinek et al., 2000). In addition, over-expression of either gene restored the viability of *iqg1* Δ without restoring the actomyosin ring, suggesting that they both are involved in septum formation (Korinek et al., 2000).

In Chapter III, I will describe recent work to show that Hof1 and Cyk3 are involved in coupling actomyosin ring contraction with septum formation. Both interact with a newly identified C2-domain containing protein Inn1, which is necessary for the activation, but not localization, of the CSII catalytic subunit Chs2 to form the primary septum.

HOF1- an F-BAR protein

Hof1 is a member of an evolutionarily conserved family of proteins called PCH (pombe Cdc15 homology) proteins. The founding member of this family is the *Schizosaccharomyces pombe* Cdc15 protein. Mutations in this protein can cause a cytokinesis failure in fission yeast (Balasubramanian et al., 1998; Fankhauser et al., 1995). Homologs of Cdc15 have been found in many other organisms including mammals (review in Lippincott and Li, 2000). These proteins

have low sequence similarity but share similar domains including PCH (FCH), CC, and SH3 domains (Heath and Insall, 2008; Chitu and Stanley, 2007). They are divided into 6 subfamilies based on domain organization. Some of the subfamilies have proteins that can also contain kinase and small GTPase binding (HR1) domains (Chitu and Stanley, 2007).

Initially, PCH proteins were thought to regulate cellular functions through F-actin assembly (Lippincott and Li, 2000). However, recently they have been found to function more broadly in linking membranes and the cytoskeleton. In mammalian cells, they have been shown to bind lipids, deform membranes, and bundle F-actin (Itoh et al., 2005; Tsujita et al., 2006; Chitu et al., 2005) to lead to their involvement in exocytosis (Kessels et al., 2006; Qian et al., 2005), endocytosis (Itoh et al., 2005; Tsujita et al., 2006; Kamioka et al., 2004; Kessels and Qualmann, 2002; Anggono et al., 2006; Modregger et al., 2000; Schilling et al., 2006; Perez-Otano et al., 2006), and endosomal recycling (Braun et al., 2005).

F-BAR domain and endocytosis

Recent work in mammalian cells showed that together the PCH and CC domains bear a striking structural and functional resemblance to the BAR domain and so are jointly called an F-BAR domain (Itoh et al., 2005; Tsujita et al., 2006). Similar to BAR domains, F-BAR domains are composed of α -helical dimers (though of a different radius) and can sense and bind highly curved lipid membranes (Henne et al., 2007, Shimada et al., 2007). The F-BAR domains of several PCH proteins, including FBP17, CIP4, Toca-1, PSTPIP1 and PSTPIP2, can bind liposomes enriched with phosphatidyl-serine (PS) and phosphatidyl inositol(4,5)biphosphate (PtdIns(4,5)P₂) and induce tubule formation *in vitro*. In cells, overexpression of the F-BAR domain can induce the formation of tubular membrane invaginations (Itoh et al., 2005; Tsujita et al., 2006).

Initial work in mammalian cells shows that some F-BAR proteins are involved in endocytosis. The FBP-17/CIP4 subfamily contributes to the formation of a protein complex, together with N-WASP and dynamin-2, in the early stages of endocytosis. FBP17 and CIP4 can dimerize, tubulate liposomes *in vitro*, deform the plasma membrane, and bind PS and PI(4,5)P₂.

RNAi against FBP17 and CIP4 reduced uptake of Texas red-labeled EGF (Itoh et al., 2005; Tsujita et al., 2006). The model of action predicts that these F-BAR proteins will bind to budding vesicle membranes via their F-BAR domains and then connect to actin-binding proteins via their C-terminal SH3 domains (Figure 1.5a) (Chitu and Stanley, 2007). In a second model, F-BAR proteins without SH3 domains, such as PSTPIP2 and CIP4b, cannot directly interact with WASP or dynamin and are proposed to contribute to the generation of membrane protrusions such as filopodia (Figure 1.5b) (Chitu and Stanley, 2007).

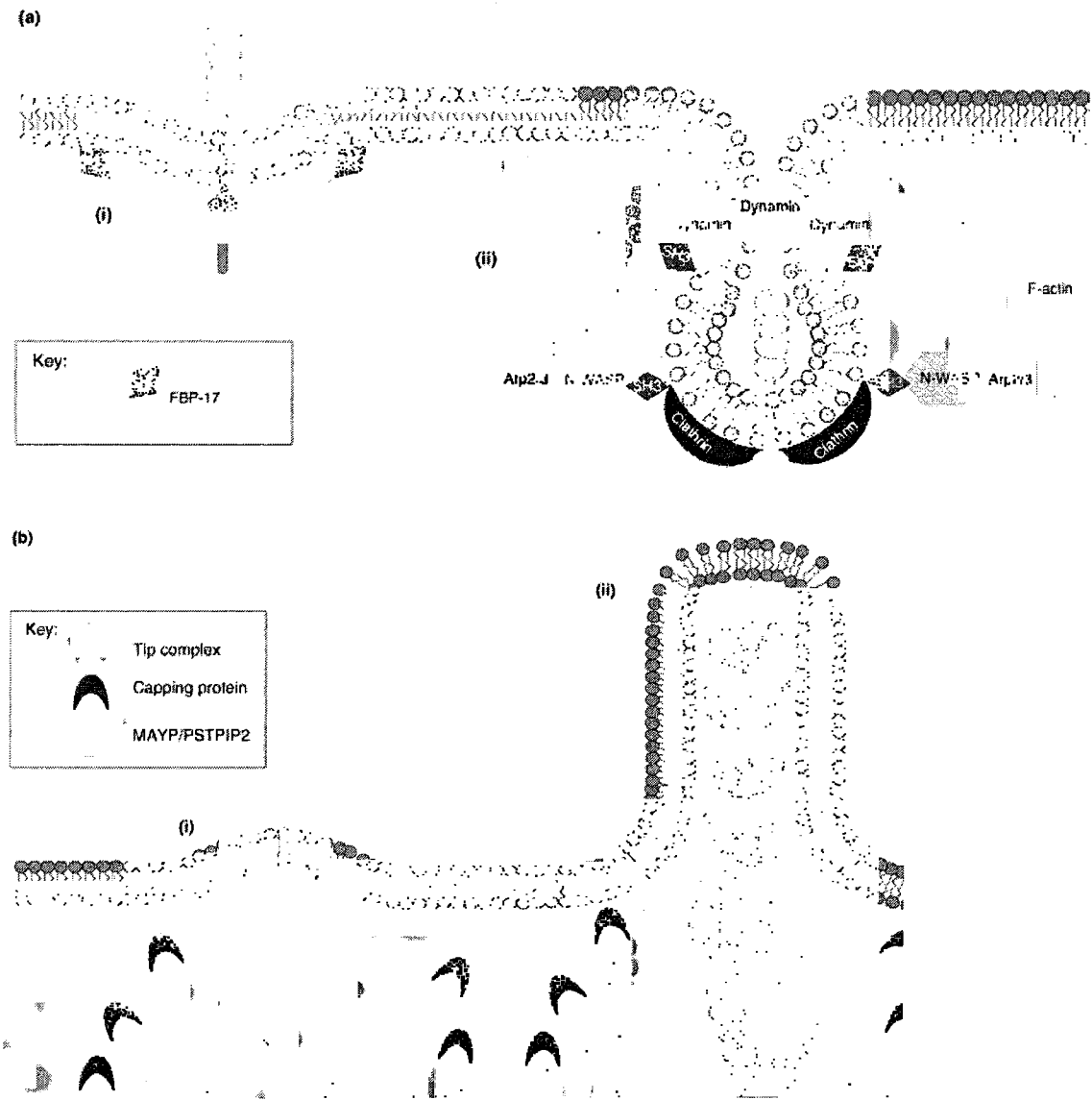


Figure 1.5 **Known processes involving PCH proteins.** (from Chitu and Stanley, 2007).

Hof1 function

Budding yeast contain three F-BAR proteins: Hof1, Bzz1, and Rgd1. Rgd1p (rho GTPase-activating protein) negatively regulates the GTPase activity of Rho3p and Rho4p, which are involved in bud growth and cytokinesis, respectively. It contains an F-BAR domain at its N-terminal end and a RhoGAP domain at its C-terminal end. Different phosphoinositides regulate the recruitment and trafficking of Rgd1p to the Golgi and the plasma membrane via the F-BAR domain (Prouzet-Mauléon, et al., 2008). Bzz1 is a WASP/Las17-interacting protein that is found in actin patches and is involved in the early steps of endocytosis along with other actin nucleators (Soulard et al., 2005).

The third F-BAR protein, Hof1 (homolog of fifteen), has been shown to be involved in cytokinesis (Vallen et al., 2000), though the mechanisms are not understood and will be explored in this thesis. Hof1 has three distinct domains, including the N-terminus F-BAR domain, a PEST sequence in the middle of the protein, and a C-terminal SH3 domain. The deletion of *HOF1* causes a temperature sensitive phenotype with cells normal in appearance and growth at 25°C (Vallen et al., 2000), though closer examination by EM reveals some cells with asymmetric primary septum formation and abnormal secondary septum formation (Figure 1.6).

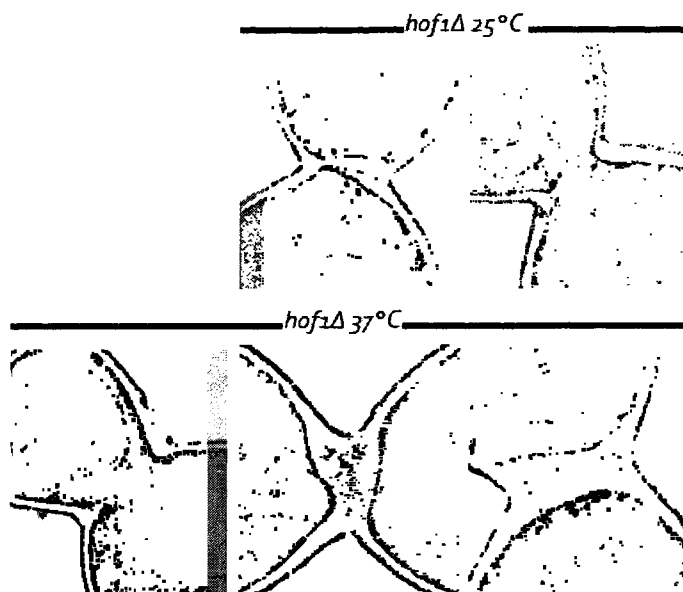


Figure 1.6 Primary septum formation in *hof1Δ* cells (EM by R. Nishihama)

At the non-permissive temperature of 37°C, the cells can no longer grow and arrest in chains with the actomyosin ring forming but not contracting normally. In addition, the primary septum cannot form, or cannot form efficiently (Figure 1.6) and chitin is found in increased amounts over the entire cell surface in addition to its bud neck concentration (Vallen et al, 2000; Kamei et al, 1998).

Hof1 localizes to the bud neck in a septin-dependent manner (Vallen et al., 2000) and has a distinct localization pattern. It localizes to the mother side of the bud neck in G2/M. During anaphase, the ring splits into two rings on either side of the bud neck before forming a single ring again in the middle of the neck. In telophase, the single ring appears to contract with the actomyosin ring and then splits into two fuzzy rings on either side of the bud neck during septum formation (Vallen, et al., 2000). Hof1 undergoes MEN-dependent phosphorylation which may be in part responsible for its localization pattern (Vallen et al., 2000). It is also degraded at the end of each cell cycle by the SCF^{Grr1} E3 ligase, and this requires its PEST sequence (Blondel et al., 2005).

Hof1 has genetic and physical interactions with several proteins that hint at its possible functions. The SH3 domain of Hof1 can directly interact with the FH1 domain on the formin Bnr1 (Kamei et al., 1998) and also has been reported to interact with the Wiskott-Aldrich syndrome protein (WASP)-interacting protein (WIP) ortholog Vrp1 (Naqvi et al., 2001; Ren et al., 2005). In addition, *hof1Δ* was also found to be synthetic lethal with *cyk3Δ* and *bni1Δ* (Korinek et al., 2000; Vallen et al., 2000). As mentioned above, Cyk3 is a SH3 domain protein that shares the telophase/cytokinesis localization pattern with Hof1 (Korinek et al., 2000), and together with Hof1 is important for primary septum formation. Bni1 is the other formin in yeast; it localizes to the presumptive bud site, the bud tip, and the bud neck in large-budded cells (Evangelista et al., 1997; Fujiwara et al., 1998), and is required for actin ring assembly during cytokinesis. *hof1Δ* was also synthetic lethal in combination with *myo1Δ* but not with *bnr1Δ* (Vallen et al., 2000), consistent with the fact that Bnr1 disappears from the neck prior to actin ring contraction (Buttery et al., 2007). This suggests that Hof1/Bnr1 and Myo1/Bni1 are likely involved in parallel pathways in cytokinesis.

The synthetic lethal interactions, deletion phenotype, and localization pattern of Hof1 suggest that it is involved in the coordination of actomyosin ring contraction and septum formation. In Chapter III, I will explore the mechanisms of the coordination. The unique mother-side of the bud neck localization pattern of Hof1 during G2/M and the chitin mis-localization in *hof1* Δ cells at the non-permissive temperature suggest that Hof1 is involved in the regulation of chitin synthesis. In Chapter II, I will show that Hof1 interacts with a component of chitin synthase III, Chs4, and likely regulates chitin synthesis at G2/M and also late in the cell cycle during cytokinesis.

CHAPTER II

REGULATION OF CHITIN SYNTHESIS BY THE F-BAR PROTEIN HOF1

Modified from **Schreiter, J. H., Nishihama, R., Bi, E.** (2009) Regulation of chitin synthesis by the F-BAR protein Hof1 (in submission)

Introduction

Localized synthesis and remodeling of the extracellular matrix (ECM) plays an important role in cell biology. Budding yeast cells are surrounded by an ECM-like structure, the cell wall, which contains an essential though minor component called chitin. Ninety percent of the chitin in the cell wall is found in a chitin ring at the base of the bud that is made by the enzyme chitin synthase III (Chs3). CSIII localizes to the bud neck at two points in the cell cycle. It first localizes to the incipient bud site and starts to synthesize a ring of chitin on the mother side of the bud neck at the base of the growing bud (Shaw et al., 1991). It disappears from the bud neck around G2/M and then re-localizes during telophase (Chuang and Schekman, 1996; Kozubowski et al., 2003). There are several interacting proteins required for CSIII activity. Chs3 is the catalytic subunit, Chs4 is the activator, and Bni4 along with the yeast protein phosphatase (PP1) catalytic subunit Glc7 are required to recruit active CSIII to the bud neck (DeMarini et al., 1997; Grabinska et al., 2007; Reyes et al., 2007; Larson et al., 2008). Chs3 and Chs4 are independently delivered in vesicles to the bud neck where Chs4 promotes the translocation of a stable and active form of Chs3 into the plasma membrane (Reyes et al., 2007). Chs3 is then endocytosed from the plasma membrane (Holthuis et al., 1998) to populate the chitosome, a pool of stable vesicles in the early endosomal compartment, from where it can then be delivered again to the bud neck (Ziman et al., 1996; Valdivia and Schekman, 2003). This endocytic recycling of Chs3 continues until about G2/M of the cell cycle when Chs3 and Chs4 both disappear from the bud neck. Later in the cell cycle during cytokinesis, both Chs3 and Chs4 re-appear at the bud neck (Chuang and Schekman, 1996; Kozubowski et al., 2003). The mechanism behind the endocytic removal of

Chs3 and presumably Chs4 from the bud neck during both G2/M and cytokinesis is completely unknown.

At G2/M, when Chs3 and Chs4 disappear from the bud neck, another protein localizes to the mother side of the bud neck, the F-BAR domain containing protein, Hof1 (Vallen et al., 2000). The deletion of *HOF1* causes a temperature sensitive growth defect with the cells appearing normal at 25°C but arresting in chains at 37°C. The actomyosin ring can form but cannot contract normally at the non-permissive temperature. Also, the septum cannot form and chitin is found in increased amounts over the entire cell surface in addition to its bud neck concentration (Vallen et al, 2000; Kamei et al, 1998). Like other proteins involved in cytokinesis, Hof1 can localize as a single band in the center of the bud neck and contract with the actomyosin ring but then lingers at either side of the neck in diffuse bands as the septum forms. As a result, we have proposed that Hof1 helps couple the two processes important for efficient cytokinesis in budding yeast, actomyosin ring contraction and septum formation (Vallen et al, 2000, unpublished results).

However, Hof1 also localizes to the mother side of the bud neck during G2/M, long before other cytokinesis proteins such as Cyk3 and Inn1 localize to the bud neck (Vallen et al., 2000; Sanchez-Diaz et al., 2008). Only a few other proteins share this mother side of the neck localization pattern, including the formin Bnr1 (Kamei et al., 1998) and components of chitin synthase III. In fact, Hof1 localizes to the bud neck at about the time Chs3 and Chs4 disappear, and we raise the possibility that Hof1 plays a role in the endocytic removal of Chs3 and Chs4 from the bud neck during G2/M. Hof1 also lingers at the bud neck during cytokinesis, after the actomyosin ring has contracted and while the septum is forming, and it is possible that it is involved in the removal of Chs3 and Chs4 from the bud neck at this point in the cell cycle as well.

In this report, we show that Hof1 directly binds the activator of CSIII, Chs4. Surprisingly, the F-BAR domain of Hof1 appears to be responsible for the interaction. Up to this point, F-BAR domains were only thought to bind to lipid membranes (Itoh et al., 2005; Tsujita et al., 2006). The Sel1-like repeats (SLR) in Chs4 (Grant and Greenwald, 1996), whose family members possess different cellular functions but seem to be involved as adapter proteins in the assembly of

macromolecular complexes (Mittl and Schneider-Brachert, 2007), also appear to be involved in the interaction. We further suggest that Hof1 might be involved in the endocytic removal of CSIII from the bud neck in both G2/M and cytokinesis.

Materials and Methods

Yeast strains, growth conditions, and genetic procedures

Yeast strains are listed in Appendix 1. Standard culture media and genetic techniques were used (Guthrie and Fink, 1991). Where noted, cells were grown in YM-P, a rich, buffered liquid medium (Lillie and Pringle, 1980). All yeast strains were grown at 25°C, unless otherwise indicated. To select for the loss of *URA3*-containing plasmids, 1 mg/ml 5-fluoroorotic acid (5-FOA) (Research Products International, Prospect, IL) was added to media. Oligonucleotide primers were purchased from Integrated DNA Technologies (Coralville, IA).

Plasmids

Plasmids are listed in Appendix 2 and/or described below. A genomic-DNA library in the low-copy vector YCp50-LEU2 was kindly supplied from F. Spencer and P. Hieter [see (Bi and Pringle, 1996)]. Plasmid YCp50LEU2-HOF1, carrying full-length *HOF1*, was isolated from this library by complementing the temperature-sensitive growth of a *hof1*Δ strain (YEF1951). Plasmids YCp50LEU2-HOF1-GFP, YCp50LEU2-HOF1-FBAR-GFP (1-340aa), and YCp50LEU2-HOF1-Cterm-GFP (341-669aa) were constructed by PCR-amplification of superbright GFP (from pFA6a-GFP(S65T,F64L)-kanMX6) and transformation into YEF473A with YCp50LEU2-HOF1 (Longtine et al., 1998). Plasmids YCp50LEU2-HOF1-FBAR (1-340aa) and YCp50LEU2-HOF1-Cterm (341-669aa) were constructed similarly (from pFA6a-His3MX6). Plasmids YCp50LEU2-PGAL-HOF1-GFP, YCp50LEU2-PGAL-HOF1-Cterm-GFP (341-669aa), YCp50LEU2-PGAL-HOF1-FBAR-GFP (1-340aa), and YCp50LEU2-PGAL-HOF1-SH3Δ-GFP (1-601aa) were made similarly by tagging the GFP plasmids described above with PGAL (from pFA6a-His3MX6-PGAL1).

The parent vectors for two-hybrid analyses were the DNA-binding-domain (DBD) plasmid pEG202 (2 μ , *HIS3*) and the activation-domain (AD) plasmid pJG4-5 (2 μ , *TRP1*) (Gyuris et al., 1993). pEG202-CHS4, pEG202-Chs4 C-S, and pEG202-Chs4RI were supplied by John Pringle (Stanford University). CHS4 is the full-length gene (DeMarini et al., 1997). The *chs4*^{C693S} allele (CHS4 C-S) mutation in the CAAX box and the *chs4* ^{Δ 610} allele (CHS4RI) encodes amino acids 1-610 and is missing the CAAX box. Other plasmids were constructed by PCR-amplifying and cloning full-length *HOF1* and fragments of this gene (see Figure 4) into pJG4-5. The structures of these plasmids were confirmed by sequencing.

Plasmids for *in vitro* protein-interaction assays were constructed as follows. Axl2-C was obtained from Sergei Tcheperegine. *Bam*HI-*Xho*I-digested DNA fragments encoding Chs4 C-S, Chs4 220-610aa (Sel1 repeats), and Chs4 1-260aa were subcloned from pEG202 plasmids into the corresponding sites of pGEX-5X-1 (GE Healthcare, Buckinghamshire, UK) to create plasmids encoding GST-fusion proteins. A DNA fragment encoding *HOF1* 1-340aa (FBAR) was PCR-amplified, digested with *Bam*HI and *Sal*I (sites included in the primers), and cloned into *Bam*HI/*Sal*I-digested pCOLADuet-1 (EMD Biosciences, Darmstadt, Germany) to create a plasmid encoding a His6-tagged protein.

Two-hybrid interactions

Strain Y1026 carrying various DBD plasmids (see above) was mated to strain Y860 carrying various AD plasmids. Diploids were selected on SC-His-Trp plates, replica-plated to SC-His-Trp-Ade plates containing 1% raffinose plus 2% galactose (to induce production of the fusion proteins), and incubated at 30°C for \geq 4 days to detect interactions.

In vitro protein-binding assays

To purify His6-tagged proteins, *E. coli* strain BL21 (Invitrogen) was transformed with pCOLADuet-based plasmids (see above), grown to exponential phase at 37°C for 4 h, and induced with 1 mM IPTG for 3 h at 23°C. Cells were washed twice with double-distilled water,

frozen at -20°C, thawed in freshly-prepared Ni-NTA lysis buffer (300 mM NaCl, 20 mM Tris-HCl, pH 8.0, 20 mM imidazole, 10 mM β-mercaptoethanol, 0.1% NP-40) containing a cocktail of protease inhibitors, sonicated seven times, placed on ice for 30 min, and centrifuged at 15,000 rpm for 20 min. The supernatant was mixed with Ni-NTA beads that had been freshly washed with Ni-NTA lysis buffer. After rocking for 1 h at 4°C, the beads were collected by centrifugation, washed three times with Ni-NTA buffer, and eluted five times with freshly-prepared elution buffer (PBS containing 5 mM EDTA, 5 mM DTT, and 0.1% NP-40). To purify GST-tagged proteins, *E. coli* BL21 was transformed with pGEX-5X-based plasmids (see above). Protein extracts were then prepared essentially as described for the His6-tagged proteins, except that the lysis buffer was PBS containing 5 mM EDTA, 5 mM DTT, and 0.1% NP-40. The 15,000-rpm supernatant was mixed with pre-washed glutathione beads and rocked for 1 h at 4°C. The beads were collected by centrifugation, washed three times with lysis buffer, and resuspended in lysis buffer.

To test for protein binding *in vitro*, 20 μg of His6-tagged protein was mixed with 10 μg of GST (as negative control) or GST-tagged protein that was still bound to the glutathione beads (400 μl total volume) and rocked for 1 h at 4°C. The beads were washed five times with freshly-prepared GST-fusion lysis buffer (see above) and resuspended in 50 μl SDS sample buffer, and proteins were analyzed by SDS-PAGE (10% gel) and Western blotting using mouse monoclonal anti-penta-His (Qiagen, Valencia, CA) and anti-GST (Covance, Emeryville, CA) primary antibodies and an HRP-conjugated rabbit anti-mouse-IgG secondary antibody (Jackson ImmunoResearch, West Grove, PA). The anti-His signal was detected using the Millipore Immobilon Western Chemiluminescent HRP Substrate (Billerica, MA), and the blot was incubated with the Restore Blot-stripping Buffer (Pierce, Rockford, IL) for 2 hours at 37°C before re-probing with the anti-GST antibody, which was then detected by ECL (GE Healthcare).

BiFC assay

BiFC yeast strains were constructed by chromosome tagging YEF473A and YEF473B on the N-terminus of CHS4 and HOF1 with the split YFP gene as described (Sung and Huh, 2007)

and mated to each other. Diploids were selected on SC-His-Trp plates and examined for fluorescent signal using the spinning-disk confocal microscope system (see below).

Measurement of the chitin content of cells

Yeast cells were grown in YM-1+2%Dex culture for 48 hours on a roller drum at 23°C to stationary phase. Measured the OD of the cells and diluted approximately 1:100 into duplicate 5 mL YM-1+2%Dex cultures trying to get roughly the same amount of starting cells. Grew cultures again for 22-24 hours on a roller drum at 23°C, centrifuged a total of 3 mL of culture into a pre-weighed 1.5 mL Eppendorf tube at 15,000rpm for 2 min, and placed the tubes in a 37° incubator for 48-96 hours to dry the pellets. Weighed the tubes again and subtracted the initial weight of the empty tube to determine the dry weight of the cell pellet. Added 1 mL 6% KOH to the cell pellets, heated to 80°C for 90 min with occasional mixing, pelleted alkaline insoluble material at 15,000rpm for 20 min, and neutralized with 1mL phosphate-buffered saline (PBS) for 10-20 min with occasional mixing. Centrifuged at top speed for 20 minutes and discarded the supernatant. Added 200 uL of McIlvaine's Buffer (0.2 M Na₂HPO₄/0.1 M citric acid, pH 6.0) to the pellets and stored extracts at -20°C until ready to process for chitin measurements. Thawed samples and digested with 10 uL of *Serratia marcescens* chitinase (0.004 g freshly dissolved in 1 mL cold 200 mM potassium phosphate buffer, pH 6.0, with 2 mM CaCl₂; Sigma-Aldrich, St. Louis, MO) 18-20 hours on shaking 23°C platform. Mixed 10 uL of supernatant with 10 uL of 0.27 M sodium borate (pH 9.0) in a 0.2-mL PCR tube, heated in a thermocycler to 99.9°C for about 60 s, mixed gently, and incubated at 99.9°C for 10 minutes. Immediately after cooling to room temperature, added 100 uL of freshly diluted DMAB solution (Ehrlich's reagent, consisting of 10 g of *p*-dimethylaminobenzaldehyde in 12.5 ml of concentrated HCl and 87.5 ml of glacial acetic acid, diluted 1:10 with glacial acetic acid) to samples, and incubated at 37°C for 20 minutes. Immediately recorded the absorbance at 585 nm. Standard curves were prepared from stocks of 0.2 to 2.0 mM GlcNAc. Normalized the levels of chitin, expressed as GlcNAc concentration, to the dry weight of the sample.

Microscopy

To visualize Hof1-GFP in Figure 2.1, fresh cells were grown to early log phase in SC-*leu2* medium and spotted on a thin layer on YPD plus 2% agarose. The images were acquired using IPLab software (BD Biosciences, Rockville, MD) and a spinning-disk confocal-microscope system comprising a Yokogawa CSU 10 scanner, an Olympus IX 71 microscope, a Plan S-Apo 100X/1.4 NA oil immersion objective, and a Hamamatsu Photonics ImagEM back-thinned EMCCD camera (C9100-13). Components were integrated by BioVision Technologies (Exton, PA). Diode lasers for excitation (488 nm for GFP; 561 nm for RFP) were housed in a launch constructed by Spectral Applied Research. A brightfield image was captured at the beginning and end of each timelapse series in the mid-cell focal plane, and Hof1-GFP and Cdc3-RFP images were captured in a Z series of 11 steps (0.4 μ m). The maximum-projection images created from the Z stacks using ImageJ were analyzed for the Hof1 localization patterns. The Chs3-GFP timelapse series in Figure 2.5 were captured similarly but the cells were grown in YM-1 media. The BiFC images in Figure 2.4 were also captured similarly except cells were grown in YM-1 media and there was no timelapse but a single Z-stack of 11 steps (0.4 μ m).

To measure the distance between Spc42-mcherry in Figure 2.5, fresh cells were grown to early log phase in YM-1 media. A single Z series of 30 steps (0.2 μ m) were taken for each field of cells. Small-budded cells were identified to possess the Chs3-GFP signal and the distance between the Spc42-mcherry labeled spindle pole bodies was measured in 3-D space using Volocity software.

The pGAL-Hof1 images in Figure 2.2 were performed using a computer-controlled Eclipse 800 (Nikon, Tokyo, Japan) equipped with a 60 X Plan Apo objective and a high-resolution CCD camera (model C4742-95; Hamamatsu Photonics, Bridgewater, NJ). Images were acquired and processed using Image-Pro Plus software (Media Cybernetics, Silver Spring, MD) and Photoshop CS4 (Adobe Systems, San Jose, CA).

Results

Different regions of Hof1 confer distinct localization patterns

Hof1, like other cytokinesis proteins, localizes to the bud neck during anaphase/telophase of the cell cycle. It appears to co-localize and contract with the actomyosin ring and then lingers at the neck as the septum forms before disappearing at the end of the cell cycle. However, it differs from other proteins involved in cytokinesis in that it first localizes to the bud neck during G2/M when the bud is still medium-sized (Vallen et al., 2000). We propose that Hof1 has two distinct functions, one during cytokinesis and another during G2/M (see Introduction). There are several distinct domains in the Hof1 protein including an SH3 domain and an FBAR domain (Figure 2.1A). We wished to determine if the different functions of Hof1 are separable, i.e. if different domains of Hof1 are more important for its G2/M and cytokinesis functions.

To look at this, we examined the localization pattern of different GFP-tagged Hof1 truncations. We first chromosome tagged the CDC3 gene with mcherry RFP (Shaner et al., 2004) to allow us to determine the stage of the cell cycle the cells were in. Cdc3 is a septin, a member of a family of filament forming proteins that localize to the bud neck throughout cell division (reviewed in Versele and Thorner, 2005). They are essential for the neck localization of cytokinesis proteins and split into two rings on either side of the bud neck during telophase (Vrabioiu and Mitchison, 2006). We then deleted *hof1* in these cells as Hof1 might dimerize (unpublished results) and we did not want endogenous Hof1 to interfere with our localization results. As before (Vallen et al. 2000), we found that full-length Hof1 localizes to the mother side of the bud neck in G2/M, briefly splits into two rings and then localizes as a single ring in the center of the bud neck during anaphase/telophase, contracts to a dot with the actomyosin ring, and then splits into two fuzzy rings on either side of the bud neck as the septum forms before finally disappearing as cell separation occurs (Figure 2.1B). In contrast, we found that Hof1-F-BAR-GFP localizes to the bud neck throughout the entire cell cycle, even in unbudded and small-budded cells when Hof1-GFP does not localize (Figure 2.1B). This is presumably due to the loss of the PEST sequence, which controls the degradation of Hof1 after every cell cycle (Blondel et

al., 2005). However, the F-BAR domain of Hof1 does not appear to contract well with the actomyosin ring (Figure 2.1B, 3'). There is some contraction but some of the protein stays localized on either side of the bud neck unlike Hof1-GFP and Hof1-C-term-GFP where all the visible protein contracts. We also found that the C-terminus of Hof1 localizes to the bud neck only during telophase, contracts with the actomyosin ring, and then disappears (Figure 2.1B). This differential localization pattern gave us our first hint that the functions of Hof1 might be separable.

The SH3 domain-containing C-terminus of Hof1 plays an important role in cytokinesis

We also found the over-expression of Hof1-GFP caused a cytokinesis defect with chains of cells and strong localization at the bud neck regions and also some puncta around the plasma membrane (Figure 2.2A). Similarly, Hof1-C-term-GFP over-expression also caused a cytokinesis defect although with much less localization at the bud neck and more cytoplasmic localization. In contrast, over-expression of Hof1-F-BAR-GFP failed to cause a cytokinesis defect although there appeared to be increased levels of cytoplasmic protein. A Hof1 allele missing its SH3 domain, Hof1-SH3 Δ -GFP, also failed to display a cytokinesis defect. The cytokinesis defect is possibly due to the C-terminus of Hof1 binding to other cytokinesis proteins, such as Inn1 and Cyk3 (unpublished results), and sequestering them away from the bud neck. These data suggest that the C-terminus of Hof1, in particular the SH3 domain, is involved in cytokinesis while the F-BAR domain has little apparent role.

Cyk3, another cytokinesis protein, has a SH3 domain and a putative transglutamase domain (Korinek et al., 2000; unpublished results). It shares the anaphase/telophase bud neck localization pattern of Hof1 and the double deletion is synthetic lethal. Somewhat surprisingly, a single extra copy of CYK3 in a *hof1* Δ cell significantly complemented the temperature sensitive growth defect at 37°C (Figure 2.2B). This suggests it is the later cytokinesis function of Hof1, which it might share with Cyk3, that is important for cell viability.

While neither Hof1 nor Cyk3 are essential at 25°C, the deletion of both is synthetic lethal. As expected, full-length Hof1 can rescue this synthetic lethality. However, while the F-BAR domain of Hof1 cannot rescue the synthetic lethality, the C-terminus of Hof1 can (Figure 2.2C). As the C-terminus can only localize to the bud neck during anaphase/telophase, this also suggests that it is this portion of Hof1 that is important for its cytokinesis function.

Hof1 binds directly to Chs4 via its FBAR domain

In a separate manuscript (unpublished data), we reported the role of Hof1 in linking actomyosin ring contraction and the formation of a septum to divide the cytoplasm of the mother and daughter cells during cytokinesis. In this study, we wish to determine the function of Hof1 earlier in the cell cycle, during G2/M, and also after the septum forms during cytokinesis. There are very few proteins that share the mother side of the bud neck localization of Hof1 during G2/M. Among them are the formin, Bnr1, and components of chitin synthase III, Chs3, Chs4, and Bni4. This enzyme is responsible for the creation of the chitin ring at the base of the bud neck (see Introduction). It has been already reported that Hof1 binds directly to Bnr1 (Kamei et al., 1998). We performed a candidate approach using yeast 2-hybrid to determine if Hof1 interacted with any component of chitin synthase III and found an interaction between Hof1 and Chs4. Surprisingly, the interaction appeared to be mediated through the F-BAR domain of Hof1 (Figure 2.3A). We truncated various lengths off the N-terminus of the protein and showed that deleting the first 55 amino acids from the F-BAR domain abrogated the interaction. We determined this was a direct interaction using *in vitro* binding and further defined the interaction by showing that the Sel-1 repeats (amino acid 220-610) in Chs4 appear to also mediate the interaction (Figure 2.3B). To our knowledge, this is the first example in any model system of an F-BAR domain binding to another protein. Previously, the F-BAR domain was thought to bind only to lipid membranes.

We then used a bimolecular complementation assay (BiFC) with a split YFP molecule attached to both Hof1 and Chs4 to show that they interact in a cell and to get a hint as to where

and when the interaction occurs. We found that the two proteins do interact in a cell and that the fluorescence signal intensifies as the cell cycle progresses; there is a faint signal at the bud neck in G2/M and telophase, and it is stronger as the septum forms and then at the mother and daughter sides of the bud neck as the cells separate (Figure 2.3C). As a control, cells with the same half of the YFP molecule (VN) tagged to the N-terminus of both Hof1 and Chs4 showed no fluorescence signal (data not shown). Now that we determined the interaction between Hof1 and Chs4 is direct and occurs in cells, we wanted to examine the functional significance of such an interaction.

Chitin levels are increased in *hof1*Δ cells

The enzyme Chs3 is carried as cargo in vesicles between the bud neck and the chitosome in a recycling mechanism from bud emergence through to G2/M when Hof1 first appears. In separate vesicles, its activator Chs4 is also carried to the bud neck. Both proteins disappear from the bud neck at G2/M but then later localize to the bud neck during telophase and are removed as the mother and daughter cells separate. From work in mammalian cells, F-BAR proteins have been shown to be involved in endocytosis (see Introduction). We believe it is possible that Hof1 is involved in the endocytic removal of Chs4 and Chs3 from the bud neck at both points in the cell cycle. If this is true, then a delay or defect in their removal in *hof1*Δ cells should result in an increase in chitin levels in the cell. Indeed, we found that *hof1*Δ cells have a growth defect on Calcafluor White (CW) plates, a fluorescent dye that stains chitin and will interfere with the growth of yeast that require high levels of chitin for survival (Figure 2.4A). The *cyk3*Δ strain was used as a positive control as it has been previously reported to contain high levels of chitin. As expected, cells missing a part of the chitin synthase III complex and thereby possessing decreased levels of chitin grew well on the plates (Figure 2.4A). We confirmed these results using a quantitative colorimetric assay to measure the level of chitin in cells (Figure 2.4B). Both assays showed that *hof1*Δ cells contain higher levels of chitin.

Chs3 lingers at the bud neck for longer in *hof1*Δ cells than in wild-type cells

If our hypothesis is correct and a delayed endocytosis of Chs3 leads to higher levels of chitin, Chs3-GFP should remain at the bud neck for longer in *hof1*Δ cells than wt cells. We attempted to perform this experiment with Chs4 as well, but the fluorescent signal in Chs3 was much easier to see. We tagged the spindle pole body protein Spc42 with mcherry RFP to determine cell cycle progression. The spindle pole body duplicates around G2 and then the two bodies will separate during mitosis. We found that in wild-type cells, Chs3-GFP localized to the bud neck mostly before spindle pole body separation. In contrast, in *hof1*Δ cells, there was a larger percentage of cells with Chs3-GFP localization persisting at the bud neck even after the spindle pole bodies were more than 1 μm apart (Figure 2.5A). Timelapse imaging also shows this same phenomenon (Figure 2.5B). This suggests that the removal of Chs3 from the bud neck in G2/M by endocytosis is impaired in *hof1*Δ cells.

Discussion

Role of Hof1 in cytokinesis

Previously we have shown that Hof1 is involved in cytokinesis but the underlying mechanism was unknown (Vallen et al., 2000). In this study, we performed a structure-function analysis of Hof1 and found that different domains of Hof1 have distinct functions. The F-BAR domain appears to be important for localization. Similar results were found with Hof1 in filamentous fungi (Kaufmann and Philippsen, 2009). The SH3 domain of Hof1 appears to be important for the protein's interaction with other proteins involved in cytokinesis, such as Inn1 (see Chapter III). The Hof1-Cterm, which contains the SH3 domain, can rescue the *hof1*Δ *cyk3*Δ synthetic lethal interaction (Figure 2.2) and only can localize to the bud neck during telophase. This suggests the cytokinesis role of Hof1 is its essential function.

Role of Hof1 in chitin synthesis

However, the localization pattern of Hof1 in the cell cycle suggests that it might have another function. We found that Hof1 is involved in the regulation of other proteins also found at the mother side of the bud neck around G2/M and at the bud neck during cytokinesis, Chs3 and Chs4. Surprisingly, we found that the F-BAR domain of Hof1 can bind to Chs4, another protein (Figure 2.3). This was unexpected as F-BAR domains have only been shown to bind lipid membranes (Itoh et al., 2005; Tsujita et al., 2006). While there are no other F-BAR domain protein binding partners as far as we know, there are a few examples of BAR domain protein binding partners (Tarricone et al., 2001; Inoue et al., 2008; Zhu et al., 2007). It will be interesting to see if other F-BAR domains in yeast and mammalian cells have protein binding partners as well.

Hof1 can bind to Chs4 and appears to have an effect on the regulation of chitin synthesis. Chs3 and Chs4 are both required for the deposition of a ring of chitin at the base of the bud neck as the yeast cell divides (see Introduction). They are secreted independently to the incipient bud site and are maintained on the mother side of the bud neck as the bud grows. Chs3 is maintained through a process of endocytosis and polarized delivery. An unknown process occurs in G2/M to shift the 'balance' of endocytosis/exocytosis towards the endocytic removal of Chs3 and Chs4 (the latter also presumably by endocytosis) from the bud neck. Hof1, which first appears at the bud neck at this time, appears to be involved in that process. In *hof1Δ* cells, Chs3 is localized at the bud neck for longer than in wt cells (Figure 2.5) and there is a concomitant increase in cellular chitin levels (Figure 2.4).

One pathway by which Hof1 could be involved in the removal of Chs3 and Chs4 from the bud neck is to mediate endocytosis by acting as a direct linker between the chitin synthase III components and endocytic machinery (Figure 2.6). The SH3 domain of Hof1 has been published to interact directly with the Wiskott-Aldrich syndrome protein (WASP)-interacting protein (WIP) homolog in budding yeast, verprolin (Vrp1) (Naqvi et al., 2001; Ren et al., 2005). Vrp1 has also been found to interact with actin, the WASP homolog, Las17, and the type I myosins, Myo3 and

Myo5 (Vaduva et al., 1997; Naqvi et al., 1998; Anderson et al., 1998; Evangelista et al., 2000). These proteins are involved in actin filament assembly through activation of the yeast Arp2/3

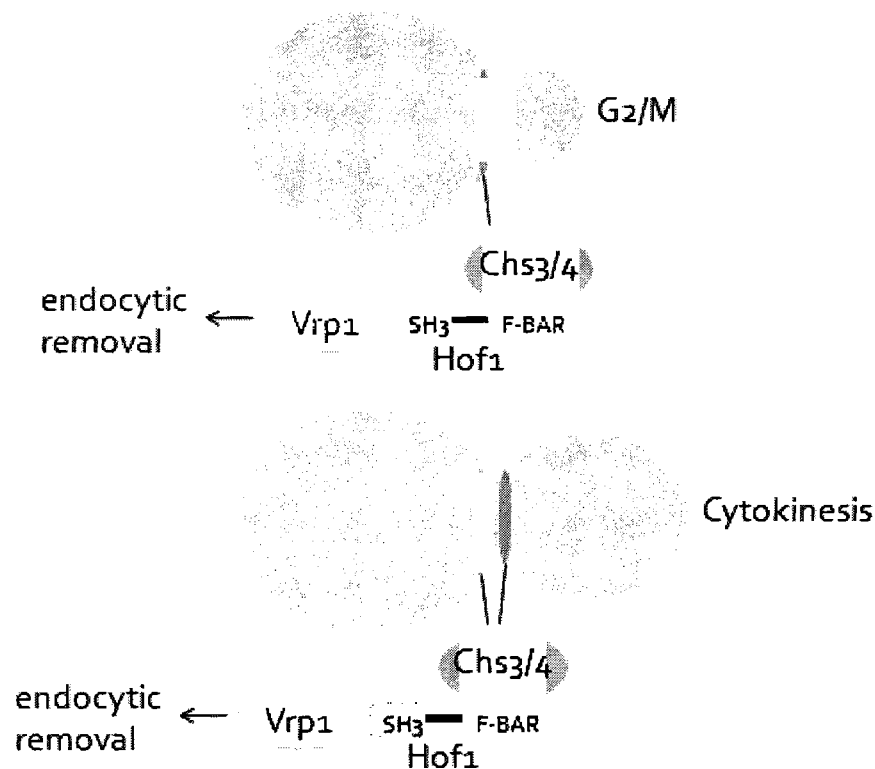


Figure 2.6 Model: Hof1 is a direct linker between chitin synthase III and endocytic machinery

complex and localize in cortical actin patches that are found at the bud neck during the cell division process and are the sites of endocytosis (Moseley and Goode, 2006). We propose that Hof1 acts as a direct linker between the endocytic machinery and chitin synthase III removal via its SH3 mediated interaction with Vrp1 and its F-BAR mediated interaction with Chs4. The removal of Chs3 and Chs4 probably occurs via different vesicles but if Hof1 facilitates the removal of Chs4, Chs3 has been shown to no longer be able to stay localized at the bud neck without Chs4 present (Reyes et al., 2007). More experiments are needed to test this model.

There is also the possibility that the binding of Hof1 to Chs4 can interfere with the latter protein's ability to activate chitin synthase III activity, possibly by interfering with the binding of

Chs3 and Chs4. This is probably in addition to a role of Hof1 in the removal of Chs4 from the bud neck as we have shown that Chs3 localizes to the bud neck for longer in *hof1Δ* cells than in wt cells (Figure 2.5).

Another possible way that Hof1 could be involved in reducing the levels of Chs3 and Chs4 at the bud neck is by interfering with their exocytic delivery to the bud neck. One way Chs3 and Chs4 could be delivered to the bud neck is along formin nucleated actin cables. Bnr1 localizes to the bud neck in small and medium budded cells and Bni1 is localized at the bud tip at the similar stages. At the start of cytokinesis, Bnr1 disappears from the bud neck and Bni1 localizes to the bud neck (Kamei et al., 1998; Pruyne et al., 2004). Each nucleates actin cables directed to the bud neck of the mother cell and bud tip of the daughter cell. A direct interaction between the SH3 domain of Hof1 and the FH1 domain of Bnr1 has been reported and it is possible this interaction interferes with Bnr1's actin cable nucleating ability (Kamei et al., 1998; Pruyne et al., 2002), thereby decrease the targeting of Chs3 to the bud neck. It is possible that this decrease in Chs3 and Chs4 delivery occurs in combination with an increase in their endocytic removal.

Chs3 and Chs4 also localize to the bud neck late in the cell cycle. For Chs4 at least, this later localization occurs through a Bni4-independent mechanism (Kozubowski et al., 2003). This late localization of Chs4 gives credence to the theory that the synthesis of chitin by chitin synthase III is necessary for the function of the remedial septa in *chs2Δ* cells (Schmidt et al, 2002). The BiFC results in Figure 2.3 suggest that Hof1 and Chs4 interact late in the cell cycle during cytokinesis. Therefore, it appears that Hof1 is involved in the process of Chs3 and Chs4 removal at this point in the cell cycle as well. The mechanism of Hof1 involvement in the disappearance of Chs3 and Chs4 localization during cytokinesis and G2/M will require further investigation.

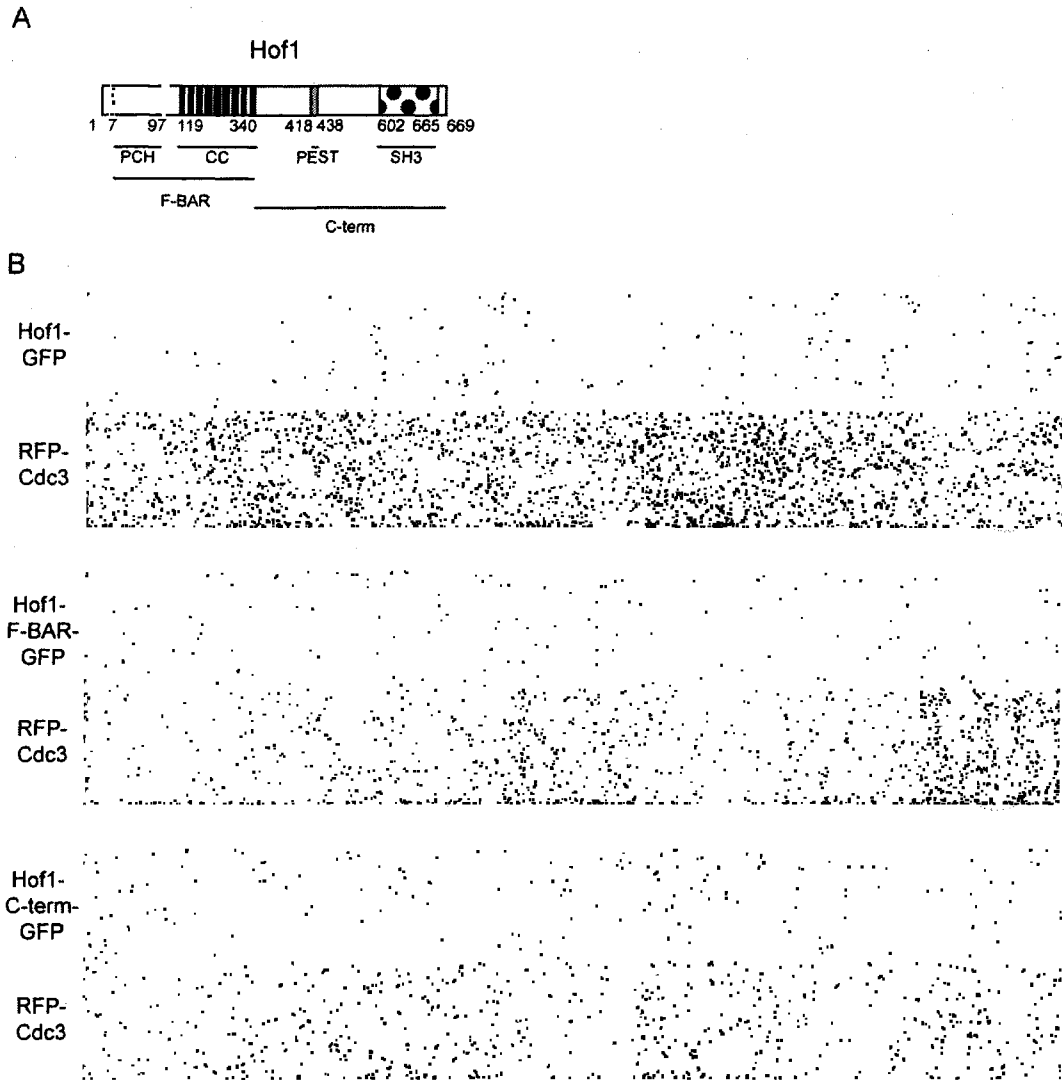


Figure 2.1 Distinct localization pattern of the F-BAR domain and C-terminus of Hof1 in the cell cycle. (A) Putative domains of Hof1. (B) Hof1-F-BAR-GFP localizes to the bud neck throughout the cell cycle while Hof1-C-term-GFP localizes only during telophase. Strains with integrated Cdc3-mcherry RFP and plasmids containing GFP-tagged Hof1 truncations (YEF5479, YEF5421, YEF5423) were grown to early log phase in SC-leu media at 23°C and examined by timelapse microscopy on a spinning disk confocal microscope. Times are from the start of filming and vary by sample. Time-lapse series shown is typical of all those examined, N=18 (Hof1-GFP), N=10 (Hof1-F-BAR-GFP), N=16 (Hof1-C-term-GFP). (Data from JHS)

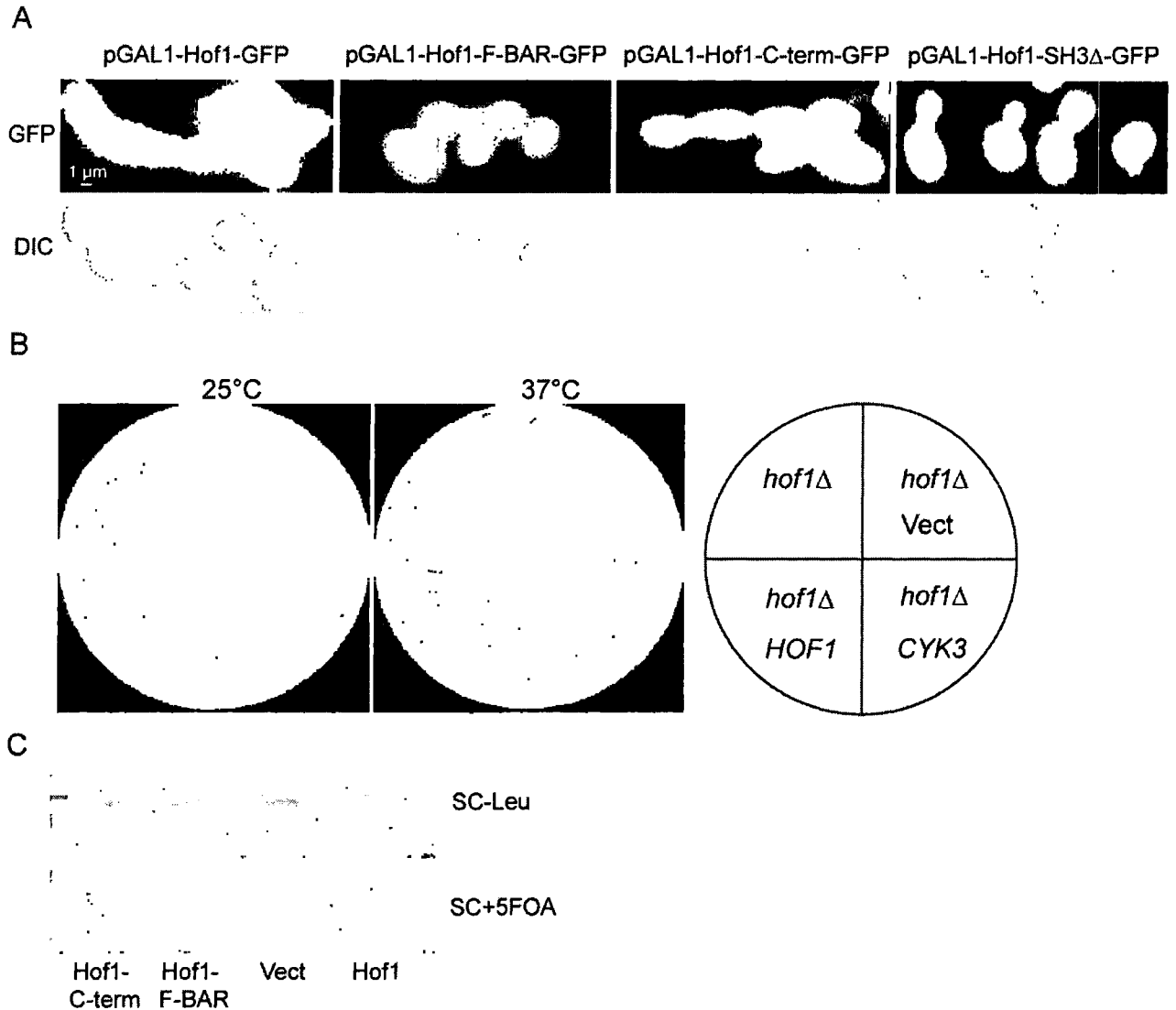


Figure 2.2 The C-terminus of Hof1 is important for cytokinesis. (A) Over-expression of Hof1-GFP and Hof1-C-term-GFP, but not Hof1-F-BAR-GFP, causes a cytokinesis defect. Strains containing GFP-tagged Hof1 FL and truncations under the control of the GAL promoter (YEF4915, YEF4916, YEF4917, YEF4918) were grown overnight in SC-leu media and then grown for about 4 hours in SC-leu +2%Gal +1%Raff and examined using fluorescent microscopy. (B) A single-copy plasmid with CYK3 can suppress the *hof1Δ* temperature sensitive growth defect. *hof1Δ* cells containing HOF1 and CYK3 plasmids were streaked on YPD plates and grown at 25°C and 37°C for two days. (C) The C-terminus of Hof1, but not the F-BAR domain,

can suppress the *hof1*Δ *cyk3*Δ synthetic lethal interaction. Strains YEFYEF4966, YEF4945, YEF4949, YEF4970 containing plasmids with Hof1-FL and truncations along with pRS316-HOF1 were patched on SC-Leu, replica plated onto SC-His and SC+5FOA (to select against pRS316-HOF1) plates, and incubated at 25°C for 2 day to assess the functionality of the *HOF1* fragments.

(Data from JHS)

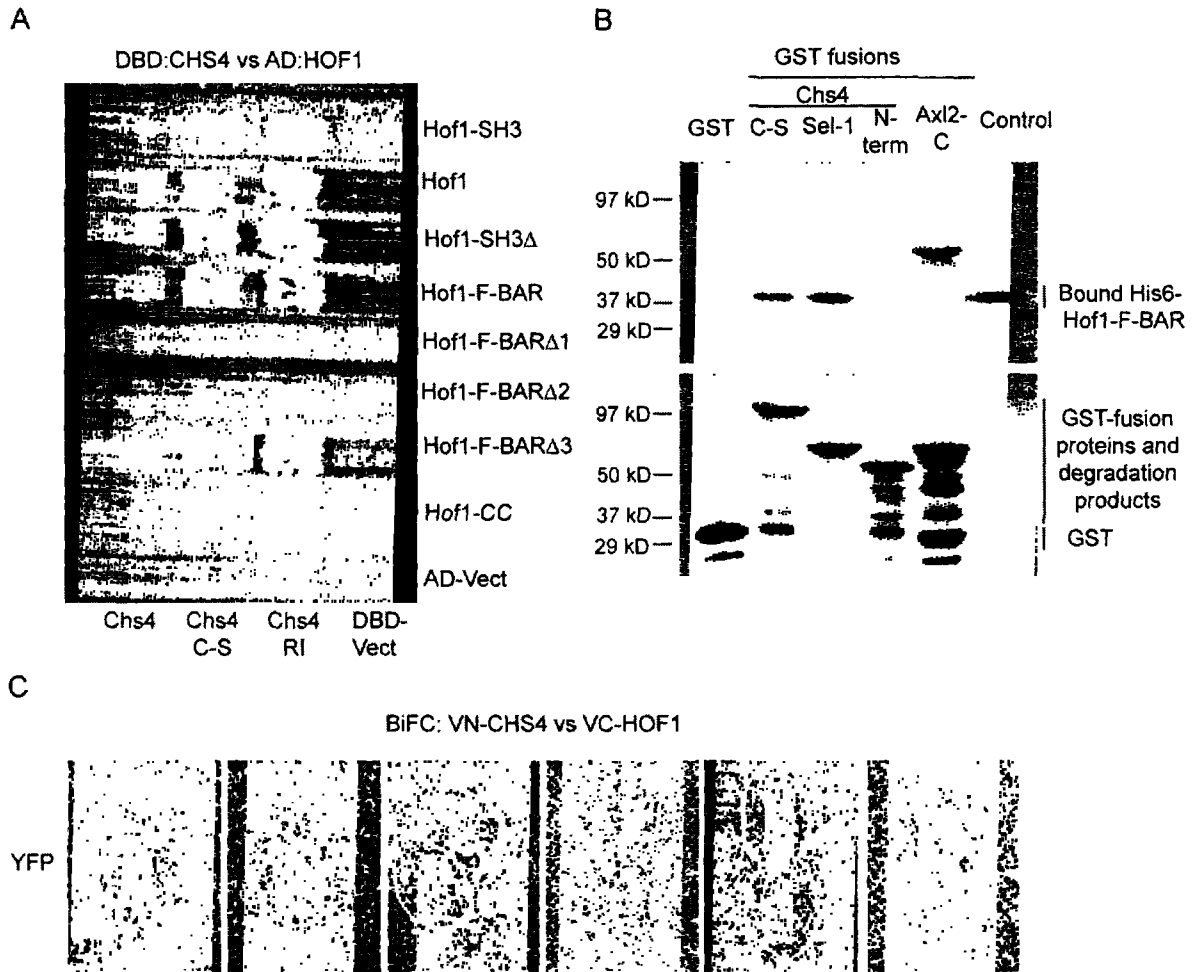
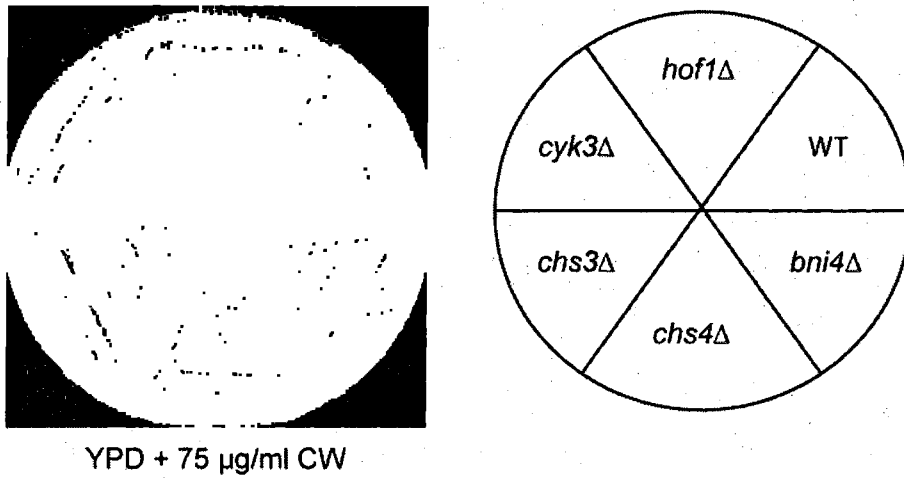


Figure 2.3 The interaction of Hof1 and Chs4 *in vitro* and in cells. (A) The F-BAR domain of Hof1 interacts with Chs4 by yeast two-hybrid analysis. Various Hof1 fragments were tested pairwise for interaction with Chs4-FL, and two Chs4 constructs with a mutated (Chs4 C-S) or missing (Chs4 RI) CAAX box. Hof1-FBARΔ1 contains amino acids 80-340, Hof1-FBARΔ2 contains amino acids 55-340, and Hof1-FBARΔ3 contains amino acids 30-340. (B) *in vitro* binding of Hof1-FBAR to Chs4-Sel-1 repeats. Purified GST-Chs4 fragments including Sel-1 repeats (220-610 aa) and His6-Hof1-FBAR were tested for binding *in vitro* as described in Materials and Methods. (C) Hof1 and Chs4 interact in yeast cells using BiFC. Strains YEF5529 and YEF5533 were mated on a YPD plate, selected on a SC-Trp-His plate, and grown to early log phase in YM-1 media before analysis on the spinning disk confocal microscope. (Data from JHS)

A



B

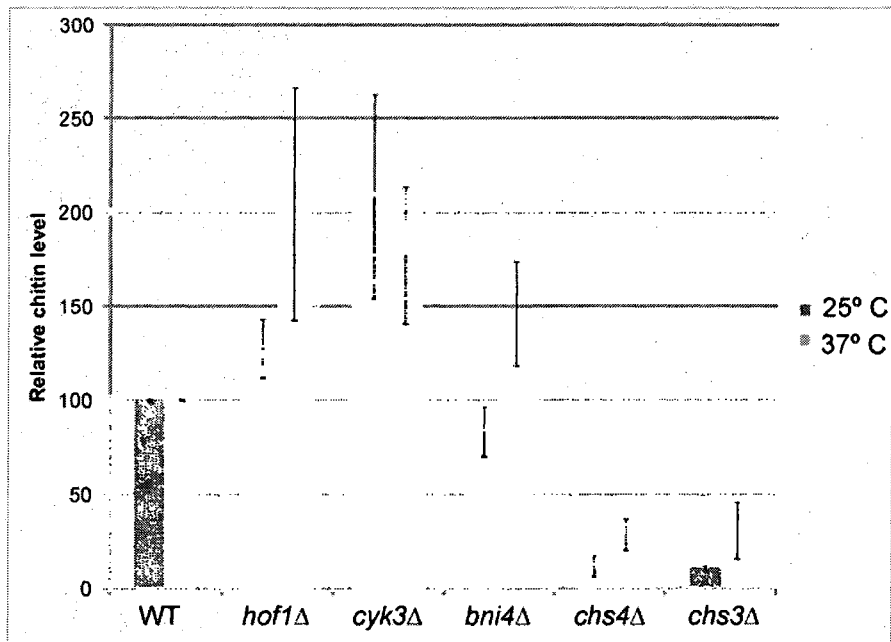


Figure 2.4 **Higher chitin levels in *hof1Δ* cells.** (A) *hof1Δ* cells are sensitive to calcafluor white (CW). YEF473A (wildtype), YEF4600 (*hof1Δ*), YEF2368 (*cyk3Δ*), YEF4633 (*bnr1Δ*), YEF4559 (*chs3Δ*), YEF2197 (*chs4Δ*), and YEF2769 (*bni4Δ*) were streaked out on a YPD plate with 75 ug/mL CW and grown at 25°C for 2 days. (B) *hof1Δ* cells have higher levels of chitin. Data are averages of 7 different experiments. (Data from JHS)

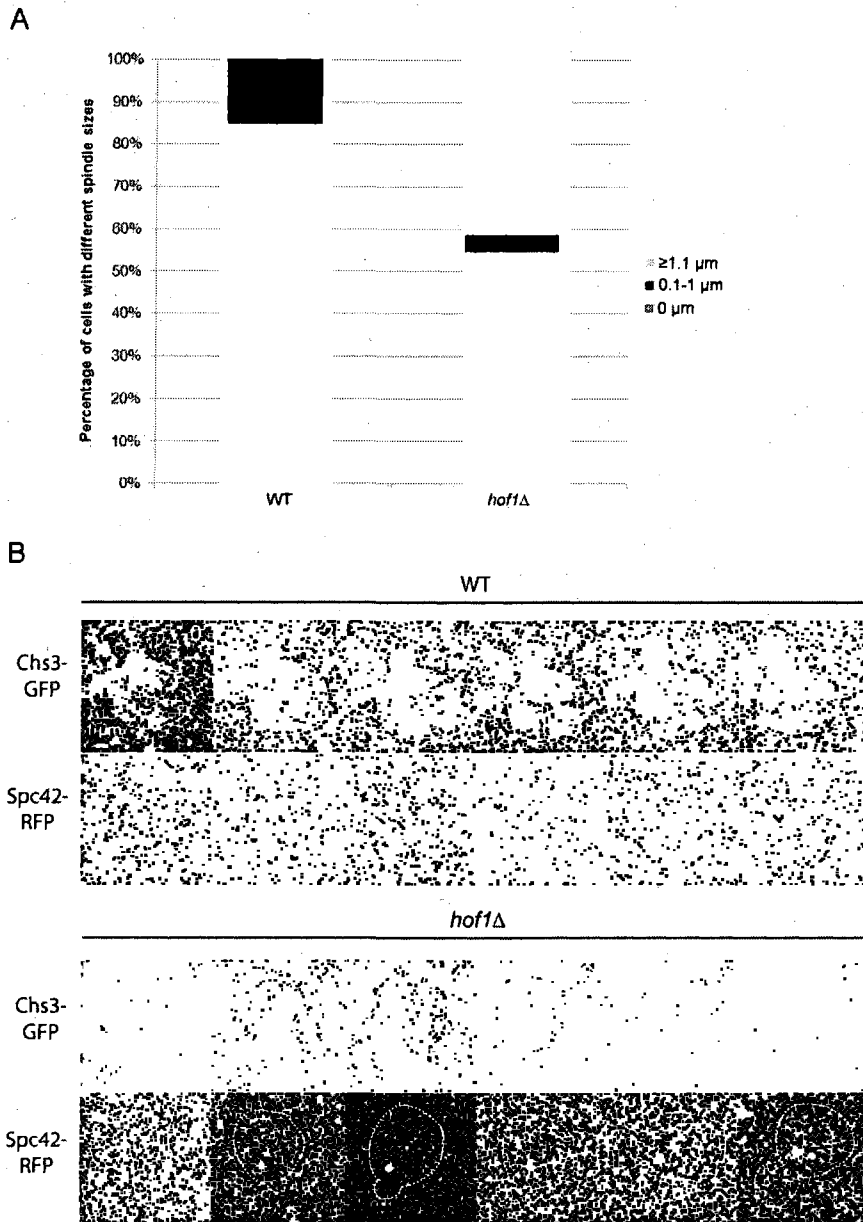


Figure 2.5 Chs3 localization in wild-type and *hof1Δ* cells. (A) Chs3-GFP localizes to the bud neck for longer in *hof1Δ* cells than in wild-type cells. Strains YEF5469 and YEF5454 were grown to early log phase at 23°C in YM-1 media and small budded cells with Chs3-GFP localization were examined in 11 Z-steps using spinning disk confocal microscopy. The distance between spindle pole bodies was measured in 3D using Volocity (wt= 33 cells analyzed, *hof1Δ*= 53 cells analyzed). (B) One representative time-lapse series from (A) for each wt and *hof1Δ* cells. Times are from the start of filming and vary by sample. (Data from JHS)

CHAPTER III

HOF1 IS INVOLVED IN COUPLING ACTOMYOSIN RING CONTRACTION TO SEPTUM FORMATION

Modified from **Nishihama, R., Schreiter, J. H., Onishi, M., Vallen, E. A., Hanna, J., Moravcevic, K., Lippincott, M. F., Han, H., Lemmon, M. A., Pringle, J. R., Bi, E.** (2009) Role of Inn1 and its interactions with Hof1 and Cyk3 in promoting cleavage-furrow and septum formation during cytokinesis in yeast (in submission)

Introduction

Cytokinesis in animal and fungal cells involves actomyosin-ring (AMR) contraction and targeted plasma-membrane and ECM rearrangements, which appear to be interdependent processes (Balasubramanian et al., 2004; Strickland and Burgess, 2004). Many components of the AMR and many proteins involved in targeted membrane trafficking have been identified, most of which are conserved from yeast to humans (Balasubramanian et al., 2004; Echard et al., 2004; Skop et al., 2004). Key questions at present are how these components interact to form the contractile and cortex-remodeling "machines" that drive cytokinesis, and how these machines, which operate with high efficiency and fidelity, are coordinated in space and time at the molecular level.

Targeted membrane trafficking presumably increases membrane surface area in the cleavage furrow and also delivers specific molecules that are required for cytokinesis. Although the precise nature of these molecules may differ in different cell types, it seems likely that the general underlying mechanisms are conserved. In the budding yeast *Saccharomyces cerevisiae*, one important function of targeted membrane trafficking is delivery of the chitin synthase Chs2 (Chuang and Schekman, 1996; VerPlank and Li, 2005), which is chiefly responsible for assembly of the primary septum (PS) (Shaw et al., 1991). The PS is a thin chitin-rich layer of cell wall that forms centripetally at the mother-bud neck during AMR contraction; once PS formation is

complete, secondary septa (SS) are laid down on both sides of the PS. Deletion of *MYO1*, which encodes the sole type-II myosin in *S. cerevisiae*, eliminates the AMR but is not lethal in most strain backgrounds. However, *myo1Δ* cells are typically delayed in cytokinesis and/or cell separation (Rodriguez and Paterson, 1990; Bi et al., 1998), and transmission EM has shown that although both PS and SS can form, they are frequently misoriented and/or disorganized in structure (Schmidt et al., 2002; Nishihama et al., 2009). Thus, the AMR and its contraction appear to guide membrane trafficking such that cleavage-furrow and PS formation are properly oriented and organized (Vallen et al., 2000; Bi, 2001). In contrast, deletion of *CHS2* completely blocks PS formation and results in abortive AMR contraction, suggesting that the PS may stabilize the contracting ring or the associated plasma membrane (Bi, 2001; Schmidt et al., 2002; VerPlank and Li, 2005).

The viability of *myo1Δ* cells indicates that AMR-independent mechanisms, presumably involving septum formation, can sustain cytokinesis in yeast (Bi et al., 1998). The proteins Iqg1, Cyk3, Hof1, and Mlc1 appear to play important roles in the AMR-independent pathway. Iqg1 is the sole IQGAP protein in *S. cerevisiae* and is essential for AMR formation (Epp and Chant, 1997; Lippincott and Li, 1998a; Shannon and Li, 1999), but the near-lethality of an *iqg1Δ* mutation can be suppressed by overexpression of Cyk3 without restoration of the AMR (Korinek et al., 2000). In addition, the growth defect of a *myo1Δ* mutant can be suppressed by overexpression of either Iqg1 or Cyk3 (Ko et al., 2007). Cyk3 contains an SH3 domain near its N-terminus and a possible transglutaminase domain near the middle of the protein. Hof1 contains an F-BAR domain (Heath and Insall, 2008) near its N-terminus and an SH3 domain near its C-terminus. Deletion of either *CYK3* or *HOF1* has no effect on AMR assembly, but either deletion causes severe synthetic growth defects in combination with *myo1Δ* (Korinek et al., 2000; Vallen et al., 2000). In addition, *hof1Δ* and *cyk3Δ* are synthetically lethal (or nearly so) with each other. Mlc1 is a light chain both for Myo1 and for the type V myosin Myo2, as well as for Iqg1, whose localization to the neck it appears to mediate (Stevens and Davis, 1998; Boyne et al., 2000; Shannon and Li, 2000; Luo et al., 2004).

Taken together, the observations described above have led to the hypotheses that Hof1 and Cyk3 play distinct roles in septum formation downstream of Iqg1/Mlc1 (Bi, 2001; Luo et al., 2004; Nishihama et al., 2009) and that yeast cells can tolerate either loss of the AMR (*myo1Δ*) or a partial defect in septum formation (*hof1Δ* or *cyk3Δ*), but not both. To identify other genes involved in the AMR-dependent and -independent pathways of cytokinesis, we performed a screen for mutations that are synthetically lethal in combination with a *hof1Δ* mutation. Along with a variety of previously known cytokinesis genes, we identified a previously uncharacterized gene, ORF *YNL152W*, which has also recently been studied (and named *INN1*) by Sanchez-Diaz et al. (2008). We report here our functional analyses of the role of Inn1 in cytokinesis, which suggest that Inn1 interacts with Hof1 and Cyk3 to promote PS formation in coordination with AMR contraction. Our conclusions differ radically from those reached by Sanchez-Diaz et al. (2008).

Materials and methods

Strains, growth conditions, and genetic methods

Yeast strains are described in Appendix 3. Standard culture media and genetic techniques were used (Guthrie and Fink, 1991); where noted, cells were grown in YM-P, a rich, buffered liquid medium (Lillie and Pringle, 1980). To select for the loss of *URA3*-containing plasmids, 1 mg/ml 5-fluoroorotic acid (FOA) (Research Products International, Prospect, IL) was added to media. To depolymerize filamentous actin (Ayscough et al., 1997), latrunculin A (latA) (Wako Chemicals, Richmond, VA) was dissolved in DMSO as a 20 mM stock solution and added to media at a final concentration of 200 μM; an identical concentration of DMSO alone was added to control cultures. Oligonucleotide primers were purchased from Integrated DNA Technologies (Coralville, IA).

Plasmids

Plasmids are listed in Appendix 4 and/or described below. A genomic-DNA library in the low-copy vector YCp50-LEU2 was kindly supplied by F. Spencer and P. Hieter (see Bi and

Pringle, 1996). Plasmid YCp50LEU2-HOF1, carrying full-length *HOF1*, was isolated from this library by complementing the temperature-sensitive growth of a *hof1* Δ strain (YEF1951). Plasmids pTSV30A-HOF1 and pTSV31A-HOF1 were constructed by first subcloning an ~6.3-kb *Bam*HI fragment containing *HOF1* from YCp50LEU2-HOF1 into the *Bam*HI sites of pTSV30A (2 μ , *LEU2*, *ADE3*) and pTSV31A (2 μ , *URA3*, *ADE3*) (M. Tibbetts and J. Pringle, unpublished results); in each case, an ~2.9-kb *Xba*I fragment (one site in the insert DNA and the other in the vector) was then deleted to remove the neighboring gene *ARP9* to avoid possible complications during the synthetic-lethal screen.

Plasmid YCp50LEU2-INN1-17C, carrying the full-length ORF *YNL152W/INN1* and flanking DNA, was isolated from the YCp50-LEU2 library by rescuing the sectoring ability of mutant 5033 from the synthetic-lethal screen (see below). Mutant 5033 showed a temperature-sensitive growth defect even in the presence of the *HOF1* plasmid. To recover the mutant *inn1-5033* allele by gap-repair, mutant 5033 was transformed with a *Pvu*II-digested plasmid (derived in several steps from YCp50LEU2-INN1-17C) in which the *INN1* ORF had been replaced by a *Pvu*II site. After selection for a Leu⁺ phenotype, a plasmid was isolated and shown to confer Ts growth to strain LY1310 in the absence of plasmid pUG36-INN1. Sequencing of this plasmid revealed a single mutation in the *INN1* ORF (see Fig. 3.11).

To generate plasmid pUG34mCherry, the *mCherry* red fluorescent protein (RFP) ORF without its stop codon was PCR-amplified from pKT355 (or pFA6a-link-mCherry-His3MX6), provided by K. Thorn (University of California, San Francisco) and gap-repaired into *Xba*I-digested pUG34 (provided by J. Hedgemann, Heinrich-Heine-Universität, Düsseldorf) to replace the *yEGFP* allele in pUG34 (confirmed by sequencing). Plasmids pUG36-INN1 and pUG34mCherry-INN1 were constructed by gap-repairing the PCR-amplified *INN1* ORF into *Eco*RI-digested pUG36 (J. Hedgemann) or pUG34mCherry, generating N-terminally tagged *GFP-INN1* and *RFP-INN1* fusions that are under *MET25*-promoter control. pUG34mCherry-INN1-C2 and pUG34mCherry-INN1-Tail were made similarly and contain *INN1* codons 1-140 and 130-409, respectively. pUG34mCherry-INN1 was subjected to site-directed

mutagenesis using the QuickChange Site-directed Mutagenesis Kit (Stratagene, La Jolla, CA) to generate plasmids containing PXXP-motif mutations (*m1* to *m4*, either individually or in different combinations; see Results and Fig. 3.11).

To generate plasmid pRS315GW-C2-HOF1, the *HOF1* gene (-1000 to +2510 bp relative to the start codon) was amplified by PCR from yeast genomic DNA and cloned into the pCR8/GW/TOPO vector (Invitrogen, Carlsbad, CA). A *NotI* site was introduced at the position immediately downstream of the *HOF1* start codon by site-directed mutagenesis using the QuickChange Site-directed Mutagenesis Kit (Stratagene), creating plasmid pCR8/GW-*NotI*-*HOF1*. A DNA fragment encoding the putative C2 domain of Inn1 (amino acids 1-134), flanked by two *NotI* sites, was amplified by PCR, digested with *NotI*, and cloned into the *NotI* site of pCR8/GW-*NotI*-*HOF1*. The resulting plasmid was subjected to Gateway recombination (Invitrogen) into pRS315-attR (unpublished data), yielding pRS315GW-C2-HOF1.

The parent vectors for two-hybrid analyses were the DNA-binding-domain (DBD) plasmid pEG202 (2 μ , *HIS3*) and the activation-domain (AD) plasmid pJG4-5 (2 μ , *TRP1*) (Gyuris et al., 1993). pEG202-HOF1-SH3 (residues 576-669) was supplied by C. Boone (University of Toronto, Canada). Other two-hybrid plasmids were constructed by PCR-amplifying and cloning full-length *INN1*, *HOF1*, and *CYK3*, and fragments of these genes (see Figs. 3.4 and 3.5), into plasmids pEG202 and pJG4-5. In addition, pJG4-5-INN1-Tail (residues 131-409) was subjected to site-directed mutagenesis to generate plasmids containing PXXP-motif mutations (see Fig 3.11). The structures of these plasmids were confirmed by sequencing.

Plasmids for lipid-binding and *in vitro* protein-interaction assays were constructed as follows. DNA fragments encoding Inn1 amino acids 1-134 and Tcb1 amino acids 979-1186 (the third C2 domain in Tcb1) were PCR-amplified, digested with *Bam*HI and *Xho*I (sites included in the primers), and cloned into *Bam*HI/*Xho*I-digested pGStag3vM (Narayan and Lemmon, 2006) to create plasmids encoding GST-fusion proteins. DNA fragments encoding *HOF1* amino acids 341-669 and *CYK3* amino acids 1-70 were PCR-amplified, digested with *Bam*HI and *Sal*I (sites included in the primers), and cloned into *Bam*HI/*Sal*I-digested pCOLADuet-1 (EMD Biosciences,

Darmstadt, Germany) to create plasmids encoding His₆-tagged proteins. An ~840-bp *Bam*HI-*Xho*I fragment encoding the wild-type or PXXP-mutant derivatives of *INN1* amino acids 131-409 was subcloned from wild-type or mutant pJG4-5-INN1-Tail into the corresponding sites of pGEX-5X-1 (GE Healthcare, Buckinghamshire, UK) to create plasmids encoding GST-fusion proteins.

Identification of synthetic-lethal mutations

To screen for mutations synthetically lethal with *hof1*Δ, we used a *hof1*Δ *ade2* *ade3* *leu2* *ura3* strain harboring a high-copy *HOF1 ADE3 URA3* plasmid (strain LY1067). After mutagenesis with EMS to ~50% viability, cells were grown overnight at 23°C to allow the expression of mutant phenotypes, plated, and screened for an inability to lose the *HOF1* plasmid. Colonies lacking white sectors (indicating an inability to lose *ADE3*) were screened for sensitivity to FOA (indicating an inability to lose *URA3*) and then for recovery of growth on FOA after transformation with a *HOF1 LEU2* plasmid (YCp50LEU2-HOF1), but not with a similar plasmid lacking *HOF1*, indicating that growth depended on *HOF1* and not on some other feature of the plasmid.

To identify the genes defined by the synthetic-lethal mutations, each mutant was crossed to strain LY1065, and appropriate segregants were then mated and tested for complementation as judged by the ability to grow without plasmid-borne *HOF1*. Similar tests asked if the new mutations could complement mutations in genes previously known to be synthetically lethal with *hof1*Δ. We also tested for the ability of low-copy plasmids carrying known cytokinesis genes to rescue the mutants and/or analyzed the genes on plasmids obtained by rescuing the mutants using a YCp50LEU2-based genomic library (Bi and Pringle, 1996). Taken together, these tests showed that the mutations fell into 13-18 genes (see Results and Table 1).

Light and electron microscopy

The differential-interference-contrast (DIC) and fluorescence-microscopy images in Figs. 3.1B, D, and E; 3.2C; 3.5F; 3.6C and D; and 3.12 were acquired and processed using a

computer-controlled Eclipse 800 microscope (Nikon, Tokyo, Japan), a 60 X Plan Apo objective, a high-resolution CCD camera (model C4742-95; Hamamatsu Photonics, Bridgewater, NJ), Image-Pro Plus software (Media Cybernetics, Silver Spring, MD), and Photoshop CS3 (Adobe Systems, San Jose, CA). Time-lapse microscopy was performed as described by Vallen et al. (2000). Actin rings and DNA were stained with Alexa 568-phalloidin (Molecular Probes, Eugene, OR) and bis-benzimide (Sigma, St. Louis, MO) as described by Bi et al. (1998).

The images in Fig. 3.7A were acquired using IPLab software (BD Biosciences, Rockville MD) and a spinning-disk confocal-microscope system comprising a Yokogawa CSU 10 scanner, an Olympus IX 71 microscope, a Plan S-Apo 100X/1.4 NA oil immersion objective, and a Hamamatsu Photonics Imagem back-thinned EMCCD camera (C9100-13); components were integrated by BioVision Technologies (Exton, PA). Diode lasers for excitation (488 nm for GFP; 561 nm for RFP) were housed in a launch constructed by Spectral Applied Research.

Other DIC and fluorescence images were acquired using a Nikon Eclipse 600-FN microscope, an Apo 100X/1.40 NA oil-immersion objective, an ORCA-2 cooled CCD camera (Hamamatsu Photonics), and MetaMorph version 5.0 or 7.0 software (Molecular Devices, Downingtown, PA). Image contrast was enhanced using the MetaMorph and/or Photoshop software. GFP signal was observed using a triple-band filter set except in experiments involving GFP/CFP double staining, in which YFP and CFP filter sets were used. To assess the asymmetry of Inn1 localization, DIC and Cdc3-CFP images were captured in the mid-cell focal plane, and a Z series of 11 steps (0.2 μm) was captured for Inn1-GFP. The maximum-projection images created from the Z stacks using MetaMorph were analyzed for the Inn1 distribution patterns. Time-lapse microscopy was performed essentially as described by Salmon *et al.* (1998). To determine cluster indices [number of clusters with ≥ 3 connected cell bodies divided by this number plus the numbers of unbudded (one cell body) and budded (two cell bodies) cells], 400 cells + clusters were scored for strain LY1310 transformed with either pRS425 or pRS425-CYK3, cured of plasmid pUG36-INN1 by growth on SC-Leu+FOA medium, and grown to exponential phase in SC-Leu medium.

For EM, cells were fixed with glutaraldehyde and potassium permanganate, embedded in LR White resin, and stained with uranyl acetate and lead citrate, as described in detail elsewhere (Nishihama *et al.*, 2009). Images were obtained and processed using a JEOL (Tokyo, Japan) JEM1230 electron microscope, a Gatan (Pleasanton, CA) Model 967 cooled CCD camera, and DigitalMicrograph software (Gatan) and Photoshop.

Lipid-binding assays

The lipid-overlay and surface-plasmon-resonance (SPR) assays were performed as described by Narayan and Lemmon (2006).

Co-immunoprecipitation and phosphatase treatment

Samples of cells from a synchronized culture (see Fig. 3.4) were collected by centrifugation and frozen immediately in liquid nitrogen. Protein extracts were prepared using glass beads in NP-40 buffer (6 mM Na₂HPO₄, 4 mM NaH₂PO₄, 1% NONIDET P-40, 150 mM NaCl, 2 mM EDTA) supplemented with 1 mM DTT, 50 mM NaF, 0.1 mM Na₃VO₄, and a complete protease inhibitor cocktail (Roche Applied Science, Mannheim, Germany) and centrifuged at 2000 X g for 10 min. To precipitate Hof1-TAP, 15 mg of each extract were incubated with 15 µl Dynabeads® pan-mouse IgG (Invitrogen; Cat. No. 110.41) for 1 h at 4°C, washed three times with NP-40 buffer, and eluted with SDS sample buffer. Samples were analyzed by SDS-PAGE (7.5% gel) and Western blotting using a mouse anti-GFP antibody (Roche; Cat. No. 11814460007) and an HRP-conjugated rabbit anti-mouse antibody (ICN Pharmaceuticals, Bryan, OH; Cat. No. 55564) to detect Inn1-GFP and peroxidase anti-peroxidase soluble complex (Sigma; Cat. No. P1291) to detect Hof1-TAP.

For the phosphatase-treatment experiment, 10 mg of protein extract (prepared as described above) was incubated for 1 h at 4°C with 4 µg of a mouse anti-GFP antibody (Roche) bound to 40 µl of protein G sepharose. The beads were washed three times with NP-40 buffer and separated into four aliquots. As a control, SDS sample buffer was added to one aliquot. The

other aliquots were washed twice with lambda protein-phosphatase buffer (New England Biolabs, Ipswich, MA) and incubated for 30 min at 30°C in 30 µl of the same buffer with or without lambda protein phosphatase (New England Biolabs) and phosphatase inhibitors (50 mM NaF and 1 mM Na₃VO₄). Reactions were terminated by adding 10 µl of 4X SDS sample buffer, and samples were analyzed by SDS-PAGE and Western blotting using anti-GFP and HRP-conjugated antibodies (see above).

Two-hybrid interactions

Strain Y1026 carrying various DBD plasmids (see above) was mated to strain Y860 carrying various AD plasmids. Diploids were selected on SC-His-Trp plates, replica-plated to SC-His-Trp-Ade plates containing 1% raffinose plus 2% galactose (to induce production of the fusion proteins), and incubated at 30°C for ≥4 days to detect interactions.

In vitro protein-binding assays

To purify His₆-tagged proteins, *E. coli* strain BL21 (Invitrogen) was transformed with pCOLADuet-based plasmids (see above), grown to exponential phase at 37°C, and induced with 1 mM IPTG for 3 h at 23°C. Cells were washed twice with double-distilled water, frozen at -20°C, thawed in Ni-NTA lysis buffer (300 mM NaCl, 20 mM Tris-HCl, pH 8.0, 20 mM imidazole, 10 mM β-mercaptoethanol, 0.1% NP-40) containing a cocktail of protease inhibitors, sonicated seven times, placed on ice for 30-60 min, and centrifuged at 15,000 rpm for 20 min. The supernatant was mixed with Ni-NTA beads that had been freshly washed with Ni-NTA lysis buffer. After rocking for 1 h at 4°C, the beads were collected by centrifugation, washed three times with Ni-NTA buffer, and eluted five times with elution buffer (PBS containing 5 mM EDTA, 5 mM DTT, and 0.1% NP-40).

To purify GST-tagged proteins, *E. coli* BL21 was transformed with pGEX-5X-based plasmids (see above). Protein extracts were then prepared essentially as described for the His₆-tagged proteins, except that the lysis buffer was PBS containing 5 mM EDTA, 5 mM DTT,

and 0.1% NP-40. The 15,000-rpm supernatant was mixed with pre-washed glutathione beads and rocked for 1 h at 4°C. The beads were collected by centrifugation, washed three times with lysis buffer, and resuspended in lysis buffer.

To test for protein binding *in vitro*, ~3 µg of His₆-tagged protein was mixed with ~5-7 µg of GST (as negative control) or GST-tagged protein that was still bound to the glutathione beads (400 ml total volume) and rocked for 1 h at 4°C. The beads were washed five times with the GST-fusion lysis buffer (see above) and resuspended in 50 ml SDS sample buffer, and proteins were analyzed by SDS-PAGE (12% gel) and Western blotting using mouse monoclonal anti-penta-His (Qiagen, Valencia, CA) and anti-GST (Covance, Emeryville, CA) primary antibodies and an HRP-conjugated rabbit anti-mouse-IgG secondary antibody (Jackson ImmunoResearch, West Grove, PA). The anti-His signal was detected using the Millipore Immobilon Western Chemiluminescent HRP Substrate (Billerica, MA), and the blot was incubated with the Restore Blot-stripping Buffer (Pierce, Rockford, IL) for 15 min at 37°C before re-probing with the anti-GST antibody, which was then detected by ECL (GE Healthcare).

Results

Identification of *INN1* and other cytokinesis genes in a screen for mutations synthetically lethal with *hof1*Δ

A *hof1*Δ mutation is not lethal by itself but is lethal in combination with several other mutations affecting cytokinesis proteins (see Introduction). To identify additional cytokinesis proteins, we used a colony-sectoring assay (Bender and Pringle, 1991) to screen systematically for EMS-induced mutations that were synthetically lethal with *hof1*Δ (see Materials and methods). From ~33,000 colonies screened, we found 38 such mutations, which defined at least 13 genes (Table 1), 11 of which encode proteins already known to be involved in cytokinesis. These proteins are in four general groups: septins and proteins that regulate septin function (Cdc12, Gin4, Elm1, and Bni5); proteins involved in the function of the actomyosin contractile ring (Myo1 and Bni1); proteins that appear to regulate both the AMR and some aspect(s) of membrane

and/or cell-wall deposition (*Mlc1* and *Iqg1*); and proteins that regulate septal-cell-wall assembly and/or cell separation (*Chs2*, *Cyk3*, and *Psa1*). The synthetic lethality of *hof1Δ* with mutations in *MYO1*, *BNI1*, *CYK3*, and *BNI5* was known previously. It should be noted that we recovered point mutations in several essential (or nearly essential) genes (*CDC12*, *CHS2*, *MLC1*, *IQG1*, and *PSA1*), which would have been missed in a genome-wide synthetic-genetic-array analysis using the viable deletion strains (Tong et al., 2001).

The twelfth gene identified was *YNL152W/INN1*, uncharacterized at the time but subsequently studied also by Sanchez-Diaz et al. (2008). *INN1* is predicted to encode a protein of 409 amino acids with a possible C2 domain at its N-terminus (Sanchez-Diaz et al., 2008) and multiple PXXP motifs in its C-terminal region (Fig. 3.11). The roles of these domains are discussed below. *Inn1* has unambiguous homologues in a variety of other fungi; homologies outside the fungi are less clear and may be limited to the putative C2 domains.

An essential role of *Inn1* in primary-septum formation

Tetrad analysis of an *INN1/inn1Δ* heterozygous diploid on YPD rich medium suggested that *INN1* is an essential gene (unpublished data; Sanchez-Diaz et al., 2008), but we found that *inn1Δ* cells were viable, although slow growing, when streaked on synthetic minimal medium (Fig. 3.1A). Similar effects of growth medium on yeast mutant phenotypes have been seen with other genes (Bulawa and Osmond, 1990; Abelovska et al., 2007; unpublished data). The *inn1Δ* cells formed extensive cell clusters with abnormal-looking septal regions (Fig. 3.1B, left); decoration of the plasma membrane with GFP-Ras2 (Fig. 3.1B, right) revealed that cytokinesis (cytoplasmic separation) was complete in some of these septal regions (neck 1) but not in others (neck 2). These data suggest that *Inn1* plays a role in membrane invagination, septum synthesis, and/or cell separation.

To explore these possibilities, we used TEM. In wild-type cells, a thin, chitinous PS forms first and then is sandwiched by layers of SS (see Introduction; Fig. 3.1C, left). In contrast, in 50 *inn1Δ* cells scored, no sign of a PS could be seen; instead, the necks filled with SS-like material

(Fig. 3.1C, right). Similar results were obtained when temperature-sensitive *inn1* mutants (created by PCR mutagenesis) were incubated at restrictive temperature (unpublished data). Because digestion of the PS normally leads to cell separation (Yeong, 2005), the absence of the PS in *inn1* mutant cells presumably accounts for the delay in cell separation and resultant formation of cell clusters.

The lack of PS formation might mean that Inn1 is required for recruitment to the mother-bud neck of Chs2, the catalytic subunit of chitin synthase II (Shaw et al., 1991). However, as shown in Fig. 3.1D, the localization of GFP-tagged Chs2 to the vicinity of the neck was similar to that seen in wild type (Chuang and Schekman, 1996; VerPlank and Li, 2005; Zhang et al., 2006). This finding argues that Inn1 controls PS formation by controlling the activation and/or precise localization of Chs2, rather than simply its recruitment to the neck region.

Assembly and contraction of the AMR occurred in *inn1* Δ cells. However, the actin rings were generally less tight and stained more faintly than those in wild-type cells (Fig. 3.12), and the Myo1-GFP rings invariably (n = 7) appeared to detach from part of the plasma membrane within 3-4 min following the initiation of contraction, resulting in an asymmetrically localized dot at on one side of the neck (Fig. 3.1E), in contrast to the symmetrical ring contraction seen in wild-type cells, which takes 6-8 min under the same experimental conditions (Bi et al., 1998; Vallen et al., 2000). This behavior is similar to that of the AMR in *chs2* Δ cells (Bi, 2001; Schmidt et al., 2002; VerPlank and Li, 2005), consistent with the hypothesis that Inn1 plays an essential role in PS formation.

MEN-dependent, AMR-independent localization of Inn1 to the division site

Analysis of Inn1 levels using α -factor-synchronized cells expressing HA-tagged Inn1 indicated that Inn1 is present at an approximately constant level throughout the cell cycle (unpublished data). However, time-lapse analysis showed that Inn1-GFP did not localize to the neck until the septin hourglass split into two cortical rings (Fig. 3.2A), an event that is under the control of the mitotic-exit network (MEN) (Lippincott et al., 2001). Once a ring of Inn1-GFP was

visible at the neck, it began to contract almost immediately. The contraction from a full-sized ring to a dot took ~8 min ($n = 9$), as did the centripetal synthesis of the septum (Fig. 3.2A, DIC images). Immediately after contraction, Inn1-GFP disappeared from the neck, and cell separation occurred 12-14 min later.

These data suggest that the localization of Inn1 is regulated post-translationally and might occur in response to activation of the MEN, in which a Polo kinase (Cdc5) and a GTPase-controlled kinase cascade (Cdc15, Dbf2, and Dbf20) lead to activation of the protein phosphatase Cdc14 (Stegmeier and Amon, 2004). The MEN controls mitotic exit by down-regulating CDK/mitotic cyclins and cytokinesis in a largely independent manner whose mechanisms remain obscure (Balasubramanian et al., 2004). The MEN is not required for assembly of the AMR but is required for its contraction as well as for septum formation (Vallen et al., 2000; Lippincott et al., 2001; Hwa Lim et al., 2003). To ask if Inn1 localization depends on the MEN, we examined various temperature-sensitive mutants. As expected, Inn1-GFP localized to the neck in large-budded cells of all MEN mutants at permissive temperature (Fig. 3.3A, top), although the percentage of cells in which localized Inn1-GFP could be seen was decreased in comparison to wild-type cells (Fig. 3.3B). In contrast, at restrictive temperature, Inn1-GFP failed to accumulate at the necks of large-budded cells in all MEN mutants (Fig. 3.3A, bottom; Fig. 3.3B), suggesting that Inn1 localization to the bud neck is directly or indirectly regulated by the MEN.

The "contractile" behavior of the Inn1-GFP ring was almost identical to that of the Myo1-GFP (Bi et al., 1998) and Iqg1-GFP (Shannon and Li, 1999) rings, suggesting that Inn1 might be associated with the AMR. Indeed, Sanchez-Diaz et al. (2008) reported that Inn1 failed to localize in either Myo1- or Iqg1-depleted cells. In contrast, we observed that Inn1-GFP localized to the neck at the normal time in *myo1* Δ cells (Fig. 3.2B; Table 2). However, the appearance and behavior of the Inn1-GFP signal were abnormal: it usually appeared either as a faint band that never displayed a clear contraction (in 10 of the 19 cells observed by time-lapse analysis: Fig. 3.2B, top) or as one or two relatively bright dots that moved asymmetrically across

the bud neck (in the other 9 cells: Fig. 3.2B, bottom). Similarly, in random fields of cells, 16% of *myo1D* cells with split septin rings displayed an asymmetric line or dot of Inn1-GFP at the neck, whereas this was rarely seen in control cells (Table 2). This behavior might reflect the asymmetric PS formation that occurs in some *myo1D* cells (unpublished data). We also observed Inn1-GFP localization to the neck in *iqg1Δ* cells (Fig. 3.2C), although the signal was generally weaker than in wild type. Taken together, our results indicate that the normal contraction of the Inn1 ring depends on the AMR, but the initial localization of Inn1 does not. This suggests that Inn1 is not a true component of the AMR but rather part of a functional complex that associates and cooperates with it.

Inn1-Hof1 interaction and its role in the symmetric localization of Inn1 at the neck

The C-terminal region of Inn1 contains eight PXXP motifs, which represent generic binding sites for SH3 domains (Feller et al., 1994). Hof1 contains an SH3 domain (see Fig. 3.4C), and genome-wide screens for SH3-domain ligands have suggested that it might interact with Inn1 (Ito et al., 2001; Tong et al., 2002). Inn1 was also one of the Hof1-binding proteins identified by mass spectrometry (unpublished data). To determine whether and when Inn1 interacts with Hof1 during the cell cycle, we used a co-immunoprecipitation assay. We observed that Inn1 interacted strongly with Hof1 throughout the 90 min following release from an MEN block (Fig. 3.4A), suggesting that Inn1 forms a tight complex with Hof1 before, during, and after cytokinesis.

Like Hof1 (Fig. 3.4A; Vallen et al., 2000; Blondel et al., 2005; Corbett et al., 2006), Inn1 also undergoes cell cycle-regulated modification, as indicated by the multiple retarded forms of Inn1 in SDS-PAGE analysis (Fig. 3.4A). The modified forms of Inn1 apparently result from phosphorylation, as phosphatase treatment reduced all high-molecular-weight forms of Inn1 to a single band (Fig. 3.4B). The modified forms of both Inn1 and Hof1 first appear at ~40 min after release from the MEN block, which corresponds closely to the time at which PS formation and AMR contraction occur under these conditions, as judged from parallel time-course analyses

(unpublished data).

To define the regions of Inn1 and Hof1 involved in their interaction, we used two-hybrid analysis. As shown in Fig. 3.4C, full-length Hof1 interacted with the Inn1 C-terminus (residues 180-409), but not with the N-terminus (residues 1-180). Any Hof1 fragment lacking the C-terminal SH3 domain failed to interact with any region of Inn1, whereas the isolated Hof1 SH3 domain was sufficient for binding to the Inn1 C-terminus (and also, weakly or perhaps artifactually, to the Inn1 N-terminus) (Fig. 3.4C and unpublished data). When P-to-A mutations (*m1-m4*; Figs. 4C and S1) were introduced into the Inn1 PXXP motifs, mutations *m1-m3*, alone or in combination, had no detectable effect on binding to full-length Hof1, but mutation *m4* dramatically reduced binding, particularly when combined with *m2* or *m3* (Fig. 3.4D). These data suggest that the PKLPPLP motif at Inn1 amino acids 377-383 is primarily responsible for interaction with the Hof1 SH3 domain, although there may also be some interaction with the PIPPLP (amino acids 160-165) and PPLPIP (amino acids 329-325) motifs.

To determine whether Inn1 interacts directly with Hof1, we employed a pull-down assay using the GST-tagged Inn1 C-terminus (wild type or mutant) and His₆-tagged Hof1 C-terminus that were purified after expression in bacteria. His₆-Hof1 bound strongly to both wild-type and *m2*-mutant GST-Inn1 in comparison to the negative control, GST alone (Fig. 3.4E). In contrast, the *m4* mutation nearly eliminated the interaction between Inn1 and Hof1. These results support the conclusion from two-hybrid analysis that Hof1 binds to Inn1 primarily via the Inn1 PKLPPLP motif.

Hof1 localizes to the neck much earlier in the cell cycle than does Inn1 (Vallen et al., 2000), so it seemed possible that Inn1 localization might depend on Hof1. We found that Inn1-GFP localized to the neck with essentially normal timing in *hof1*Δ cells: 44% of cells with split septin rings had detectable signal, compared to 33% in wild type (Fig. 3.4F; Table 2). However, although Inn1-GFP localization was almost always (~95%) symmetric in wild-type cells, it was asymmetric in 39% of the *hof1*Δ cells with detectable signal (Fig. 3.4F; Table 2). Thus, Hof1 appears to be required for the initiation or maintenance of symmetric Inn1 localization at the neck.

Functional and physical interactions between Inn1 and Cyk3

In addition to Hof1, three other proteins important for AMR-independent cytokinesis are Iqg1, Cyk3, and Mlc1 (see Introduction). To explore further the interactions among these proteins, we asked if overexpression of any of them could suppress the growth and cytokinesis defects of an *inn1Δ* strain. We found that Cyk3, but not the other three proteins, could partially suppress the growth (Fig. 3.5A) and cytokinesis defects of *inn1Δ* cells. The cluster index for *inn1Δ* cells (indicative of a cytokinesis and/or cell separation defect; see Materials and methods) was reduced from 67% to 44% by a *CYK3* plasmid. Remarkably, this suppression involved the formation of almost normal-looking PS in many cells (38% of the 50 cells examined; Fig. 3.5B).

We next tested for physical interaction between Inn1 and Cyk3. Yeast two-hybrid analyses and *in vitro* protein-binding assays parallel to those used to characterize the Inn1-Hof1 interaction (see above) indicated that Inn1 and Cyk3 interact directly and that this interaction is mediated by the SH3 domain of Cyk3 and the PIPPLP motif (amino acids 159-165) of Inn1 (Fig. 3.5C-E). Cyk3-GFP could localize to the neck in *inn1Δ* cells (Fig. 3.5F), although its localization was somewhat less well ordered than the tight band observed in wild-type cells (Korinek et al., 2000).

One possible interpretation of these data is that Cyk3 localizes to the neck independently of Inn1 but then is activated by Inn1 for a role in promoting PS formation; on this model, overexpression of Cyk3 would partially bypass the activation requirement. Alternatively, Inn1 and Cyk3 might act in parallel to promote PS formation.

Dependence of Inn1 localization on both Hof1 and the AMR

Inn1 could also localize to the neck in *cyk3Δ* cells, and, unlike *hof1Δ*, *cyk3Δ* did not affect the symmetry of Inn1 localization: as in wild type, nearly all cells with detectable Inn1-GFP signal at the neck showed a symmetric pattern (Fig. 3.6A; Table 2). The fraction of *cyk3Δ* cells with split septin rings that showed localized Inn1-GFP was significantly increased over that in wild type (Table 2), presumably reflecting the increased duration of cytokinesis (accompanied by persistent

Inn1-GFP at the neck) that results from the delayed PS formation in *cyk3Δ* cells (Nishihama et al., 2009). Although Inn1 interacts physically with both Hof1 and Cyk3 (see above), these interactions do not appear sufficient to account for the neck localization of Inn1, because Inn1 could localize to the neck both in *hof1Δ cyk3Δ* cells (Fig. 3.6B; Table 2) and when the PXXP motifs involved in the interactions were mutated (Fig. 3.6C).

Because Inn1-GFP localized weakly and/or asymmetrically to the neck in both AMR-deficient (*myo1Δ* and *iqg1Δ*) and *hof1Δ* mutants (see above), it seemed possible that the AMR and Hof1 might act in concert to localize Inn1 during cytokinesis. Because *myo1Δ* and *hof1Δ* are synthetically lethal (Vallen et al., 2000), we could not examine Inn1 localization in the double mutant. Thus, we instead examined Inn1 localization in wild-type, *hof1Δ*, and *cyk3Δ* cells that had been treated with latrunculin A (latA), which disrupts all F-actin structures including the actin ring (Ayscough et al., 1997). Inn1-GFP localized efficiently to the neck in latA-treated wild-type and *cyk3Δ* cells, but not in latA-treated *hof1Δ* cells (Fig. 3.6D), consistent with the hypothesis that Hof1 and the AMR cooperate in Inn1 localization.

Distinct roles of the C-terminal and N-terminal domains of Inn1 in localization and the activation of PS formation

To further analyze the function of the Inn1 N-terminal and C-terminal regions, appropriate fragments were tagged with RFP at their N-termini, expressed from a methionine-regulatable promoter, and assessed for their abilities to localize and to provide Inn1 function. Consistent with its binding to Hof1 (and Cyk3), the C-terminal region was able to localize to the bud neck in telophase in either the presence (Fig. 3.7A) or absence (unpublished data) of full-length Inn1. However, the RFP signal was less intense than with the full-length protein (Fig. 3.7A), and no contraction was seen in the absence of full-length protein (unpublished data). Despite its ability to localize to the neck, the C-terminal fragment showed no detectable ability to rescue the growth of an *inn1Δ* mutant (Fig. 3.7B).

In striking contrast, the RFP-tagged N-terminal fragment showed no detectable

localization to the neck and appeared to be cytosolic as judged by confocal microscopy (Fig. 3.7A), but it could nonetheless rescue the growth (Fig. 3.7B) and PS-formation (Fig. 3.7C) defects of an *inn1Δ* mutant. Most of the *inn1Δ* cells expressing the N-terminal fragment formed either a seemingly normal PS (Fig. 3.7C, cells 1 and 2) or a seemingly normal PS with additional “PS-like” structures (cell 3); some cells formed an asymmetrically localized PS sandwiched by SS (unpublished data). The ability of the N-terminal fragment to provide Inn1 function appears to depend on its overexpression, because a single chromosomal copy under the normal *INN1* promoter was not sufficient for colony formation (Fig. 3.13A), whereas the same construct rescued the growth of *inn1Δ* cells when overexpressed from a *GAL* promoter (Fig. 3.13B); presumably, the overexpression allows a sufficient concentration of the fragment to be present at its site of action despite its inability to localize efficiently to this site. The ability of the N-terminal fragment to provide Inn1 function also appears to depend on Cyk3, as the overexpressed N-terminal fragment was unable to rescue the growth of an *inn1Δ cyk3Δ* double mutant (Fig. 3.7D).

Taken together, these results suggest that the Inn1 N-terminal domain collaborates with Cyk3 to provide the activity necessary for PS formation and cytokinesis, whereas the C-terminal domain is responsible for targeting Inn1 to its site of action.

Apparent lack of phospholipid binding by the putative C2 domain of Inn1

Sanchez-Diaz et al. (2008) proposed that Inn1 might help to physically link the AMR to the plasma membrane, based in part on the resemblance of the Inn1 N-terminal region to C2 domains, which are typically involved in calcium-dependent lipid binding (Rizo and Sudhof, 1998; Cho and Stahelin, 2006). However, C2 domains have also been implicated in protein-protein interactions (Benes et al., 2005; Lu et al., 2006; Dai et al., 2007), and the Inn1 N-terminal domain does not appear to possess aspartates in positions corresponding to those critical for Ca^{2+} binding in the C2 domains of the rat synaptotagmin-I (Shao et al., 1996) and the *S. cerevisiae* Tcb proteins (Schulz and Creutz, 2004). Moreover, in lipid-overlay assays, we could not detect significant lipid binding by Inn1 in either the presence or absence of Ca^{2+} (Fig. 3.14A), although

Ca²⁺-dependent binding of various phospholipids was observed with a positive control (Fig. 3.14B).

To analyze possible phospholipid binding in a membrane environment and in a more quantitative manner, we also used the surface-plasmon-resonance (SPR) approach (Narayan and Lemmon, 2006). As shown in Fig. 3.8, the Inn1 N-terminal region showed no significant binding to surfaces containing 20% (mole/mole) PtdSer or 10% (mole/mole) PtdIns(4,5)P₂ in a dioleoylphosphatidylcholine background in the presence or absence of Ca²⁺. In contrast, the positive control Tcb1-C2C showed robust binding to PtdSer in the presence of Ca²⁺ ($K_D = 0.95 \pm 0.57 \mu\text{M}$) but did not bind significantly to PtdIns(4,5)P₂ (a low level of binding was observed in the absence of Ca²⁺). Because phospholipid binding by the Inn1 N-terminal region was barely above background even when 10 mM protein was applied, the K_D for binding is likely to exceed 100 μM . Based on other studies with GST-fusion proteins (which are known to dimerize), the monomeric Inn1 N-terminal region presumably binds phospholipids with a K_D in the 1 mM range or weaker. No binding of either the Tcb1 C2 domain or Inn1 N-terminal region was detected by SPR for PtdIns3P, PtdIns4P, or PtdIns(3,5)P₂ surfaces, regardless of Ca²⁺ levels (unpublished data).

In summary, the apparently cytosolic localization of the Inn1 N-terminal fragment (see above), the apparent lack of amino acids critical for Ca²⁺-dependent lipid binding, and the biochemical data all suggest that the Inn1 N-terminal region is not a lipid-binding domain.

Function of Inn1 in AMR-independent cytokinesis

In the model of Sanchez-Diaz et al. (2008), Inn1 couples plasma-membrane ingression to contraction of the AMR. However, we found that an Inn1-N-terminus-Hof1 fusion similar to that described by Sanchez-Diaz et al. (2008) could not only provide Hof1 function [Fig. 3.9, sector 5; note that the *hof1* Δ *myo1* Δ double mutant is essentially inviable (see Introduction)] and Inn1 function (Fig. 3.9, compare sectors 3 and 4 to sectors 1 and 2), but it could do so in the absence of Myo1 and hence of an AMR (Fig. 3.9, sector 6). Moreover, the fusion protein could also

suppress an *iqg1* Δ mutation (Fig. 3.9, compare sector 9 to sectors 7 and 8), even though *Iqg1* is essential for AMR formation (see Introduction). In striking contrast, the *Inn1-N-terminus-Hof1* fusion protein showed no detectable suppression of a *chs2* Δ mutation (Fig. 3.9, compare sector 10 to sectors 11 and 12), consistent with the other evidence that the primary function of *Inn1* is to stimulate synthesis of the PS by *Chs2* (see Discussion). Because *Iqg1* is also essential for PS formation (Nishihama et al., 2009), the data suggest that *Inn1* functions downstream of *Iqg1* but upstream of *Chs2* in PS formation. It should also be noted that the *Inn1-N-terminus-Hof1* fusion protein could provide *Inn1* function even when expressed from low-copy vectors (Fig. 3.9), whereas the free *Inn1* N-terminus required overexpression to do so (Fig. 3.13). This difference presumably reflects the ability of the *Hof1* portion of the fusion protein to target the *Inn1* N-terminus to the neck (Sanchez-Diaz et al., 2008), thus increasing its effective concentration at that site.

Discussion

In most if not all animal and fungal cells, the contractile AMR is important for efficient cytokinesis. However, it is also clear that a variety of cell types, including yeast, *Dictyostelium* amoebae (DeLozanne and Spudich, 1987; Neujahr et al., 1997; Hibi et al., 2004), and at least some kinds of mammalian cells (Kanada et al., 2008), can undergo cell-cycle-regulated division at appropriate sites in the absence of AMR function when grown under appropriate conditions. These observations focus attention on the processes of membrane deformation, membrane addition and compositional specialization, and ECM (e.g., cell-wall) formation that normally work in close concert with AMR contraction but can also form a cleavage furrow even when the AMR is absent or nonfunctional (Finger and White, 2002; Mizuguchi et al., 2003; Strickland and Burgess, 2004; Albertson et al., 2005; Szafer-Glusman et al., 2008). They also suggest that animal and fungal cytokinesis may have more in common mechanistically with plant cytokinesis than has traditionally been thought (Hales et al., 1999; Otegui et al., 2005).

In yeast, Iqg1, Mlc1, Hof1, and Cyk3 have all been implicated in the AMR-independent processes of cytokinesis (see Introduction). In this study, we have identified Inn1 as another critical contributor to these processes. Specifically, we have shown that Inn1 interacts directly with Hof1 and Cyk3, plays an essential role in PS formation, and can function in cytokinesis independently of the AMR, as summarized in Fig. 3.10. Our study has some overlap with an independent study of Inn1 (Sanchez-Diaz et al., 2008) but reaches a very different conclusion about the role of Inn1 in cytokinesis.

Assembly of cytokinesis proteins at the mother-bud neck

In late G1, Myo1 forms a ring at the presumptive bud site (Bi et al., 1998; Lippincott and Li, 1998). Myo1-ring formation is septin dependent, and after bud emergence, the Myo1 ring lies near the center of the hourglass-shaped septin assembly. The mechanism(s) by which Myo1 associates with the septins and/or the plasma membrane remain obscure. Later in the cell cycle, other cytokinesis proteins are recruited to the neck. By anaphase (Fig. 3.10A), Mlc1 has joined Myo1 and has also helped to recruit Iqg1 to the neck (Shannon and Li, 2000; Luo et al., 2004). Actin recruitment occurs just before mitotic exit and depends on Myo1, Mlc1, and Iqg1 (Bi et al., 1998; Shannon and Li, 1999; Korinek et al., 2000; Yoshida et al., 2006) but not on Inn1 (Fig. 3.12; Sanchez-Diaz et al., 2008), which is not yet localized to the neck (Fig. 3.2A; Fig. 3.3). At this stage, Hof1 forms a double ring at the neck; its recruitment depends on the septins but not on the other proteins discussed here (Vallen et al., 2000). Some Hof1 also appears to be present in complexes (mediated by an SH3-PXXP interaction) with the as-yet-unlocalized Inn1 (Fig. 3.4A, C, D, E).

As cells enter cytokinesis, multiple events occur that depend directly or indirectly on the MEN (Fig. 3.10B). The septin ring splits (Kim et al., 1991; Lippincott et al., 2001) and defines a domain to which other proteins are confined (Dobbelaere and Barral, 2004). Chs2 is recruited to the neck (Chuang and Schekman, 1996; Zhang et al., 2006), an event that depends on the septins and the secretory apparatus (VerPlank and Li, 2005), but not on the other proteins

discussed here (Fig. 3.1D; Nishihama et al., 2009). Cyk3 is also recruited to the neck (Korinek et al., 2000); this recruitment is less efficient (or the recruited Cyk3 is less well organized) in the absence of either Hof1 or Inn1 (Fig. 3.5F; unpublished data). Cyk3 presumably is bound to Inn1 at this time by an SH3-PXXP interaction (Fig. 3.5C-E), although it is not yet known whether this binding also occurs earlier in the cell cycle. Hof1 reorganizes into a single ring, an event that is correlated with its MEN-dependent phosphorylation (Fig. 3.4A and B; Vallen et al., 2000; Corbett et al., 2006). Inn1 is recruited to the neck, an event that depends on its C-terminal region but not on its N-terminal region (Fig. 3.7A; Sanchez-Diaz et al., 2008) or the presence of Cyk3 (Fig. 3.6A; Table 2). Inn1 localization also occurs in *myo1Δ*, *iqg1Δ*, and *hof1Δ* cells (Fig. 3.2B and C; Fig. 3.4F; Table 2), as well as when interactions with Hof1 and Cyk3 are disrupted by mutation of the Inn1 PXXP motifs (Fig. 3.6C). However, Inn1 localization appears weak and/or asymmetric in each case and was abolished when *hof1Δ* cells (but not wild-type or *cyk3Δ* cells) were treated with latA (Fig. 3.6D), suggesting that Inn1 localization depends jointly on Hof1 and the AMR.

Like Hof1, Inn1 undergoes MEN-dependent phosphorylation (Fig. 3.4B), and it seems likely that the rearranged protein localizations and associations that occur at this time depend, at least in part, on these phosphorylations. Because the MEN component Dbf2 is also targeted to the neck upon actin-ring assembly and is required for the phosphorylation and/or localization of both Hof1 and Inn1 (Fig. 3.3; Vallen et al., 2000; Corbett et al., 2006), Inn1, Hof1, or both may be direct substrates of this protein kinase.

Functions of the assembled proteins during cytokinesis

Once the cytokinesis apparatus is fully assembled, contraction of the AMR, membrane ingression, and PS synthesis all normally begin almost immediately. AMR contraction has long been presumed to involve motor activity of Myo1 upon actin filaments. This view has been challenged by the findings that the Myo1 tail (lacking the motor domain) assembles at the neck and supports efficient cytokinesis (Lord et al., 2005) and that even some *myo1Δ* cells form nearly normal-looking cleavage furrows and PSs (Nishihama et al., 2009). However, a role for Myo1-

actin force generation is supported by the observations that in *inn1Δ* (Fig. 3.1E) and *chs2Δ* (VerPlank et al., 2005) mutants, the AMR can apparently continue to contract after it has pulled away from the plasma membrane over much of its circumference.

These observations also suggest one possible role for Inn1, namely that it might help to physically tether the AMR to the membrane during contraction (see also Sanchez-Diaz et al., 2008). However, such a role appears to be ruled out by the following arguments. First, the myosin (later actomyosin) ring can associate with the cell cortex in *inn1Δ* cells (Fig. 3.1E) and, in wild-type cells, does so long before Inn1 has localized to the neck (see above). Second, the plasma membrane can ingress without force production by the AMR (see above). Third, the putative C2 domain of Inn1 does not appear to bind phospholipids (Figs. 3.8 and 3.14), and indeed its sequence is sufficiently different from C2 domains that are known to bind lipids (Cho and Stahelin, 2006) that there seems little reason to expect such binding. Fourth, although the Inn1-binding partner Hof1 might possibly help to tether the AMR to the membrane via the presumed interaction of its F-BAR domain with the membrane (Fig. 3.10B), there is no good evidence for a role of Inn1 in linking Hof1 to the AMR. The contraction of the Inn1 ring (Fig. 3.2A; Sanchez-Diaz et al., 2008) would be seen with any protein that is associated with the leading edge of the cleavage furrow, and although Sanchez-Diaz et al. (2008) detected weak binding of Inn1 to Iqg1, Iqg1 is a multifunctional protein that is involved in AMR-independent processes as well as in AMR formation (see Introduction). More compellingly, an N-terminal fragment of Inn1 can provide Inn1 function when overexpressed (Fig. 3.7B and C; Fig. 3.13) despite its inability to bind Hof1 (Fig. 3.4C-E) or concentrate at the neck (Fig. 3.7A). Fifth, a fusion of Inn1(1-134) to Hof1 can provide Inn1 function not only in otherwise wild-type cells (Sanchez-Diaz et al., 2008) but also in *myo1Δ* and *iqg1Δ* cells (Fig. 3.9), showing that Inn1 function does not depend on the AMR. Finally, the formation of reasonably well oriented PSs in *inn1Δ* cells overexpressing either Cyk3 (Fig. 3.5B) or an Inn1 fragment that cannot concentrate at the division site (Fig. 3.7C) shows that the AMR can direct furrow ingression without an Inn1-dependent link to the membrane.

Thus, we favor a different model in which the role of Inn1 is to cooperate with Cyk3 in the activation of Chs2 for PS formation (Fig. 3.10B). This model is supported by (1) the absence of PS formation in *inn1* Δ cells (Fig. 3.1C) and its delay in *cyk3* Δ cells (Nishihama et al., 2009); (2) the restoration of PS formation in *inn1* Δ cells overexpressing either Cyk3 (Fig. 3.5B) or an N-terminal fragment of Inn1 (Fig. 3.7C); (3) the observation that the Inn1 N-terminal fragment (whose function is presumably inefficient because of its inability to localize) can only provide Inn1 function when Cyk3 is present (Fig. 3.7D); and (4) the inability of the Inn1(1-134)-Hof1 fusion to suppress the growth defect of a *chs2* Δ mutant (Fig. 3.9). Moreover, the behavior of the AMR in *inn1* Δ cells (Fig. 3.1E) appears very similar to that in *chs2* Δ cells (VerPlank et al., 2005); thus, in the absence of PS formation, the membrane apparently cannot ingress rapidly enough to keep pace with AMR contraction, resulting in detachment of the ring from the membrane and/or its disassembly. Because the Inn1(1-134)-Hof1 fusion rescues an *iqg1* Δ but not a *chs2* Δ mutant (Fig. 3.9), Inn1 presumably functions downstream of *iqg1* but upstream of Chs2 in the PS-formation pathway, as also suggested for Cyk3 (Korinek et al., 2000; Nishihama et al., 2009). Because the PS-formation defects of *iqg1* Δ and *inn1* Δ mutants are more severe than that of a *cyk3* Δ mutant, Inn1 and Cyk3 presumably function in parallel to activate Chs2 by a mechanism(s) that remains to be determined. The MEN-regulated localization of Inn1 and Cyk3 to the division site presumably allows proper coordination of PS formation and furrow ingression with AMR contraction. It will be interesting to explore the interplay between AMR contraction and ECM synthesis during cytokinesis in other types of cells.

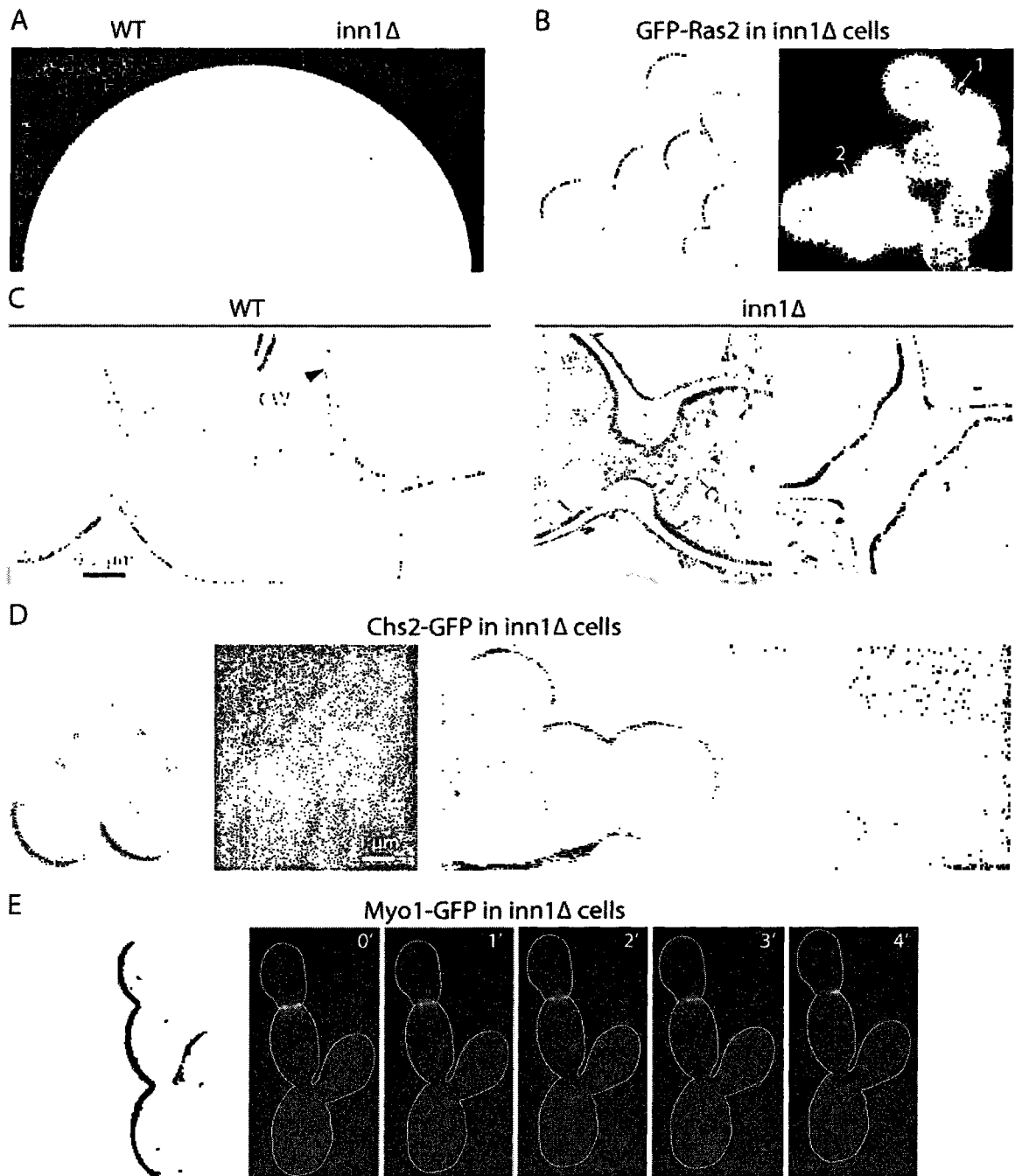


Figure 3.1 **Dependence of PS formation on *Inn1*.** (A) Slow growth of *inn1Δ* cells. Wild-type (YEF473A) and *inn1Δ* (YEF5216) cells were streaked on an SC plate and incubated at 25°C for 3 days. (B) Abnormal but complete cytokinesis in *inn1Δ* cells. YEF5216 cells carrying plasmid

pRS315-GFP-RAS2 were grown to exponential phase in SC-Leu liquid medium at 23°C and imaged by DIC and fluorescence microscopy. (C) Absence of PS formation in *inn1Δ* cells. Strains YEF473A and YEF5216 were grown to exponential phase in SC medium at 24°C and examined by TEM. CW, cell wall; PM, plasma membrane; PS, primary septum; SS, secondary septum. (D) Localization of Chs2 to the neck in *inn1Δ* cells. Strain LY1373 (*inn1Δ* □ *CHS2-GFP* [pUG36-INN1]) was transferred from an SC plate to an SC+FOA plate, incubated overnight at 25°C to select for loss of the *URA3*-marked *INN1* plasmid, and examined by fluorescence microscopy. (E) Abnormal contraction of the AMR in *inn1Δ* cells. *inn1Δ MYO1-GFP* cells (YEF5291) were observed by time-lapse microscopy; cell bodies are outlined in the GFP panels. Scale bars, 0.5 or 1 μm. (Data from EAV, RN, JH)

See also Videos 1-4. (C) Wild-type (RNY2395) and *iqg1* Δ (RNY2393) cells expressing Inn1-GFP and containing plasmid YCp50-IQG1 were grown overnight at 25°C on an SC+FOA plate to eliminate the plasmid, scraped from the plate, and imaged by DIC and fluorescence microscopy. Scale bars, 2 μ m. (Data from JH, EAV)

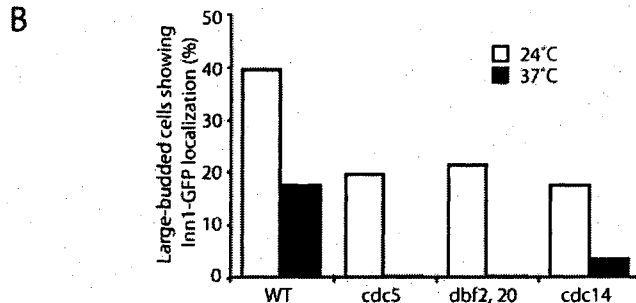
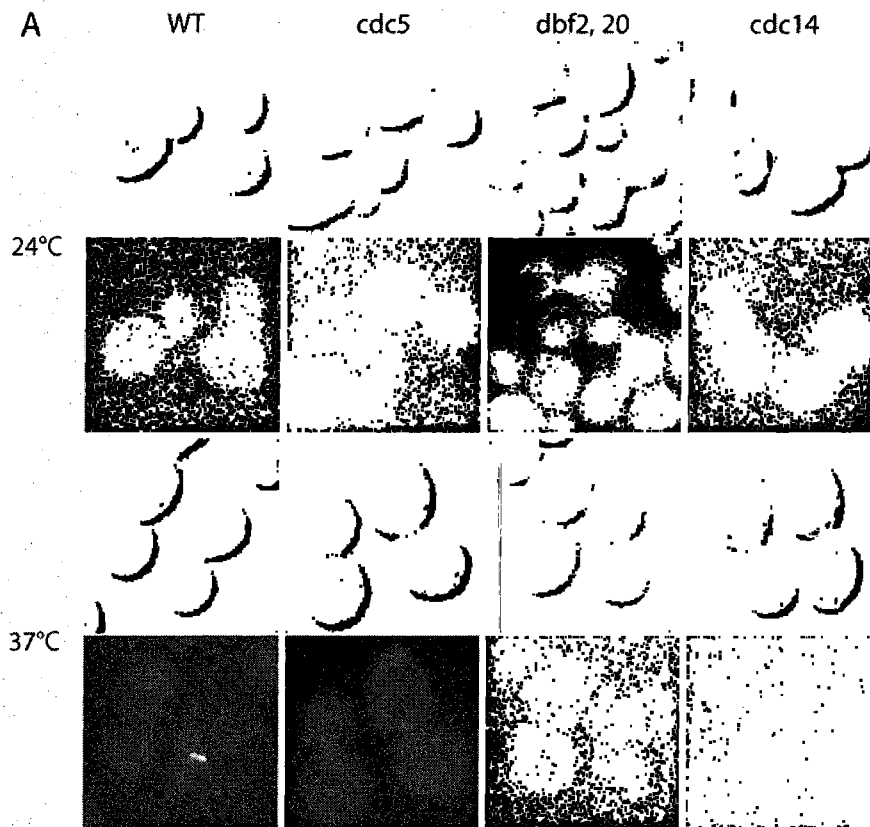


Figure 3.3 Dependence of Inn1 localization on the MEN. Wild-type (LY1313), *cdc5* (LY1357), *dbf2 dbf20* (LY1355), and *cdc14* (LY1360) cells expressing Inn1-GFP were grown to exponential phase in YM-P rich medium at 24°C and then shifted to 37°C for 3.5 h (LY1360) or 2.5 h (the other strains) before imaging (A) and scoring large-budded cells (B) for Inn1-GFP localization. In B, the numbers of cells scored were: (24°C) 62 for wild type and 102-131 for the mutants; (37°C) 78 for wild type and 177-199 for the mutants. Scale bar, 2 μ m. (Data from RN)

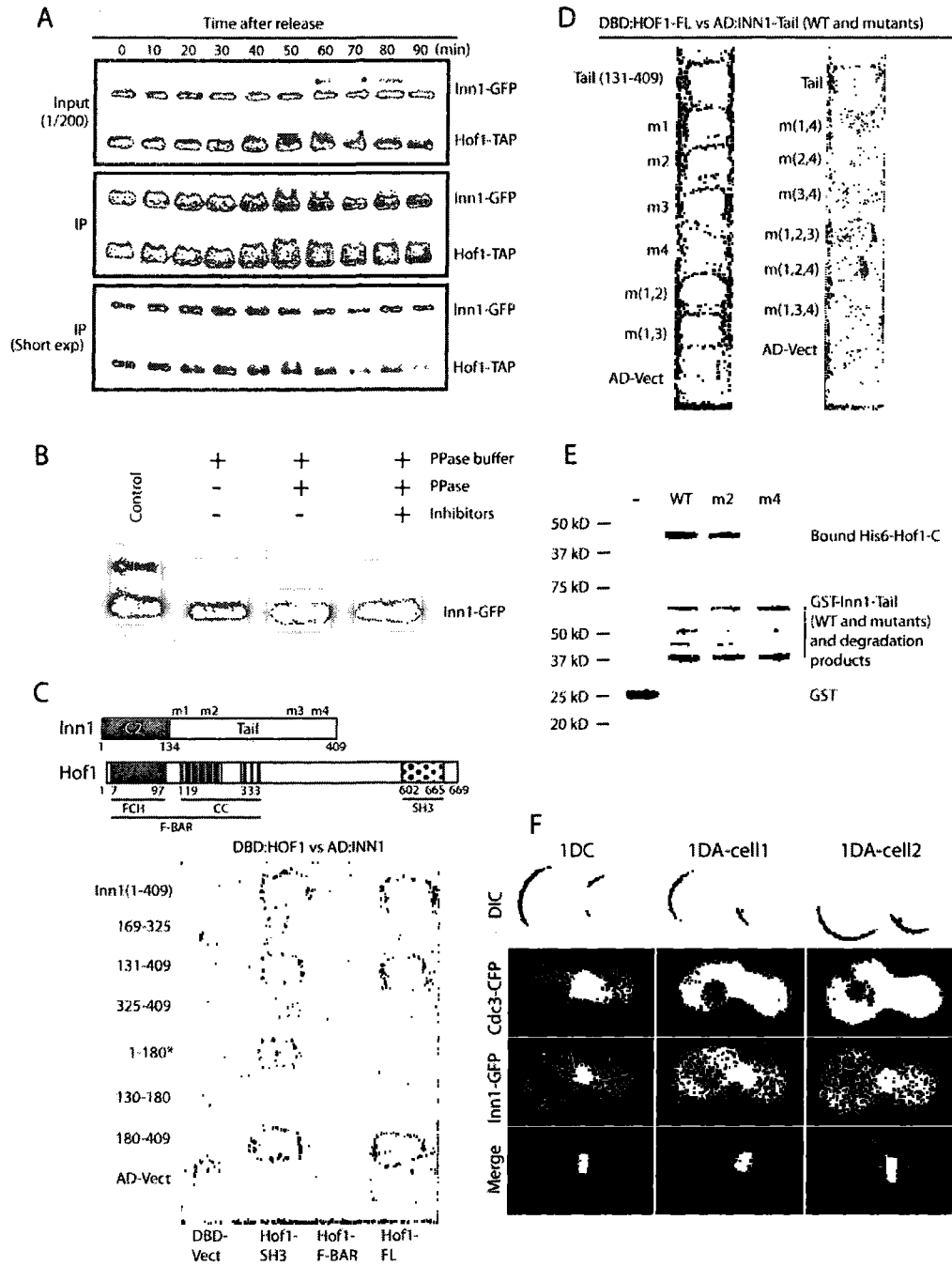


Figure 3.4 Inn1-Hof1 interaction and its role in the symmetric localization of Inn1 at the neck. (A) Co-immunoprecipitation and cell-cycle-dependent modification of Inn1 and Hof1.

Strain MOY157 (*INN1-GFP HOF-TAP cdc15-2*) was grown to exponential phase in YM-P medium at 24°C, shifted to 37°C for 2.5 h to synchronize cells at mitotic exit using the *cdc15-2* block,

released to permissive temperature by rapidly cooling to 24°C, and sampled at intervals. Hof1-TAP was precipitated from protein extracts, and samples of the extracts (Input) and precipitates (IP) were analyzed by SDS-PAGE and immunoblotting (see Materials and methods). In a control in which no TAP-tagged protein was present, no Inn1-GFP was detected in the precipitate (unpublished data). (B) Phosphorylation of Inn1. Strain MOY215 (*INN1-GFP cdc15-2*) was synchronized as in A and sampled 45 min after release. Inn1-GFP was immunoprecipitated and subjected to phosphatase treatments as indicated (see Materials and methods). (C) Two-hybrid analysis of Inn1-Hof1 interaction. The diagram shows the domain structures of Inn1 (see text and Fig. S1; m1-m4 are the mutations introduced into the PXXP motifs) and Hof1 (FCH, FER/CIP4-homology; CC, coiled coil; F-BAR, putative membrane-interaction domain; SH3, Src Homology 3). Various Inn1 fragments carried on the activation-domain vector (AD-Vect) were tested pair-wise for interaction with full-length Hof1 (Hof1-FL), Hof1 amino acids 576-669 (Hof1-SH3), and Hof1 amino acids 1-340 (Hof1-F-BAR) carried on the DNA-binding-domain vector (DBD-Vect). *: Inn1(1-180) interacted with Hof1-SH3 for unknown reasons. (D) Role of Inn1 amino acids 377-383 (PXXPPXP) in the Inn1-Hof1 interaction. Two-hybrid analysis was conducted using full-length Hof1-DBD and Inn1(131-409)-AD. The Inn1 sequence was wild type [Tail(131-409)] or carried mutations *m1*, *m2*, *m3*, and/or *m4*, individually or in combinations. (E) Direct binding of Inn1 to Hof1 and its mediation by Inn1 amino acids 377-383 (PKLPPLP). Purified GST-Inn1-tail (amino acids 131-409; wild type or carrying mutation *m2* or *m4*) and His6-Hof1-C (amino acids 341-669) were tested for binding *in vitro* as described in Materials and methods. (F) Asymmetric localization of Inn1 at the neck in *hof1Δ* cells. Strain LY1328 (*INN1-GFP hof1Δ* [pRS316-HOF1]) was transformed with plasmid YCp111-CDC3-CFP and incubated on an FOA plate to eliminate the *HOF1* plasmid. Cells from a population growing exponentially in SC-Leu medium at 24°C were examined by 3D microscopy (see Materials and methods). 1DC, 1 central dot (as typically observed in wild-type cells); 1DA, 1 asymmetric dot (as often observed in *hof1Δ* cells; see Table I and Videos 5 and 6). Scale bar, 2 μm. (Data from JHS, MO)

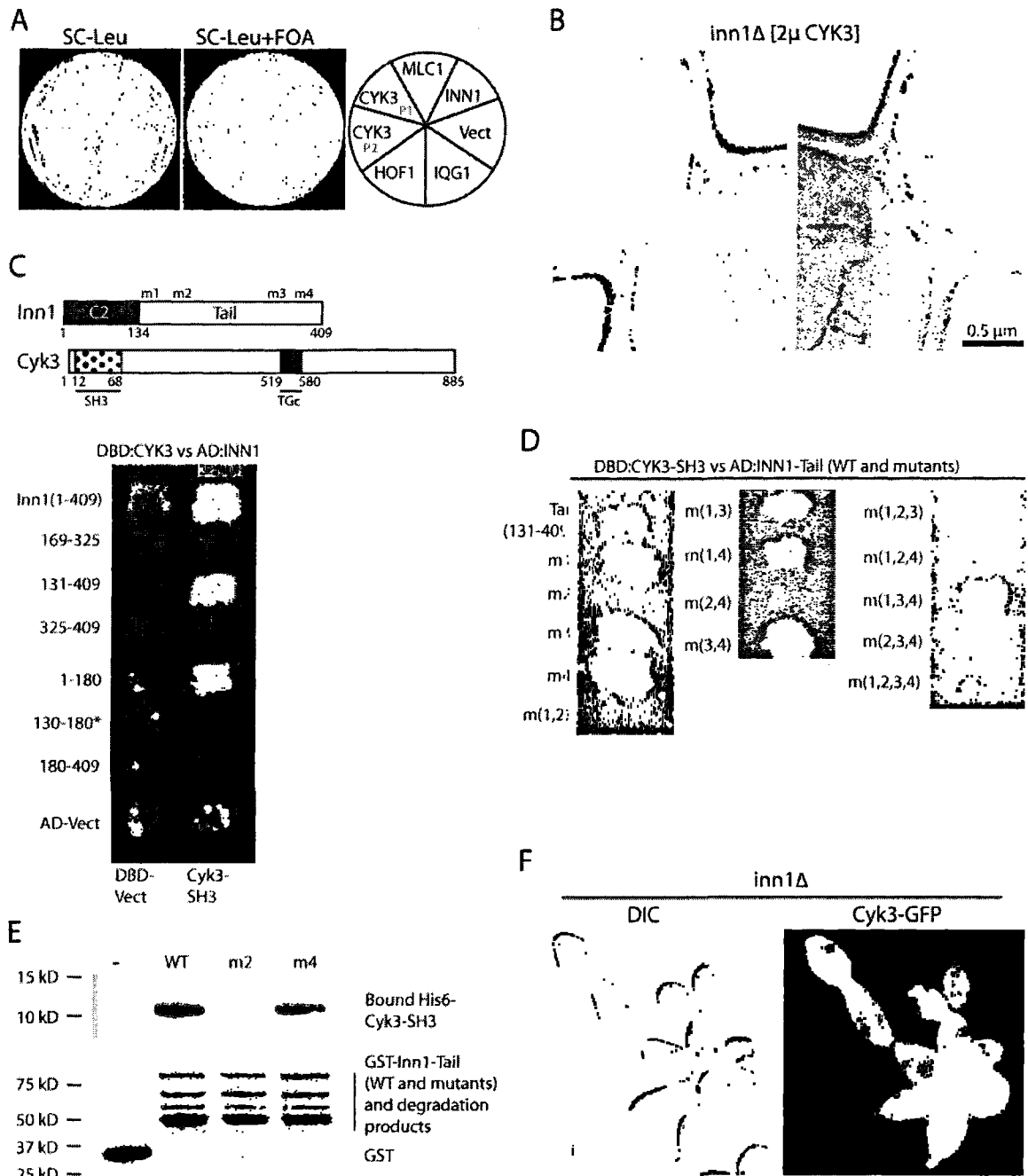


Figure 3.5 Functional and physical interactions between Inn1 and Cyk3. (A) Suppression of *inn1Δ* growth defect by overexpression of Cyk3. Strain LY1310 (*inn1Δ* [pUG36-INN1]) was transformed with a vector control (Vect; YEplac181) or with *LEU2*-marked high-copy plasmids carrying *IQG1* (YEpl81-IQG1), *HOF1* (pTSV30A-HOF1), *CYK3* (P1, pBK132; P2, pBK133),

MLC1 (pBK65), or *INN1* (pGP564-INN1). Transformants were streaked on SC-Leu and SC-Leu+FOA plates and incubated at 25°C for 3 days to ask whether any of the candidate plasmids could replace the *URA3*-marked pUG36-INN1. (B) Restoration of PS formation in *inn1Δ* cells by overexpression of Cyk3. Strain LY1310 (*inn1Δ* [pUG36-INN1]) was transformed with pRS425-CYK3, incubated on an SC-Leu+FOA plate at 24°C for 3 days to eliminate plasmid pUG36-INN1, grown to exponential phase in SC-Leu medium at 24°C, and examined by TEM. (C-E) Interaction of the SH3 domain of Cyk3 with the PIPPLP motif (amino acids 159-165) of Inn1 as determined by two-hybrid analysis (C and D) and *in vitro* protein-binding assays (E). Experiments were performed as described for Fig. 4C-E using a Cyk3 SH3-domain fragment (amino acids 1-70) instead of Hof1. In C, the diagram shows the motifs of Cyk3 (SH3; TGc, putative transglutaminase domain). *: Inn1(130-180) failed to interact with Cyk3-SH3 for unknown reasons. (F) Localization of Cyk3 in *inn1Δ* cells. Strain YEF5216 (*inn1Δ*) was transformed with plasmid pRS315GW-CYK3-2GFP, grown overnight on an SC-Leu plate at 25°C, and imaged by DIC and fluorescence microscopy. Scale bars, 0.5 or 2 μm. (Data from JHS, JH, RN)

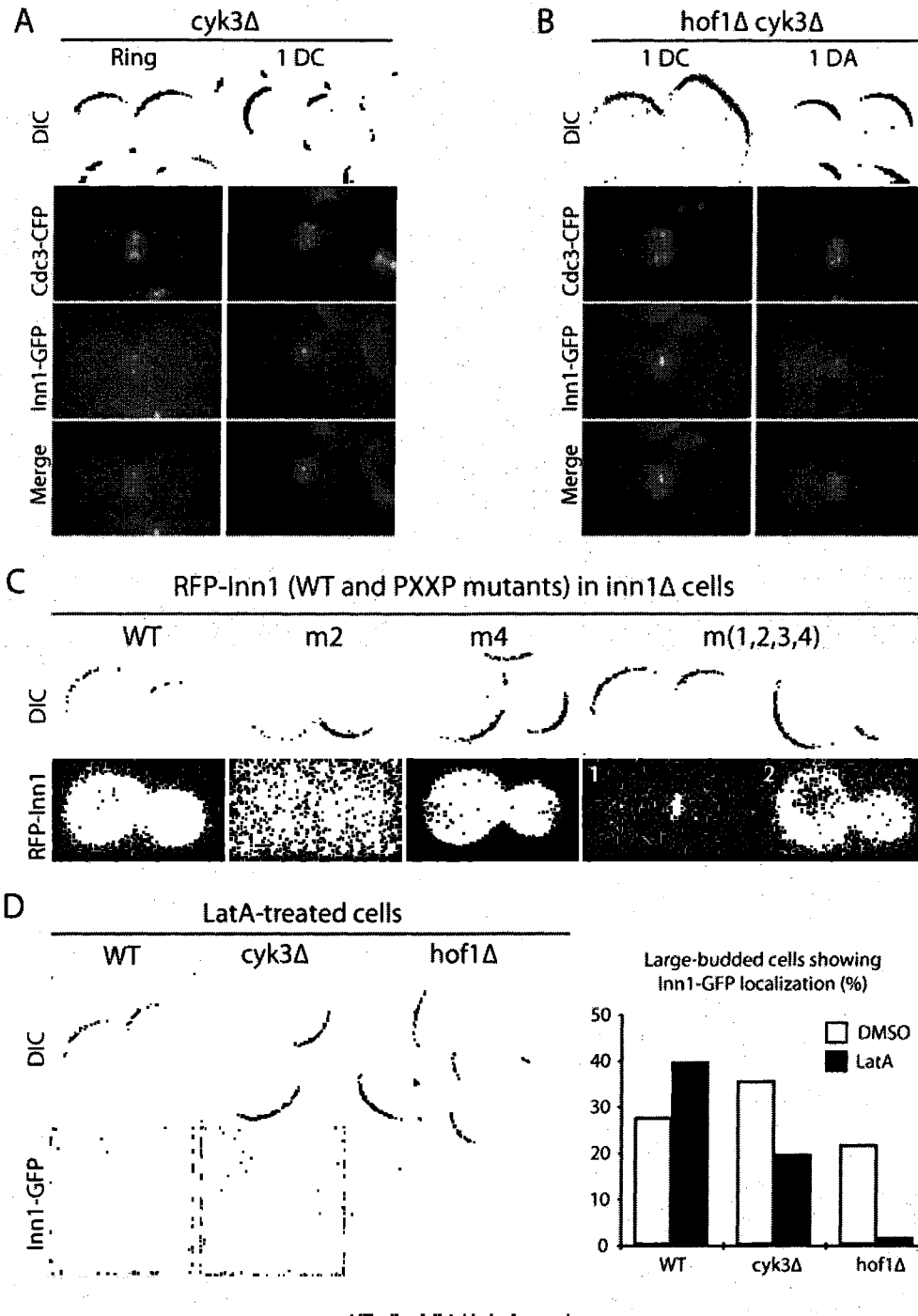


Figure 3.6 Mechanisms of Inn1 bud-neck localization. (A and B) Strains (A) LY1321 (*INN1-GFP cyk3Δ*) and (B) LY1325 (*INN1-GFP cyk3Δ hof1D* [pRS316-HOF1]) were transformed with plasmid YCp111-CDC3-CFP, and the LY1325 transformants were incubated on an FOA

plate to eliminate the *HOF1* plasmid. Cells were examined as described in Figure 4F. See also Table I and Video 7. (C) Localization of Inn1 lacking its Hof1- and Cyk3-binding sites. Strain LY1310 (*inn1* Δ [pUG36-INN1]) was transformed with *HIS3*-marked plasmids carrying RFP-tagged wild-type or mutant *INN1* alleles. After growth on an SC-His+FOA plate at 25°C to eliminate pUG36-INN1, DIC and fluorescence images were captured. (D) Loss of Inn1 localization in *latA*-treated *hof1* Δ cells. Wild-type (LY1324), *cyk3* Δ (LY1321), and *hof1* Δ (LY1328 after eliminating plasmid pRS316-HOF1 by growth on an FOA plate) strains were grown to exponential phase in YM-P medium at 25°C. Portions of each culture were treated with *latA* for 20 min (see Materials and methods), and cells were imaged by DIC and fluorescence microscopy. Images of representative *latA*-treated cells (left panels) and percentages of large-budded cells with localized Inn1-GFP (right panel) are shown. Scale bars, 2 μ m. (Data from RN, JH)

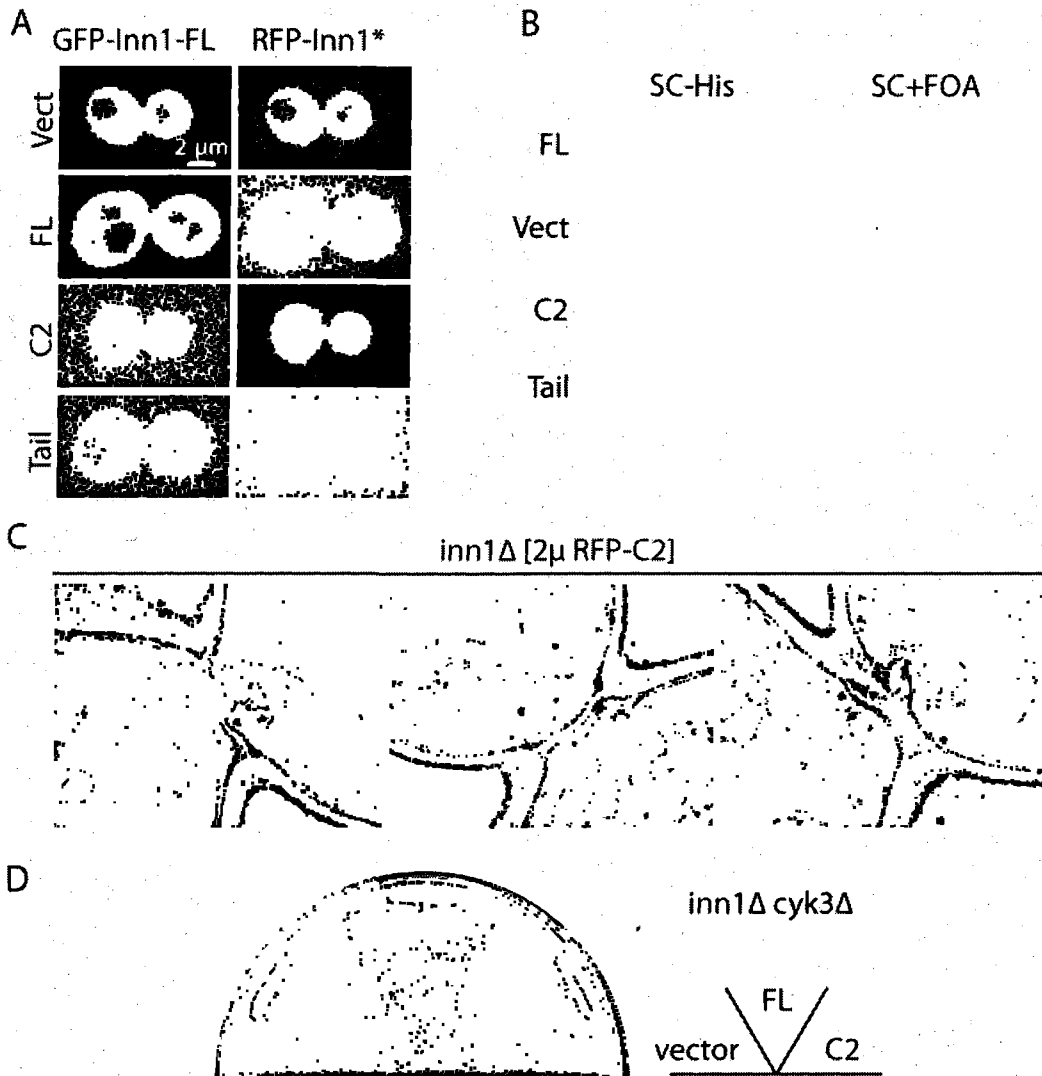


Figure 3.7 Structure-function analysis of Inn1. (A) Role of the Inn1 C-terminal region in neck localization. Strain LY1310 (*inn1Δ* [pUG36-INN1]) was transformed with the pUG34mCherry vector (Vect) or its derivatives (see Materials and methods) containing sequences encoding full-length *INN1* (FL), the putative C2 domain (amino acids 1-140), or the C-terminal tail (amino acids 130-409). Transformants were incubated on an SC-His-Ura plate for 2 days at 25°C, scraped off, and imaged by spinning-disk confocal microscopy for GFP-Inn1-FL and RFP-Inn1 derivatives (asterisk). (B) Critical role of the putative C2 domain in Inn1 function. The transformants described in (A) were patched onto SC-His and SC+FOA (to select against

pUG36-INN1) plates, and incubated at 25°C for 3 days to assess the ability of the *INN1* fragments to provide Inn1 function. (C) Restoration of PS formation in *inn1Δ* cells by the putative C2 domain. Strain YEF5202 (*inn1Δ* [pUG34mCherry-INN1-C2]), obtained as described in (B), was grown to exponential phase in SC-His medium at 24°C and examined by TEM. PS, primary septum; SS, secondary septum. (D) Cooperative function of Cyk3 and the putative C2 domain of Inn1. Strain MWY1171 (*inn1Δ cyk3Δ* [pUG36-INN1]) was transformed with the plasmids described in (A). The transformants were streaked on an SC-His-Met+FOA plate and incubated for 4 days at 24°C. (Data from EAV, RN, JH)

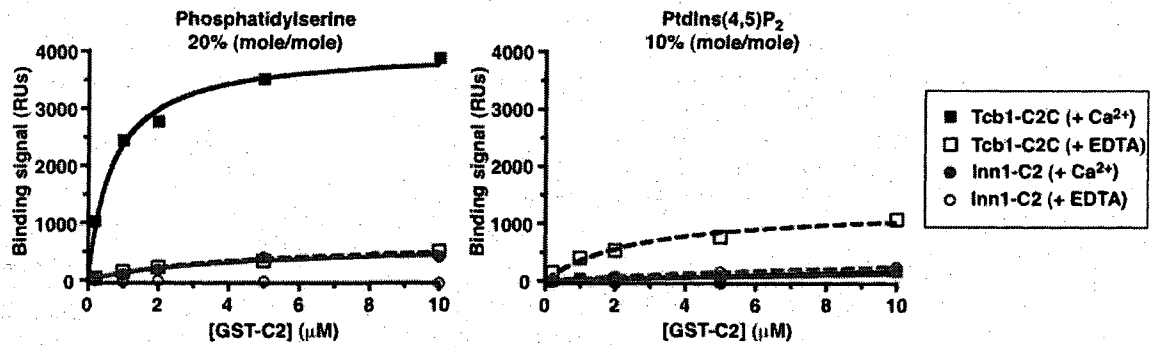


Figure 3.8 **Lack of detectable phospholipid binding by the putative C2 domain of Inn1.**

Bacterially expressed GST-Inn1(1-134) and the positive control GST-Tcb1-C2C [the third C2 domain (amino acids 979-1186) in the tricalbin Tcb1 (Schulz and Creutz, 2004)] were tested by SPR for binding of phosphatidylserine and PtdIns(4,5)P₂ (see Materials and methods). (Data from KM)

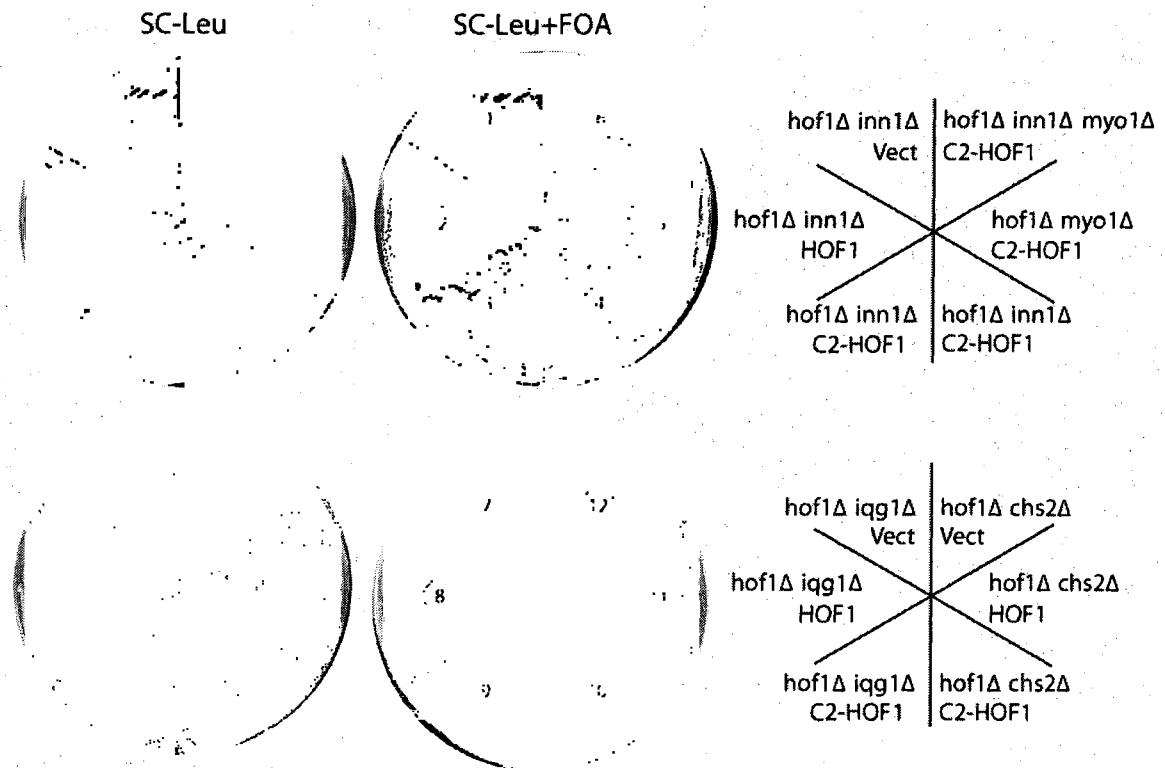
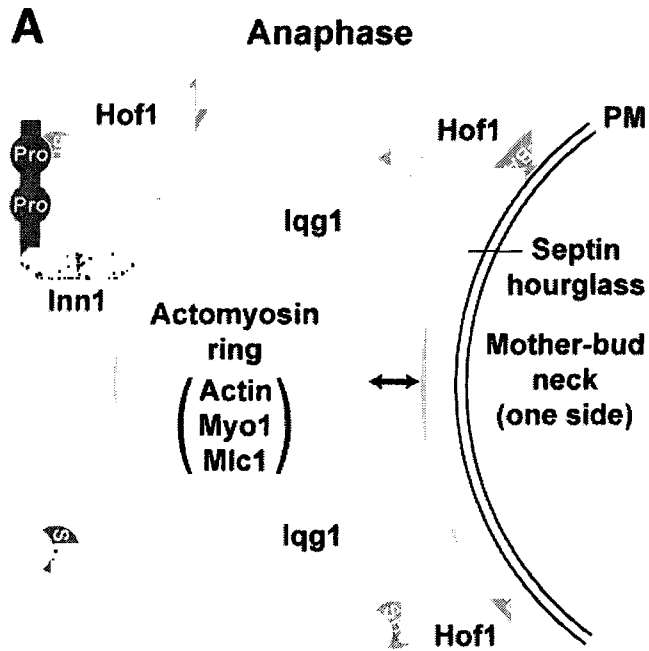


Figure 3.9 Evidence that Inn1 functions downstream of Iqq1 and upstream of Chs2 in AMR-independent cytokinesis. Strains MWY1145 (*hof1Δ inn1Δ* [pUG36-INN1]) (sectors 1-3), MWY764 (*hof1Δ iqq1Δ* [pRS316GW-IQG1]) (sectors 7-9), or RNY2225 (*hof1Δ chs2Δ* [pRS316-CHS2-myc]) (sectors 10-12) were transformed with pRS315GW, pRS315GW-NotI-HOF1, or pRS315GW-C2-HOF1. The resulting transformants and strains MOY632 (*hof1Δ innΔ* [pUG36-INN1][pRS315GW-C2-HOF1]) (sector 4), MOY630 (*hof1Δ myo1Δ* [pUG36-INN1][pRS315GW-C2-HOF1]) (sector 5), and MOY634 (*hof1Δ inn1Δ myo1Δ* [pUG36-INN1][pRS315GW-C2-HOF1]) (sector 6) were streaked on SC-Leu and SC-Leu+FOA plates and incubated at 24°C for 3 days. (Data from RN)



B Exit from mitosis / Cytokinesis

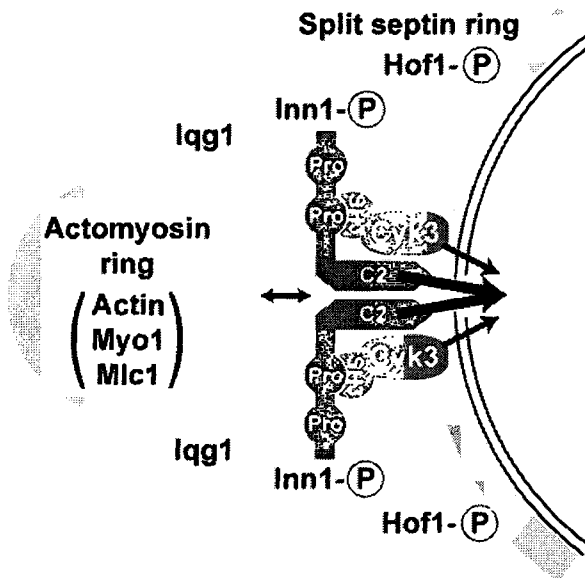


Figure 3.10 **A model for the assembly and function of Inn1 in cytokinesis.** See text for details. PM, plasma membrane; circled P symbols, phosphorylation of the proteins.

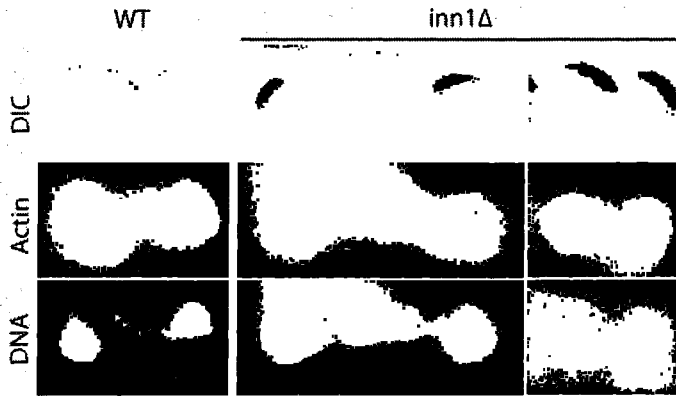


Figure 3.12 **Approximately normal assembly of the actomyosin ring in *inn1*Δ cells.** Wild-type (YEF473A) and *inn1*Δ (YEF5216) cells were grown to exponential phase in SC medium at 23°C before staining with Alexa-568-phalloidin (actin) and bis-benzimide (DNA) and observation by DIC and fluorescence microscopy. Actin rings were observed in 84% of 25 *inn1*Δ cells with fully segregated nuclei, as compared to 85% of 26 wild-type cells.

A

B

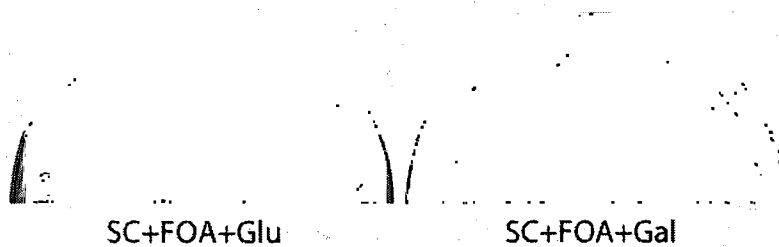


Figure 3.13 Dosage-dependent suppression of the growth defect of *inn1*Δ cells by the putative C2 domain (amino acids 1-134) of Inn1. (A) Failure of suppression by GFP-tagged Inn1(1-134) expressed from the *INN1* locus under the *INN1* promoter. None of the 24 expected *pINN1-inn1(1-134)-GFP* spores from 12 dissected tetrads of strain RNY2494 (*INN1/pINN1-inn1(1-134)-GFP*) produced colonies on a YPD plate at 24°C even after 6 days. (B) Suppression by GFP-tagged Inn1(1-134) expressed from the galactose-inducible *GAL1* promoter. Haploid segregants from strains RNY2499 (*INN1/pGAL1-GFP-INN1*) and RNY2498 (*INN1/pGAL1-GFP-inn1(1-134)*) were isolated on YPGal plates, transformed with plasmid pUG36-INN1 (*URA3, INN1*), streaked on SC+FOA plates containing either 2% glucose (Glu) or 2% galactose (Gal), and grown at 24°C for 3 days. (1) a *pGAL1-GFP-inn1(1-134)* strain; (2) a *pGAL1-GFP-INN1* strain.

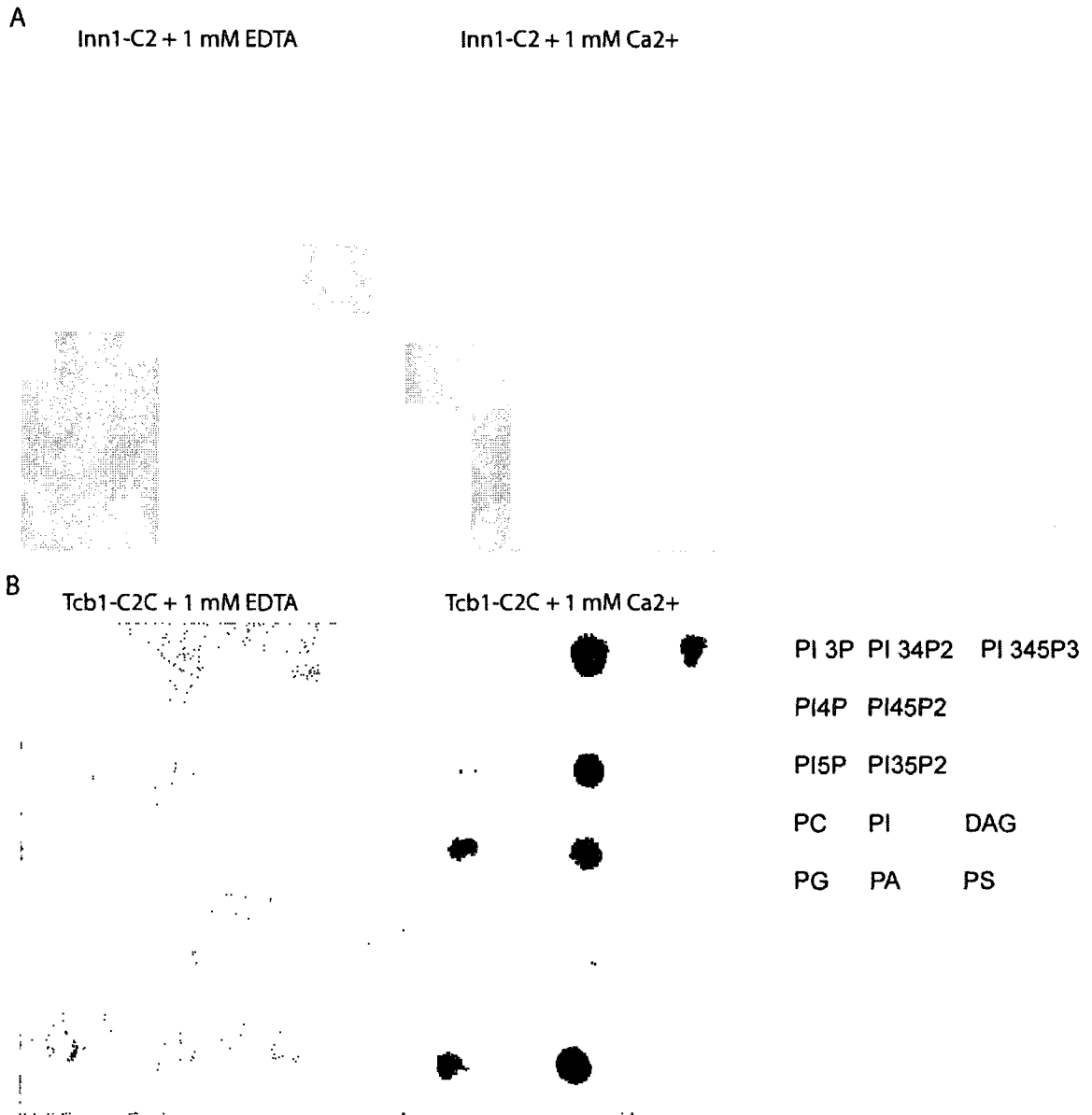


Figure 3.14 Apparent lack of binding of phospholipids by the putative C2 domain of Inn1. Bacterially expressed GST-fused Inn1(1-134) and the positive control GST-fused Tcb1-C2C [the third C2 domain (amino acids 979-1186) in the tricalbin Tcb1 (Schulz and Creutz, 2004)] were purified and tested for binding to various phospholipids by lipid-overlay assay (see Materials and methods). (Data from KM)

Table 1. Genes identified by screening for synthetic lethality with *hof1*Δ

Gene (alphabetical order)	Number of isolates	Function	Reference
<i>BNI1</i>	5	A formin that nucleates the assembly of actin cables and the actin ring	(Pruyne et al., 2002; Sagot et al., 2002)
<i>BNI5</i>	4	Septin regulator	(Lee et al., 2002; Mortensen et al., 2002)
<i>CDC12</i>	1	An essential mitotic septin	(Longtine et al., 1996; Bertin et al., 2008)
<i>CHS2</i>	2	Catalytic subunit of chitin synthase II, chiefly responsible for the synthesis of the primary septum	(Shaw et al., 1991; Chuang and Schekman, 1996)
<i>CYK3</i>	1	An SH3 domain-containing protein that is involved in actomyosin ring-independent cytokinesis	(Korinek et al., 2000)
<i>ELM1</i>	1	A protein kinase that regulates septin organization	(Bouquin et al., 2000)
<i>GIN4</i>	2	An NMR (NIM-related) protein kinase that regulates septin organization	(Altman and Kellogg, 1997; Longtine et al., 1998; Rubenstein and Schmidt, 2007)
<i>IQG1</i>	1	The sole IQGAP in <i>S. cerevisiae</i> . Involved in both actomyosin-ring-dependent and -independent cytokinesis	(Epp and Chant, 1997; Lippincott and Li, 1998; Korinek et al., 2000; Ko et al., 2007)
<i>MLC1</i>	2	"Essential" light chain for the type-II myosin Myo1; also a light chain for the type-V myosins Myo2 and Myo4 and for the IQGAP Iqg1/Cyk1	(Stevens and Davis, 1998; Shannon and Li, 2000; Boyne et al., 2000; Wagner et al., 2002; Luo et al., 2004)
<i>MYO1</i>	11	The heavy chain of the sole type-II myosin in <i>S. cerevisiae</i> . Not essential for cell viability in most strain backgrounds including that used in this study	(Rodriguez and Paterson, 1990; Lippincott and Li, 1998; Bi et al., 1998)
<i>PSA1</i>	1	An evolutionarily conserved GDP-mannose pyrophosphorylase, which synthesizes GDP-mannose that is required either directly or indirectly for N- and O-linked glycosylation as well as for GPI anchor formation. Psa1 is involved in cell separation	(Zhang et al., 1999; Tomlin et al., 2000; Warit et al., 2000)
<i>INN1/YNL152W</i>	1	See text	This study and Sanchez-Diaz et al., 2008
<i>Others</i>	6	Six mutations that do not belong to any of the complementation groups above. Five of the six were difficult to backcross, and all require further study.	This study

Table 2. Localization of Inn1-GFP in wild-type and cytokinesis-mutant strains ^a

Strain	Percent of cells with the indicated localization pattern				
	Faint or no signal	Symmetric line or 2 dots ^b	1 dot (center) ^c	Asym-metric dot or line ^c	Other ^d
<i>myo1Δ</i> [YCp50-MYO1]	62 ^e	27	11	0	0
<i>myo1Δ</i>	42	22	11	16	9
Wild type	68 ^e	20	11	2	0
<i>hof1Δ</i>	56	15	12	17	0
<i>cyk3Δ</i>	35	54	9	2	0
<i>hof1Δ cyk3Δ</i> ^f	54	24	12	10	0

^a After transformation of each strain with plasmid YCp111-CDC3-CFP and growth to exponential phase in SC-Leu or SC-Leu-Ura liquid medium at 24°C, cells with split septin rings were scored in strains LY1364 (*myo1Δ INN1-GFP* [YCp50-MYO1]; n = 81), YEF5293 (*myo1Δ INN1-GFP*; n = 95), LY1314 (*INN1-GFP*; n = 66), LY1328 (*hof1Δ INN1-GFP*; n = 94), LY1321 (*cyk3Δ INN1-GFP*; n = 117) and LY1325 (*hof1Δ cyk3Δ INN1-GFP*; n = 50). Strains LY1328 and LY1325 were first cured of their *URA3 HOF1* plasmids by growth on a 5-FOA plate. The patterns of Inn1 localization were assessed by 3D microscopy as described in Materials and methods.

^b Both types of images presumably represent views of a more-or-less normal ring of Inn1-GFP.

^c If an Inn1-GFP dot was positioned within one third the diameter of the Cdc3-CFP ring from either side, it was scored as "asymmetric"; if in the middle one third of the neck, it was scored as "1 dot, center". "Asymmetric lines" presumably represent asymmetrically contracting rings.

^d A variety of other asymmetric patterns, including asymmetries along the mother-bud axis (presumably related to the misdirected membrane invagination that occurs in many *myo1Δ* cells: Nishihama et al., unpublished data).

^e The higher number of cells with faint or no signal in wild-type strains, in comparison to *myo1Δ* and *cyk3Δ* strains, presumably reflects the more efficient completion of cytokinesis and corresponding rapid disappearance of the Inn1-GFP signal in wild-type cells.

^f Like a number of other mutants (see text), *hof1Δ cyk3Δ* strains appear to be inviable on rich medium but can be cultured on SC medium.

(Data from RN)

PERSPECTIVES

As discussed in the Introduction, remodeling of the ECM is important for cell biology. Animal, yeast, plant, and bacterial cells all possess an ECM-like structure surrounding cells although the protein and polysaccharide composition differs significantly. Despite this diversity, a common theme is that although the specific cargo differs among different cell types, all eukaryotic ECMs are shaped by a common underlying cytoskeleton that positions a highly conserved secretory machinery to deliver proteins and enzymes which synthesize the ECM. However, even though many of the components are evolutionarily conserved, it is still not known whether the cytoskeletal and secretory pathway strategies for constructing the ECM are conserved. A goal of this thesis is to deepen our understanding of the pathways responsible for the timely deposition of a budding yeast cell wall component called chitin. We hope that by studying these pathways, and the evolutionarily conserved proteins involved such as F-BAR and C2 domain proteins, we can identify unifying themes.

Localized remodeling of the ECM is important during cytokinesis, when new membrane and proteins involved in synthesizing and remodeling the cell wall are delivered specifically to the bud neck instead of globally. There are two main structures made primarily of chitin that are important for cytokinesis, the chitin ring and the primary septum. The chitin ring is synthesized as the new bud emerges by chitin synthase III (Chs3) and is important for maintaining the correct neck diameter. The primary septum is synthesized during cytokinesis by chitin synthase II (Chs2) to separate the mother and daughter cell cytoplasms. In this thesis, I have discussed work to show that the F-BAR protein Hof1 plays a role in regulating the construction of each structure.

In Chapter II, I discussed work to show that Hof1 is involved in the endocytic removal of chitin synthase III from the bud neck at G2/M when the chitin ring is finished forming. We believe that Hof1 might serve as a direct linker between Chs4, the activator of chitin synthase III, and Vrp1, the budding yeast WIP that is part of the endocytic machinery. Though some details still remain to be determined, the pathways for the synthesis, localization, and activation of Chs3 at the bud neck are fairly well understood, while the pathway for Chs3 removal is not understood at

all. The work in this thesis starts to answer an important question in the chitin synthesis field about how chitin ring formation ceases at G2/M and how chitin synthase III components are removed from the neck.

In Chapter III, I discussed work to show that Hof1 is important for the correct localization of a newly identified C2-domain protein called Inn1 that is required for the formation of the primary septum. The work in this chapter starts to answer a very important question in the field of cytokinesis about how actomyosin ring contraction is linked to septum deposition. While the role of Chs2 in synthesizing the septum is clear, less is known about the localization and activation of this protein. *In vitro* experiments show that Chs2 is activated upon proteolytic cleavage and we believe that Inn1 is the first protein shown *in vivo* to be involved in Chs2 activation. One pathway through which Inn1 functions is through the SH3 domain protein Cyk3. Cyk3 contains a putative transglutaminase domain which is likely involved in the proteolytic activation of Chs2. We are currently doing experiments to further study this question.

Another way to study the function of Hof1 is to break the protein into its individual domains and examine their properties. In Chapter II, I showed that the C-terminus of Hof1, which includes the SH3 domain, only localizes to the bud neck during telophase yet is sufficient to rescue a *hof1* Δ synthetic lethal genetic interaction. In addition, when the C-terminus is overexpressed, it causes a cytokinesis defect with cells forming chains. This data suggests it is the SH3 domain of Hof1 that is important for cytokinesis, due partly to its binding of Inn1 and the role both proteins play in forming the primary septum.

However, there could also be other functions of Hof1-SH3 that are important for cytokinesis. Clues to what these other functions are could come from looking at how Hof1 is localized to the bud neck during cytokinesis. Hof1 can interact with the actomyosin ring through the formin Bni1. Bni1 localizes to the bud neck during actomyosin ring contraction (Buttery et al., 2007) and a weak interaction with Hof1 was reported (Kamei et al., 1998). Hof1 might also be involved in the exocytic delivery of enzymes and other proteins to the bud neck. We have yeast 2-hybrid evidence that Hof1 interacts with a component of the exocyst, Exo84 (unpublished

results). The exocyst is a multisubunit tethering complex involved in the regulation of cell-surface transport (reviewed in Hsu et al., 2004). In Chapter II, we showed that Chs2 is delivered to the bud neck in *inn1Δ* cells but appears to not be active as the primary septum cannot form. Perhaps Hof1, in addition to its role in binding and localizing Inn1 properly, is involved in the delivery of Chs2 to the neck. Studying these questions and more will give hints at the mechanisms behind the role of Hof1 in cytokinesis.

Also in Chapter II, I showed that the F-BAR domain of Hof1 can localize to the bud neck throughout the cell cycle. It can even localize in very small buds where the full-length protein does not localize. This is presumably due to the loss of the PEST sequence which is required for the normal proteosomal degradation of Hof1 at the end of each cell cycle (Blondel et al., 2005). An interesting question is how can the F-BAR domain localize to the bud neck? We have looked at Hof1-F-BAR-GFP localization in cells missing all known Hof1 binding partners during the G2/M phase of the cell cycle, *bnr1Δ hof1Δ chs4Δ*, and found that it can localize (unpublished results). This raises the possibility that Hof1 might bind to phospholipids, as other members of the FBP-17/CIP4 subfamily do (et al., 2005; Tsujita et al., 2006). While we haven't looked at this question exhaustively, Katarina Marovcevic in Mark Lemmon's lab here at Penn looked at the Hof1-F-BAR domain in lipid binding assays and found that it does not appear to bind phospholipids (unpublished data). This indicates that the Hof1 F-BAR domain might function differently than previously described mammalian F-BAR domains and correlates with our results as we found that the F-BAR domain of Hof1 binds directly to another protein. This is the first example of an F-BAR domain having a protein binding partner, although there are a few examples of other BAR domains behaving this way (Tarricone et al., 2001; Inoue et al., 2008; Zhu et al., 2007). In the future, it will be interesting to compare the F-BAR domain of Hof1 with other F-BAR domains and see if they also have differential abilities to tubulate the plasma membrane and bind different proteins for different cellular functions.

One intriguing possibility for how the Hof1 F-BAR domain might localize to the bud neck during telophase is by binding to the septin ring. From the early stages of budding, the septins

form an hourglass made of filaments aligned along the yeast bud neck. However, during cytokinesis, the septin filaments rotate 90 degrees in the membrane plane and form circumferential rings on either side of the bud neck (Vrabioiu and Mitchison, 2006). It is possible that the banana shaped F-BAR domain of Hof1 can bind to these curved rings. We found that overexpressing Hof1-GFP causes ectopic localization at the bud tip and other sites away from the bud neck, and that Cdc3-RFP co-localizes with Hof1-GFP in these cells (unpublished data). This suggests that Hof1 interacts with the septins either directly or through another protein, though future experiments are needed.

Another way that Hof1 might function during cytokinesis is in the formation of the secondary septum. As discussed in Chapter II, Hof1 and Chs3/Chs4 are localized to the bud neck late in the cell cycle as the septum is forming. Chs3 and Chs4 probably function at a low level to provide some chitin in the secondary septum as it forms. In addition, Chs3 and Chs4 are thought to function as a backup mechanism to make a remedial septum in the absence of Chs2. Their activity is probably increased as part of a cell stress response. Instead of a clearly distinguished chitin-containing primary septum sandwiched by a mannan/glucan-containing secondary septum as in wild-type (wt) cells, *chs2* Δ cells have thick aberrant septa with a diffuse distribution of chitin (Shaw et al., 1991).

Chs4 might also play a more direct role in $\beta(1,3)$ glucan synthesis in normal secondary septum formation. Recently it was discovered that a SEL-1 repeat containing protein resembling Chs4 in fission yeast, Cfh3p, is a novel regulator for the glucan synthase Bgs1p (Sharifmoghadam and Valdivieso, 2009). Chs4 might play a similar role in budding yeast, and Hof1 might be involved in the regulation of Chs4 in this process.

In conclusion, we had made progress toward understanding the pathways in budding yeast for coordinating ECM remodeling during cytokinesis. While work in the past 10 years has shown that targeted membrane is essential for cytokinesis in animal cells (Hales et al., 1999; Strickland and Burgess, 2004), it has been recognized for longer as essential in fungi and plants. This thesis might then have more immediate implications for plant cell wall formation and

remodeling as each form a structure between the daughter cells, the septum in yeast and the cell plate in plants. The cell plate is formed at the cleavage plane and requires the deposition of cell wall material via the secretory pathway. This process is mediated by formation of the phragmoplast, a complex array of microtubules, actin microfilaments and different membrane compartments (Heese et al., 1998). So while this thesis focused on specific cargo pathways, deposition of enzymes involved in making essential cell wall structures containing chitin, we hope that in studying individual pathways, we can identify unifying themes for all eukaryotic cells.

APPENDICES

Appendix 1. Yeast strains used in Chapter II^a

Strain	Genotype	Source
YEF473A	<i>a his3 leu2 lys2 trp1 ura3</i>	(Bi and Pringle, 1996)
YEF473B	<i>α his3 leu2 lys2 trp1 ura3</i>	(Bi and Pringle, 1996)
YEF1951	As YEF473A except <i>hof1Δ::KanMX6</i>	(Vallen et al., 2000)
YEF2197	As YEF473A except <i>chs4Δ::TRP1</i>	(DeMarini et al., 1997)
YEF2368	As YEF473A except <i>cyk3Δ::KanMX6</i>	This study
YEF2769	As YEF473A except <i>bni4Δ::TRP1</i>	This study
YEF4559	As YEF473A except <i>chs3Δ::TRP1</i>	This study
YEF4600	As YEF473A except <i>hof1Δ::TRP1</i>	This study
YEF4633	As YEF473A except <i>bnr1Δ::TRP1</i>	This study
YEF4915	As YEF473A except <i>hof1Δ::KanMX6</i> [YCp50LEU2-PGAL-HOF1-GFP]	This study
YEF4916	As YEF473A except <i>hof1Δ::KanMX6</i> [YCp50LEU2-PGAL-HOF1-Cterm-GFP]	This study
YEF4917	As YEF473A except <i>hof1Δ::KanMX6</i> [YCp50LEU2-PGAL-HOF1-FBAR-GFP]	This study
YEF4918	As YEF473A except <i>hof1Δ::KanMX6</i> [YCp50LEU2-PGAL-HOF1-SH3Δ-GFP]	This study
YEF4945	As YEF473A except <i>hof1Δ::KanMX6 cyk3Δ::HIS3MX6</i> [YCp50LEU2-HOF1-FBAR and pRS316-HOF1]	This study
YEF4949	As YEF473A except <i>hof1Δ::KanMX6 cyk3Δ::HIS3MX6</i> [YCp50LEU2-HOF1-Cterm and pRS316-HOF1]	This study
YEF4966	As YEF473A except <i>hof1Δ::KanMX6 cyk3Δ::HIS3MX6</i> [YCp50LEU2-HOF1 and pRS316-HOF1]	This study
YEF4970	As YEF473A except <i>hof1Δ::KanMX6 cyk3Δ::HIS3MX6</i> [YCp50LEU2 and pRS316-HOF1]	This study
YEF5421	As YEF473A except <i>hof1Δ::TRP1 CDC3-mcherry:HIS3MX6</i> [YCp50LEU2-HOF1-FBAR-GFP]	This study
YEF5423	As YEF473A except <i>hof1Δ::TRP1 CDC3-mcherry:HIS3MX6</i> [YCp50LEU2-HOF1-Cterm-GFP]	This study
YEF5428	As YEF473A except <i>hof1Δ::KanMX6</i> [YCp50LEU2-HOF1]	This study

YEF5429	As YEF473A except <i>hof1Δ::KanMX6</i> [YCp50LEU2-CYK3]	This study
YEF5430	As YEF473A except <i>hof1Δ::KanMX6</i> [YCp50LEU2]	This study
YEF5454	As YEF473A except <i>hof1Δ::TRP1 SPC42-mcherry:HIS3MX6 CDC3-GFP:KanMX6</i>	This study
YEF5469	As YEF473A except <i>SPC42-mcherry:HIS3MX6 CDC3-GFP:KanMX6</i>	This study
YEF5479	As YEF473A except <i>hof1Δ::TRP1 CDC3-mcherry:HIS3MX6</i> [YCp50LEU2-HOF1-GFP]	This study
YEF5529	As YEF473A except <i>TRP1-P_{CET1}-VN:CHS4ΔCAAX</i>	This study
YEF5533	As YEF473B except <i>HIS3MX6-P_{CET1}-VC:HOF1</i>	This study

^aGenes were deleted (the entire coding region in each case) or tagged at their C-termini using a PCR method (Baudin et al., 1993). Template plasmids were as described by Longtine et al. (1998) except for pFA6a-link-mCherry-His3MX6 (see Materials and Methods). In some cases, genomic DNA from previously transformed strains was used as a template in order to generate transformation fragments with longer flanking regions. Other steps in strain construction were conventional plasmid transformations.

Appendix 2. Plasmids used in Chapter II^a

Plasmid	Description ^a	Reference or source
YCp50LEU2	<i>CEN, LEU2</i>	Spencer and Hieter
YIp211-CDC3-mcherry	<i>inte, URA3</i>	(Tong et al., 2007)
YCp50LEU2-CYK3	<i>CEN, LEU2, CYK3</i>	Spencer and Hieter
pRS316-HOF1	<i>CEN, URA3, HOF1</i>	(Vallen, et al., 2000)
YCp50LEU2-HOF1	<i>CEN, LEU2, HOF1</i>	Spencer and Hieter
YCp50LEU2-HOF1-GFP	<i>CEN, LEU2, HOF1-GFP:KanMX6</i>	See text
YCp50LEU2-HOF1-FBAR-GFP	<i>CEN, LEU2, HOF1-FBAR-GFP:KanMX6</i>	See text
YCp50LEU2-HOF1-Cterm-GFP	<i>CEN, LEU2, HOF1-Cterm-GFP:KanMX6</i>	See text
YCp50LEU2-HOF1-FBAR	<i>CEN, LEU2, HOF1-FBAR:HIS3MX6</i>	See text
YCp50LEU2-HOF1-Cterm	<i>CEN, LEU2, HOF1-Cterm:HIS3MX6</i>	See text
YCp50LEU2-PGAL-HOF1-GFP	<i>CEN, LEU2, HIS3MX6:PGAL-HOF1-GFP:KanMX</i>	See text
YCp50LEU2-PGAL-HOF1-Cterm-GFP	<i>CEN, LEU2, HIS3MX6:PGAL-HOF1-Cterm-GFP:KanMX</i>	See text
YCp50LEU2-PGAL-HOF1-FBAR-GFP	<i>CEN, LEU2, HIS3MX6:PGAL-HOF1-FBAR-GFP:KanMX</i>	See text
YCp50LEU2-PGAL-HOF1-SH3 Δ -GFP	<i>CEN, LEU2, HIS3MX6:PGAL-HOF1-SH3Δ-GFP:KanMX</i>	See text

^a*CEN* indicates low-copy-number plasmids; 2u indicates high-copy-number plasmids

Appendix 3. Yeast strains used in Chapter III^a

Strain	Genotype	Source
YEF473	<i>a</i> α <i>his3/his3 leu2/leu2 lys2/lys2 trp1/trp1 ura3/ura3</i>	(Bi and Pringle, 1996)
YEF473A	<i>a his3 leu2 lys2 trp1 ura3</i>	(Bi and Pringle, 1996)
YEF473B	α <i>his3 leu2 lys2 trp1 ura3</i>	(Bi and Pringle, 1996)
Y860	α <i>his3-11, 15 leu2-3, 112 trp1-1 ade2-1 can1-100 ura3-1::URA3:lexAop-ADE2</i>	C. Boone
Y1026	<i>a his3-11, 15 leu2-3, 112 trp1-1 ade2-1 can1-100 ura3-1::URA3:lexAop-lacZ</i>	C. Boone
MOY157	As YEF473B except <i>INN1-GFP:TRP1 HOF1-TAP:His3MX6 cdc15-2</i>	This study ^b
MOY215	As YEF473B except <i>INN1-GFP:TRP1 cdc15-2</i>	This study ^b
MOY609	As YEF473 except <i>hof1Δ::TRP1/hof1Δ::TRP1 INN1/inn1Δ::kanMX6/ MYO1/myo1Δ::kanMX6 [pUG36-INN1][pRS315GW-C2-HOF1]</i>	This study
MOY630	As YEF473B except <i>hof1Δ::TRP1 myo1Δ::kanMX6 [pUG36-INN1][pRS315GW-C2-HOF1]</i>	Segregant of MOY609
MOY632	As YEF473B except <i>hof1Δ::TRP1 innΔ::kanMX6 [pUG36-INN1][pRS315GW-C2-HOF1]</i>	Segregant of MOY609
MOY634	As YEF473B except <i>hof1Δ::TRP1 inn1Δ::kanMX6 myo1Δ::kanMX6 [pUG36-INN1][pRS315GW-C2-HOF1]</i>	Segregant of MOY609
MWY764	As YEF473A except <i>hof1Δ::TRP1 iqg1Δ::His3MX6 [pRS316GW-IQG1]</i>	This study
MWY1145	As YEF473A except <i>hof1Δ::TRP1 inn1Δ::kanMX6 [pUG36-INN1]</i>	This study
RNY2225	As YEF473A except <i>hof1Δ::TRP1 chs2Δ::kanMX6 [pRS316-CHS2-myc]</i>	This study
RNY2393	As YEF473A except <i>iqg1Δ::His3MX6 INN1-GFP:KanMX6 [YCp50-IQG1]</i>	This study
RNY2395	As YEF473A except <i>INN1-GFP:KanMX6 [YCp50-IQG1]</i>	This study

RNY2494	As YEF473 except <i>INN1/pINN1-inn1(1-134)-GFP:His3MX6</i>	This study
RNY2498	As YEF473 except <i>INN1/TRP1:pGAL1-GFP-inn1(1-134):His3MX6</i>	This study
RNY2499	As YEF473 except <i>INN1/TRP1:pGAL1-GFP-INN1</i>	This study
LY1065	α <i>hof1Δ::KanMX6 ade2 ade3 his3 leu2 trp1 ura3</i> [pTSV30A-HOF1]	This study ^c
LY1067	a <i>hof1Δ::KanMX6 ade2 ade3 leu2 lys2 ura3</i> [pTSV31A-HOF1]	This study ^c
LY1302	As YEF473 except <i>INN1-GFP:KanMX6/INN1-GFP:KanMX6</i>	This study
LY1310	As YEF473A except <i>inn1Δ::KanMX6</i> [pUG36-INN1]	This study
LY1313	As YEF473A except <i>INN1-GFP:KanMX6</i>	This study
LY1314	As YEF473B except <i>INN1-GFP:KanMX6</i>	This study
LY1321	As YEF473A except <i>INN1-GFP:KanMX6 cyk3Δ::His3MX6</i>	This study
LY1324	As YEF473A except <i>INN1-GFP:KanMX6</i>	This study
LY1325	As YEF473A except <i>INN1-GFP:KanMX6 cyk3Δ::His3MX6 hof1Δ::KanMX6</i> [pRS316-HOF1]	This study
LY1328	As YEF473A except <i>INN1-GFP:KanMX6 hof1Δ::KanMX6</i> [pRS316-HOF1]	This study
LY1355	a <i>dbf2-1 dbf20Δ::TRP1 INN1-GFP:KanMX6 ade1 leu2 trp1 ura3</i>	This study ^d
LY1357	a <i>cdc5^{ts}::URA3 INN1-GFP:KanMX6 leu2 trp1 ura3</i>	This study ^d
LY1360	a <i>cdc14 INN1-GFP:KanMX6 can1 his7 leu2 ura3</i>	This study ^d
LY1364	As YEF473A except <i>myo1Δ::His3MX6 INN1-GFP:KanMX6</i> [YCp50-MYO1]	This study
LY1373	As YEF473A except <i>inn1Δ::KanMX6 CHS2-GFP:KanMX6</i> [pUG36-INN1]	This study
YEF1951	As YEF473A except <i>hof1Δ::KanMX6</i>	(Vallen et al., 2000)

YEF5202	As YEF473A except <i>inn1Δ::KanMX6</i> [pUG34mCherry-INN1-C2]	This study
YEF5216	As YEF473A except <i>inn1Δ::KanMX6</i>	This study
YEF5291	As YEF473A except <i>inn1Δ::KanMX6 MYO1-GFP:His3MX6</i>	This study
YEF5293	As YEF473A except <i>myo1Δ::His3MX6 INN1-GFP:KanMX6</i>	This study

^a Genes were deleted (the entire coding region in each case) or tagged at their C-termini using the PCR method (Baudin et al., 1993). Template plasmids were as described by Longtine et al. (1998) except for pFA6a-TAP-His3MX6 (P. Walter, University of California, San Francisco) and pFA6a-link-mCherry-His3MX6 (see Materials and methods). In some cases, genomic DNA from previously transformed strains was used as template in order to generate transformation fragments with longer flanking regions. Other steps in strain constructions were conventional genetic crosses and plasmid transformations.

^b *cdc15-2* was derived from strain DLY3034 (D. Lew, Duke University, Durham, NC) and backcrossed >7 times into the YEF473 background.

^c Derived from strains CDV38 and CDV39 (C. De Virgilio, University of Fribourg, Switzerland).

^d Strains J230-2D (L. Johnston, National Institute for Medical Research, London, UK), KKY021 (L. Johnston), and 4078-14-3a (L. Hartwell, Fred Hutchinson Cancer Research Center, Seattle, WA) were transformed with a PCR-generated *INN1-GFP:KanMX6* cassette.

Appendix 4. Plasmids used in Chapter III

Plasmid	Description ^a	Reference or source
YEplac181	2 μ , <i>LEU2</i>	Gietz and Sugino (1988)
pRS315GW	<i>CEN</i> , <i>LEU2</i>	Pringle lab
pRS425	2 μ , <i>LEU2</i>	(Christianson et al., 1992)
pRS315-GFP-RAS2	<i>CEN</i> , <i>LEU2</i> , <i>GFP-RAS2</i>	(Luo et al., 2004)
YCp111-CDC3-CFP	<i>CEN</i> , <i>LEU2</i> , <i>CDC3-CFP</i>	Pringle lab
YCp50-MYO1	<i>CEN</i> , <i>URA3</i> , <i>MYO1</i>	S. Brown
pBK65	2 μ , <i>LEU2</i> , <i>MLC1</i>	J. Chant
pRS316-CHS2-myc	<i>CEN</i> , <i>URA3</i> , <i>CHS2-MYC</i>	Pringle lab
pRS316GW-IQG1	<i>CEN</i> , <i>URA3</i> , <i>IQG1</i>	Pringle lab
YCp50-IQG1 (= p1868)	<i>CEN</i> , <i>URA3</i> , <i>IQG1</i>	(Korinek et al., 2000)
YEp181-IQG1	2 μ , <i>LEU2</i> , <i>IQG1</i>	(Ko et al., 2007)
pBK132	2 μ , <i>LEU2</i> , <i>CYK3</i>	(Korinek et al., 2000)
pBK133	2 μ , <i>LEU2</i> , <i>CYK3</i>	(Korinek et al., 2000)
pRS425-CYK3	2 μ , <i>LEU2</i> , <i>CYK3</i>	(Ko et al., 2007)
pRS315GW-CYK3-2GFP	<i>CEN</i> , <i>LEU2</i> , <i>CYK3-2GFP</i>	Pringle lab
pRS315GW-NotI-HOF1	<i>CEN</i> , <i>LEU2</i> , <i>HOF1</i>	Pringle lab
pRS316-HOF1	<i>CEN</i> , <i>URA3</i> , <i>HOF1</i>	(Vallen et al., 2000)
YCp50LEU2-HOF1	<i>CEN</i> , <i>LEU2</i> , <i>HOF1</i>	See text
pTSV30A-HOF1	2 μ , <i>LEU2</i> , <i>ADE3</i> , <i>HOF1</i>	See text
pTSV31A-HOF1	2 μ , <i>URA3</i> , <i>ADE3</i> , <i>HOF1</i>	See text
YCp50LEU2-INN1-17C	<i>CEN</i> , <i>LEU2</i> , <i>INN1</i>	See text
pGP564-INN1	2 μ , <i>LEU2</i> , <i>INN1</i>	F. Luca
pUG34mCherry	<i>CEN</i> , <i>HIS3</i> , <i>pMET25-mCherry</i>	See text
pUG34mCherry-INN1 ^b	<i>CEN</i> , <i>HIS3</i> , <i>pMET25-mCherry-INN1</i>	See text

pUG36-INN1	<i>CEN, URA3, pMET25-yEGFP-INN1</i>	See text
pRS315GW-C2-HOF1	<i>CEN, LEU2, C2-HOF1</i>	See text

^a *CEN* indicates low-copy-number plasmids; 2 μ indicates high-copy-number plasmids.

^b Related plasmids contain the wild-type *INN1* N-terminus (amino acids 1-140) or C-terminus (amino acids 130-409), or full-length or *INN1* into which mutations *m1-m4* (Fig. 1) had been introduced singly or in combinations (see Materials and methods).

LITERATURE CITED

- Abelovska, L., Bujdos, M., Kubova, J., Petrezselyova, S., Nosek, J., Tomaska, L.** (2007) Comparison of element levels in minimal and complex yeast media. *Can. J. Microbiol.* **53**, 533-535.
- Albertson, R., Riggs, B., Sullivan, W.** (2005) Membrane traffic: a driving force in cytokinesis. *Trends Cell Biol.* **15**, 92-101.
- Altman, R., and Kellogg, D.** (1997) Control of mitotic events by Nap1 and the Gin4 kinase. *J. Cell Biol.* **138**, 119-130.
- Anderson, B. L., Boldogh, I., Evangelista, M., Boone, C., Greene, L. A., Pon, L. A.** (1998) The Src homology domain 3 (SH3) of a yeast type I myosin, Myo5p, binds to verprolin and is required for targeting to sites of actin polarization. *J. Cell Biol.* **141**, 1357-1370.
- Anggono, V., Smillie, K. J., Graham, M. E., Valova, V. A., Cousin, M. A., Robinson, P. J.** (2006) Syndapin I is the phosphorylation-regulated dynamin I partner in synaptic vesicle endocytosis. *Nat. Neurosci.* **9**, 652-660.
- Ayscough, K. R., Stryker, J., Pokala, N., Sanders, M., Crews, P., Drubin, D. G.** (1997) High rates of actin filament turnover in budding yeast and roles for actin in establishment and maintenance of cell polarity revealed using the actin inhibitor Latrunculin-A. *J. Cell Biol.* **137**, 399-416.
- Baudin, A., Ozier-Kalogeropoulos, O., Denouel, A., Lacroute, F., Cullin, C.** (1993) A simple and efficient method for direct gene deletion in *Saccharomyces cerevisiae*. *Nucleic Acids Res.* **21**, 3329-3330.
- Balasubramanian, M. K., McCollum, D., Chang, L., Wong, K. C., Naqvi, N. I., He, X., Sazer, S., Gould, K. L.** (1998) Isolation and characterization of new fission yeast cytokinesis mutants. *Genetics* **149**, 1265-1275.
- Balasubramanian, M. K., Bi, E., Glotzer, M.** (2004) Comparative analysis of cytokinesis in budding yeast, fission yeast and animal cells. *Curr. Biol.* **14**, 806-818.

- Barr, F. A., Gruneberg, U.** (2007) Cytokinesis: placing and making the final cut. *Cell* **131**, 847-860.
- Bender, A., and Pringle, J. R.** (1991) Use of a screen for synthetic lethal and multicopy suppresser mutants to identify two new genes involved in morphogenesis in *Saccharomyces cerevisiae*. *Mol. Cell. Biol.* **11**, 1295-1305.
- Benes, C.H., Wu, N., Elia, A. E., Dharia, T., Cantley, L. C., Soltoff, S. P.** (2005) The C2 domain of PKCdelta is a phosphotyrosine binding domain. *Cell* **121**,271-280.
- Bertin, A., McMurray, M. A., Grob, P., Park, S. S., Garcia, G., Patanwala, I., Ng, H. L., Alber, T., Thorner, J., Nogales, E.** (2008) *Saccharomyces cerevisiae* septins: supramolecular organization of heterooligomers and the mechanism of filament assembly. *Proc. Natl. Acad. Sci. USA.* **105**, 8274-8279.
- Bi, E., Maddox, P., Lew, D. J., Salmon, E. D., McMillan, J. N., Yeh, E., Pringle, J. R.** (1998) Involvement of an actomyosin contractile ring in *Saccharomyces cerevisiae* cytokinesis. *J. Cell Biol.* **142**, 1301-1312.
- Bi, E.** (2001) Cytokinesis in budding yeast: the relationship between actomyosin ring function and septum formation. *Cell Struct. Funct.* **26**, 529-537.
- Bi, E., and Pringle, J. R.** (1996) ZDS1 and ZDS2, genes whose products may regulate Cdc42p in *Saccharomyces cerevisiae*. *Mol. Cell. Biol.* **16**, 5264-5275.
- Blondel, M., Bach, S., Bamps, S., Dobbelaere, J., Wiget, P., Longaretti, C., Barral, Y., Meijer, L., Peter, M.** (2005) Degradation of Hof1 by SCF(Grr1) is important for actomyosin contraction during cytokinesis in yeast. *EMBO J.* **24**, 1440-1452.
- Bouquin, N., Barral, Y., Courbeyrette, R., Blondel, M., Snyder, M., Mann, C.** (2000) Regulation of cytokinesis by the Elm1 protein kinase in *Saccharomyces cerevisiae*. *J. Cell Sci.* **113**, 1435-1445.
- Boyne, J.R., Yosuf, H. M., Bieganowski, P., Brenner, C., Price, C.** (2000) Yeast myosin light chain, Mlc1p, interacts with both IQGAP and class II myosin to effect cytokinesis. *J. Cell Sci.* **113**, 4533-4543.

- Braun, A., Pinyol, R., Dahlhaus, R., Koch, D., Fonarev, P., Grant, B. D., Kessels, M. M., Qualmann, B.** (2005) EHD proteins associate with syndapin I and II and such interactions play a crucial role in endosomal recycling. *Mol. Biol. Cell* **16**, 3642-3658.
- Bulawa, C. E.** (1993). "Genetics and Molecular Biology of Chitin Synthesis in Fungi." *Annu. Rev. Microbiol.* **47**, 505-534.
- Bulawa, C.E., and Osmond, B. C.** (1990) Chitin synthase I and chitin synthase II are not required for chitin synthesis in vivo in *Saccharomyces cerevisiae*. *Proc. Natl. Acad. Sci. USA.* **87**, 7424-7428.
- Buttery, S. M., Yoshida, S., Pellman, D.** (2007) Yeast formins Bni1 and Bnr1 utilize different modes of cortical interaction during the assembly of actin cables. *Mol. Biol. Cell* **18**, 1826-1838.
- Cabib, E., Sburlati, A., Bowers, B., Silverman, S. J.** (1989). Chitin synthase 1, an auxiliary enzyme for chitin synthesis in *Saccharomyces cerevisiae*. *J. Cell Biol.* **108**, 1665-1672.
- Cabib, E., Shaw, J.A., Mol, P.C., Bowers, B., Choi, W. J.** (1996) Chitin biosynthesis and morphogenetic processes. In *The Mycota. Biochemistry and Molecular Biology.* (ed. R. Brambl and G. A. Marzluf), pp. 243-267. Berlin: Springer-Verlag.
- Cabib, E., Schmidt, M.** (2003) Chitin synthase II activity, but not the chitin ring, is required for remedial septa formation in budding yeast. *FEMS Microbiol. Lett.* **224**, 299-305.
- Caldwell, C. M., Green, R. A., Kaplan, K. B.** (2007) APC mutations lead to cytokinetic failures in vitro and tetraploid genotypes in Min mice. *J. Cell Biol.* **178**, 1109-1120.
- Caviston, J.P., Longtine, M., Pringle, J. R., Bi, E.** (2003) The role of Cdc42p GTPase-activating proteins in assembly of the septin ring in yeast. *Mol. Biol. Cell.* **14**, 4051-4066.
- Chitu, V., Pixley, F. J., Macaluso, F., Larson, D. R., Condeelis, J., Yeung, Y. G., Stanley, E. R.** (2005) The PCH family member MAYP/PSTPIP2 directly regulates F-actin bundling and enhances filopodia formation and motility in macrophages. *Mol. Biol. Cell* **16**, 2947-2959.

- Chitu, V. and Stanley, E. R.** (2007). Pombe Cdc15 homology (PCH) proteins: coordinators of membrane-cytoskeletal interactions. *Trends Cell Biol.* **17**, 145-156.
- Cho, W., and Stahelin, R. V.** (2006) Membrane binding and subcellular targeting of C2 domains. *Biochim. Biophys. Acta.* **1761**, 838-849.
- Choi, W. J., Santos, B., Duran, A., Cabib, E.** (1994). Are yeast chitin synthases regulated at the transcriptional or the posttranslational level? *Mol. Cell. Biol.* **14**, 7685-7694.
- Christianson, T.W., Sikorski, R. S., Dante, M., Shero, J. H., Hieter, P.** (1992) Multifunctional yeast high copy number shuttle vectors. *Gene.* **110**, 119-122.
- Chuang, J.S., and Schekman, R. W.** (1996) Differential trafficking and timed localization of two chitin synthase proteins, Chs2p and Chs3p. *J. Cell Biol.* **135**, 597-610.
- Corbett, M., Xiong, Y., Boyne, J. R., Wright, D. J., Munro, E., Price, C.** (2006) IQGAP and mitotic exit network (MEN) proteins are required for cytokinesis and re-polarization of the actin cytoskeleton in the budding yeast, *Saccharomyces cerevisiae*. *Eur. J. Cell Biol.* **85**, 1201-1215.
- Corson, T. W. and Gallie, B. L.** (2006) KIF14 mRNA expression is a predictor of grade and outcome in breast cancer. *Int. J. Cancer* **119**, 1088-1094.
- Creutz, C.E., Snyder, S. L., Schulz, T. A.** (2004) Characterization of the yeast tricalbins: membrane-bound multi-C2-domain proteins that form complexes involved in membrane trafficking. *Cell Mol. Life Sci.* **61**, 1208-1220.
- Dai, H., Shen, N., Arac, D., Rizo, J.** (2007) A quaternary SNARE-synaptotagmin-Ca²⁺-phospholipid complex in neurotransmitter release. *J. Mol. Biol.* **367**, 848-863.
- Danilchik, M. V., Bedrick, S. D., Brown, E. E., Ray, K.** (2003) Furrow microtubules and localized exocytosis in cleaving *Xenopus laevis* embryos. *J. Cell Sci.* **116**, 273-283.
- De Lozanne, A., and Spudich, J. A.** (1987) Disruption of the *Dictyostelium* myosin heavy chain gene by homologous recombination. *Science.* **236**, 1086-1091.

- DeMarini, D. J., Adams, A. E. M., Fares, H., De Virgilio, C., Valle, G., Chuang, J. S., Pringle, J. R.** (1997). A septin-based hierarchy of proteins required for localized deposition of chitin in the *Saccharomyces cerevisiae* cell wall. *J. Cell Biol.* **139**, 75-93.
- Dobbelaere, J., Barral, Y.** (2004) Spatial coordination of cytokinetic events by compartmentalization of the cell cortex. *Science.* **305**, 393-396.
- Dobbelaere, J., Gentry, M. S., Hallberg, R. L., Barral, Y.** (2003) Phosphorylation-dependent regulation of septin dynamics during the cell cycle. *Dev. Cell* **4**, 345-357.
- Echard, A., Hickson, G. R., Foley, E., O'Farrell, P. H.** (2004) Terminal cytokinesis events uncovered after an RNAi screen. *Curr. Biol.* **14**, 1685-1693.
- Echard, A.** (2008) Membrane traffic and polarization of lipid domains during cytokinesis. *Biochem. Soc. Trans.* **36**, 395-399.
- Epp, J. A. and Chant, J.** (1997) An IQGAP-related protein controls actin-ring formation and cytokinesis in yeast. *Curr. Biol.* **7**, 921-929.
- Evangelista, M., Blundell, K., Longtine, M. S., Chow, C. J., Adames, N., Pringle, J. R., Peter, M., Boone, C.** (1997) Bni1p, a yeast formin linking Cdc42p and the actin cytoskeleton during polarized morphogenesis. *Science* **276**, 118-122.
- Evangelista, M., Klebl, B. M., Tong, A. H., Webb, B. A., Leeuw, T., Leberer, E., Whiteway, M., Thomas, D. Y., Boone, C.** (2000) A role for myosin-I in actin assembly through interactions with Vrp1p, Bee1p, and the Arp2/3 complex. *J Cell Biol.* **148**, 353-362.
- Fankhauser, C., Reymond, A., Cerutti, L., Utzig, S., Hofmann, K., Simanis, V.** (1995) The *S. pombe* *cdc15* gene is a key element in the reorganization of F-actin at mitosis. *Cell* **82**, 435-111.
- Feller, S.M., Ren, R., Hanafusa, H., Baltimore, D.** (1994) SH2 and SH3 domains as molecular adhesives: the interactions of Crk and Abl. *Trends Biochem. Sci.* **19**, 453-458.
- Finger, F.P., White, J. G.** (2002) Fusion and fission: membrane trafficking in animal cytokinesis. *Cell.* **108**, 727-730.

- Fujiwara, T., Tanaka, K., Mino, A., Kikyo, M., Takahashi, K., Shimizu, K., Takai, Y.** (1998) Rho1p-Bni1p-Spa2p interactions: Implication in localization of Bni1p at the bud site and regulation of the actin cytoskeleton in *Saccharomyces cerevisiae*. *Mol. Biol. Cell* **9**, 1221-1233.
- Fujiwara, T., Bandi, M., Nitta, M., Ivanova, E. V., Bronson, R. T., Pellman, D.** (2005) Cytokinesis failure generating tetraploids promotes tumorigenesis in p53-null cells. *Nature* **437**, 1043-1047.
- Ganem N. J., Storchova Z, Pellman D.** (2007) Tetraploidy, aneuploidy and cancer. *Curr Opin Genet Dev.* **17**, 157-162.
- Gietz, R.D., Sugino, A.** (1988) New yeast-Escherichia coli shuttle vectors constructed with in vitro mutagenized yeast genes lacking six-base pair restriction sites. *Gene* **74**, 527-534.
- Gladfelter, A. S., Pringle, J. R., Lew, D. J.** (2001) The septin cortex at the yeast mother-bud neck. *Curr. Opin. Microbiol.* **4**, 681-689.
- Grabinska, K. A., Magnelli, P., Robbins, P. W.** (2007). Prenylation of *Saccharomyces cerevisiae* Chs4p affects chitin synthase III activity and chitin chain length. *Eukaryotic Cell* **6**, 328-336.
- Grant, B. and Greenwald, I.** (1996). The *Caenorhabditis elegans* sel-1 gene, a negative regulator of lin-12 and glp-1, encodes a predicted extracellular protein. *Genetics* **143**, 237-247.
- Guthrie, C., Fink, G. R.** (1991) Guide to Yeast Genetics and Molecular Biology. *Methods Enzymol.* Vol. **194**, 933 pp.
- Gyuris, J., Golemis, E., Chertkov, H., Brent, R.** (1993) Cdi1, a human G1 and S phase protein phosphatase that associates with Cdk2. *Cell* **75**, 791-803.
- Hales, K. G., Bi, E., Wu, J. Q., Adam, J. C., Yu, I. C., Pringle, J. R.** (1999) Cytokinesis: an emerging unified theory for eukaryotes? *Curr Opin Cell Biol.* **11**, 717-725.

- Hartland, R. P., Vermeulen, C. A., Sietsma, J. H., Wessels, J. G. H., Klis, F. M.** (2004) The linkage of (1-3)- β -glucan to chitin during cell wall assembly in *Saccharomyces cerevisiae*. *Yeast* **10**, 1591-1599.
- Heath, R.J., and Insall, R. H.** (2008) F-BAR domains: multifunctional regulators of membrane curvature. *J. Cell Sci.* **121**, 1951-1954.
- Heissig, B., Hattori, K., Friedrich, M., Rafii, S., Werb, Z.** (2003) Angiogenesis: vascular remodeling of the extracellular matrix involves metalloproteinases. *Curr. Opin. Hematol.* **10**, 136-141.
- Henne, W. M., Kent, H. M., Ford, M. G. J., Hegde, B. G., Daumke, O., Butler, P. J. G., Mittal, R., Langen, R., Evans, P. R., McMahon, H. T.** (2007). Structure and analysis of FChO2 F-BAR domain: a dimerizing and membrane recruitment module that effects membrane curvature. *Structure* **15**, 839-852.
- Heese, M., Mayer, U., Jürgens, G.** (2003) Cytokinesis in flowering plants: cellular process and developmental integration. *Curr. Opin. Plant Biol.* **1**, 486-491.
- Hibi, M., Nagasaki, A., Takahashi, M., Yamagishi, A., Uyeda, T.Q.** (2004) Dictyostelium discoideum talin A is crucial for myosin II-independent and adhesion-dependent cytokinesis. *J. Muscle Res. Cell Motil.* **25**, 127-140.
- Holthuis, J. C. M., Nichols, B. J., Pelham, H. R. B.** (1998). The syntaxin Tlg1p mediates trafficking of chitin synthase III to polarized growth sites in yeast. *Mol. Biol. Cell* **9**, 3383-3397.
- Hwa Lim, H., Yeong, F. M., Surana, U.** (2003) Inactivation of mitotic kinase triggers translocation of MEN components to mother-daughter neck in yeast. *Mol. Biol. Cell.* **14**, 4734-4743.
- Hsu, S. C., TerBush, D., Abraham, M., Guo, W.** (2004) The exocyst complex in polarized exocytosis. *Int. Rev. Cytol.* **233**, 243-265.
- Inoue, H., Ha, V. L., Prekeris, R., Randazzo, P.A.** (2008). Arf GTPase-activating protein ASAP1 interacts with Rab11 effector FIP3 and regulates pericentrosomal localization of transferring receptor-positive recycling endosome. *Mol. Biol. Cell* **19**, 4224-4237.

- Ito, T., Chiba, T., Ozawa, R., Yoshida, M., Hattori, M., Sakaki, Y.** (2001) A comprehensive two-hybrid analysis to explore the yeast protein interactome. *Proc. Natl. Acad. Sci. USA.* **98**, 4569-4574.
- Itoh, T., Erdmann, K. S., Roux, A., Habermann, B., Werner, H., De Camilli, P.** (2005). Dynamin and the actin cytoskeleton cooperatively regulate plasma membrane invagination by BAR and F-BAR proteins. *Dev. Cell* **9**: 791-804.
- Itoh, Y., Takamura, A., Ito, N., Maru, Y., Sato, H., Suenaga, N., Aoki, T., Seiki, M.** (2001) Homophilic complex formation of MT1-MMP facilitates proMMP-2 activation on the cell surface and promotes tumor cell invasion. *EMBO J.* **20**, 4782-4793.
- Joo, E., Tsang, C. W., Trimble, W. S.** (2005) Septins: traffic control at the cytokinesis intersection. *Traffic* **6**, 626-634.
- Kamei, T., Tanaka, K., Hihara, T., Umikawa, M., Imamura, H., Kikyō, M., Ozaki, K., Takai, Y.** (1998). Interaction of Bnr1p with a Novel Src Homology 3 Domain-containing Hof1p. *J. Biol. Chem.* **273**, 28341-28345.
- Kamioka, Y., Fukuhara, S., Sawa, H., Nagashima, K., Masuda, M., Matsuda, M., Mochizuki, N.** (2004) A novel dynamin-associating molecule, formin-binding protein 17, induces tubular membrane invaginations and participates in endocytosis. *J. Biol. Chem.* **279**, 40091-40099.
- Kanada, M., Nagasaki, A., Uyeda, T. Q.** (2008) Novel functions of Ect2 in polar lamellipodia formation and polarity maintenance during "contractile ring-independent" cytokinesis in adherent cells. *Mol. Biol. Cell.* **19**, 8-16.
- Kaufmann, A. and Philippsen, P.** (2009). Of bars and rings: Hof1-dependent cytokinesis in multiseptated hyphae of *Ashbya gossypii*. *Mol. Cell. Biol.* **29**, 771-783.
- Kessels, M. M. and Qualmann, B.** (2002) Syndapins integrate N-WASP in receptor-mediated endocytosis. *EMBO J.* **21**, 6083-6094.

- Kessels, M. M., Dong, J., Leibig, W., Westermann, P., Qualmann, B.** (2006) Complexes of syndapin II with dynamin II promote vesicle formation at the trans-Golgi network. *J. Cell Sci.* **119**, 1504-1516.
- Kikyo, M., Tanaka, K., Kamei, T., Ozaki, K., Fujiwara, T., Inoue, E., Takita, Y., Ohya, Y., Takai, Y.** (1999) An FH domain-containing Bnr1p is a multifunctional protein interacting with a variety of cytoskeletal proteins in *Saccharomyces cerevisiae*. *Oncogene* **18**, 7064-7054.
- Kim, H.B., Haarer, B. K., Pringle, J. R.** (1991) Cellular morphogenesis in the *Saccharomyces cerevisiae* cell cycle: localization of the CDC3 gene product and the timing of events at the budding site. *J. Cell Biol.* **112**, 535-544.
- Ko, N., Nishihama, R., Tully, G. H., Ostapenko, D., Solomon, M. J., Morgan, D. O., Pringle, J. R.** (2007) Identification of yeast IQGAP (Iqg1p) as an anaphase-promoting-complex substrate and its role in actomyosin-ring-independent cytokinesis. *Mol. Biol. Cell.* **18**, 5139-5153.
- Korinek, W. S., Bi, E., Epp, J. A., Wang, L., Ho, J., Chant, J.** (2000). Cyk3, a novel SH3-domain protein, affects cytokinesis in yeast. *Curr. Biol.* **10**, 947-954.
- Kota, J. and Ljungdahl, P. O.** (2005) Specialized membrane-localized chaperones prevent aggregation of polytopic proteins in the ER. *J. Cell Biol.* **168**, 79-88.
- Kozubowski, L., Panek, H., Rosenthal, A., Bloecher, A., DeMarini, D., Tatchell, K.** (2003). A Bni4-Glc7 phosphatase complex that recruits chitin synthase to the site of bud emergence. *Mol. Biol. Cell* **14**, 26-39.
- Kozubowski, L., Larson, J. R., Tatchell, K.** (2005) Role of the septin ring in the asymmetric localization of proteins at the mother-bud neck in *Saccharomyces cerevisiae*. *Mol. Biol. Cell.* **16**, 3455-3466.
- Larson, J. R., Bharucha, J. P., Ceaser, S., Salamon, J., Richardson, C. J., Rivera, S. M., Tatchell, K.** (2008). Protein phosphatase type 1 directs chitin synthesis at the bud neck in *Saccharomyces cerevisiae*. *Mol. Biol. Cell* **19**, 3040-3051.

- Lee, P.R., Song, S., Ro, H. S., Park, C. J., Lippincott, J., Li, R., Pringle, J. R., De Virgilio, C., Longtine, M. S., Lee, K. S.** (2002) Bni5p, a septin-interacting protein, is required for normal septin function and cytokinesis in *Saccharomyces cerevisiae*. *Mol. Cell. Biol.* **22**, 6906-6920.
- Lillie, S. H. and Pringle, J. R.** (1980). Reserve carbohydrate metabolism in *Saccharomyces cerevisiae*: responses to nutrient limitation. *J. Bacteriol.* **143**, 1384-1394.
- Lippincott, J. and Li, R.** (1998) Sequential assembly of Myosin II, an IQGAP-like protein, and filamentous actin to a ring structure involved in budding yeast cytokinesis. *J. Cell Biol.* **140**, 355-366.
- Lippincott, J. and Li, R.** (2000) Involvement of PCH family proteins in cytokinesis and actin distribution. *Microsc. Res. Tech.* **49**, 168-172.
- Lippincott, J., Shannon, K. B, Shou, W., Deshaies, R. J., Li, R.** (2001) The Tem1 small GTPase controls actomyosin and septin dynamics during cytokinesis. *J. Cell Sci.* **114**, 1379-1386.
- Longtine, M. S., DeMarini, D. J., Valencik, M. L., Al-Awar, O. S., Fares, H., De Virgilio, C., Pringle, J. R.** (1996). The septins: roles in cytokinesis and other processes. *Curr. Opin. Cell Biol.* **8**, 106-119.
- Longtine, M.S., Mckenzie, A., Demarini, D.J., Shah, N.G., Wach, A., Brachat, A., Philippsen, P., Pringle, J.R.** (1998). Additional modules for versatile and economical PCR-based gene deletion and modification in *Saccharomyces cerevisiae*. *Yeast* **14**, 953-961.
- Longtine, M. S. and Bi, E.** (2003) Regulation of septin organization and function in yeast. *Trends Cell Biol.* **13**, 403-409.
- Lord, M., Laves, E., Pollard, T. D.** (2005) Cytokinesis depends on the motor domains of myosin-II in fission yeast but not in budding yeast. *Mol. Biol. Cell.* **16**, 5346-5355.
- Lu, J., Machius, M., Dulubova, I., Dai, H., Sudhof, T. C., Tomchick, D. R., Rizo, J.** (2006) Structural basis for a Munc13-1 homodimer to Munc13-1/RIM heterodimer switch. *PLoS Biol.* **4**, e192.

- Luo, J., Vallen, E. A., Dravis, C., Tcheperegine, S. E., Drees, B., Bi, E.** (2004) Identification and functional analysis of the essential and regulatory light chains of the only type II myosin Myo1p in *Saccharomyces cerevisiae*. *J. Cell Biol.* **165**, 843-855.
- Makarova, K.S., Aravind, L., Koonin, E. V.** (1999). A superfamily of archaeal, bacterial, and eukaryotic proteins homologous to animal transglutaminases. *Protein Sci.* **8**, 1714-9.
- Mittl, P. R. E. and Schneider-Brachert, W.** (2007) Sel1-like repeat proteins in signal transduction. *Cell Signal.* **19**, 20-31.
- Mizuguchi, S., Uyama, T., Kitagawa, H., Nomura, K. H., Dejima, K., Gengyo-Ando, K., Mitani, S., Sugahara, K., Nomura, K.** (2003) Chondroitin proteoglycans are involved in cell division of *Caenorhabditis elegans*. *Nature (London)*. **423**, 443-448.
- Modregger, J., Ritter, B., Witter, B., Paulsson, M., Plomann, M.** (2000) All three PACSIN isoforms bind to endocytic proteins and inhibit endocytosis. *J. Cell Sci.* **113**, 4511-4521.
- Montagnac, G., Echard, A., Chavier, P.** (2008) Endocytic traffic in animal cell cytokinesis. *Curr. Opin. Cell Biol.* **2008**, 454-461.
- Mori, H., Tomari, T., Koshikawa, N., Kajita, M., Itoh, Y., Sato, H., Tojo, H., Yana, I., Seiki, M.** (2002) CD44 directs membrane-type 1 matrix metalloproteinase to lamellipodia by associating with its hemopexin-like domain. *EMBO J* **21**, 3949-3959.
- Mortensen, E.M., McDonald, H., Yates, J., Kellogg, D. R.** (2002) Cell cycle-dependent assembly of a Gin4-septin complex. *Mol. Biol. Cell.* **13**, 2091-2105.
- Moseley, J. B., Goode, B. L.** (2006) The yeast actin cytoskeleton: from cellular function to biochemical mechanism. *Microbiol Mol Biol Rev.* **70**, 605-645.
- Naqvi, S. N., Zahn, R., Mitchell, D. A., Stevenson, B. J., Munn, A. L.** (1998) The WASp homologue Las17p functions with the WIP homologue End5p/verprolin and is essential for endocytosis in yeast. *Curr Biol.* **8**, 959-962.
- Naqvi, S. N., Feng, Q., Boulton, V. J., Zahn, R., Munn, A. L.** (2001) Vrp1 functions in both actomyosin ring-dependent and Hof1p-dependent pathways of cytokinesis. *Traffic* **2**, 189-201.

- Narayan, K., Lemmon, M. A.** (2006) Determining selectivity of phosphoinositide-binding domains. *Methods* **39**, 122-133.
- Neujahr, R., Heizer, C., Gerisch, G.** (1997) Myosin II-independent processes in mitotic cells of *Dictyostelium discoideum*: redistribution of the nuclei, re-arrangement of the actin system and formation of the cleavage furrow. *J. Cell Sci.* **110**, 123-137.
- Ng, M.M., Chang, F., Burgess, D. R.** (2005) Movement of membrane domains and requirement of membrane signaling molecules for cytokinesis. *Dev. Cell* **9**, 781-790.
- Nguyen, M., Arkell, J., Jackson, C. J.** (2001) Human endothelial gelatinases and angiogenesis. *Int. J. Biochem. Cell Biol.* **2001**, 960-970.
- Nishihama, R., Ko, N., Perdue, T. D., Pringle, J. R.** (2009) Roles of yeast Iqg1p (IQGAP) and Cyk3p in actomyosin-ring-independent cleavage-furrow formation. In preparation.
- Otegui, M.S., Verbrugghe, K. J., Skop, A. R.** (2005) Midbodies and phragmoplasts: analogous structures involved in cytokinesis. *Trends Cell Biol.* **15**, 404-413.
- Pan, F., Malmberg, R. L., Momany, M.** (2007) Analysis of septins across kingdoms reveals orthology and new motifs. *BMC Evol. Biol.* **7**, 103.
- Pérez-Otaño, I., Luján, R., Tavalin, S. J., Plomann, M., Modregger, J., Liu, X. B., Jones, E. G., Heinemann, S. F., Lo, D. C., Ehlers, M. D.** (2006) Endocytosis and synaptic removal of NR3A-containing NMDA receptors by PACSIN1/syndapin1. *Nat. Neurosci.* **9**, 611-621.
- Popolo, L., Gilardelli, D., Bonfante, P., Vai, M.** (1997) Increase in chitin as an essential response to defects in assembly of cell wall polymers in the *gpp1delta* mutant of *Saccharomyces cerevisiae*. *J. Bacteriol.* **179**, 463-469.
- Prouzet-Mauléon, V., Lefebvre, F., Thoraval, D., Crouzet, M., Doignon, F.** (2008) Phosphoinositides affect both the cellular distribution and activity of the F-BAR-containing RhoGAP Rgd1p in yeast. *J. Biol. Chem.* **283**, 33249-33257.
- Pruyne, D., Bretscher, A.** (2000) Polarization of cell grown in yeast. *J. Cell Sci.* **113**, 571-585.

- Pruyne, D., Evangelista, M., Yang, C., Bi, E., Zigmond, S., Bretscher, A., Boone, C. (2002)**
 Role of formins in actin assembly: nucleation and barbed-end association. *Science* **297**, 612-615.
- Qian, J., Chen, W., Lettau, M., Podda, G., Zörnig, M., Kabelitz, D., Janssen, O. (2005)**
 Regulation of FasL expression: a SH3 domain containing protein family involved in the lysosomal association of FasL. *Cell. Signal.* **18**, 1327-1337.
- Ram, A. F. J., Kapteyn, J. C., Montijn, R. C., Caro, L. H. P., Douwes, J. E., Baginsky, W., Mazur, P., van den Ende, H., Klis, F. M. (1998)** Loss of the plasma membrane-bound protein Gas1p in *Saccharomyces cerevisiae* Results in the Release of beta 1,3-Glucan into the Medium and Induces a Compensation Mechanism To Ensure Cell Wall Integrity. *J. Bacteriol.* **180**, 1418-1424.
- Ren, G., Wang, J., Brinkworth, R., Winsor, B., Kobe, B., Munn, A. L. (2005)** Verprolin cytokinesis function mediated by the Hof1 one trap domain. *Traffic* **6**, 575-593.
- Reyes, A., Sanz, M., Duran, A., Roncero, C., (2007)** Chitin synthase III requires Chs4p-dependent translocation of Chs3p into the plasma membrane. *J. Cell. Sci.* **120**, 1998-2009.
- Rizo, J., and Sudhof, T.C. (1998)** C2-domains, structure and function of a universal Ca²⁺-binding domain. *J. Biol. Chem.* **273**, 15879-15882.
- Rodriguez, J. R. and Paterson, B. M. (1990)** Yeast myosin heavy chain mutant: maintenance of the cell type specific budding pattern and the normal deposition of chitin and cell wall components requires an intact myosin heavy chain gene. *Cell Motil Cytoskeleton* **17**, 301-308.
- Rodriguez-Pena, J.M., Rodriguez, C., Alvarez, A., Nombela, C., Arroyo, J. (2002)**
 Mechanisms for targeting of the *Saccharomyces cerevisiae* GPI-anchored cell wall protein Crh2p to polarised growth sites. *J. Cell Sci.* **115**, 2549-2558.

- Roversi, G., Pfundt, R., Moroni, R. F., Magnani, I., van Reijmersdal, S., Pollo, B., Straatman, H., Larizza, L., Schoenmakers, E. F. P. M.** (2006) Identification of novel genomic markers related to progression to glioblastoma through genomic profiling of 25 primary glioma cell lines. *Oncogene* **25**, 1571-1583.
- Rubenstein, E.M., Schmidt, M. C.** (2007) Mechanisms regulating the protein kinases of *Saccharomyces cerevisiae*. *Eukaryot. Cell*. **6**, 222-230.
- Sagot, I., Rodal, A. A., Moseley, J., Goode, B. L., Pellman, D.** (2002) An actin nucleation mechanism mediated by Bni1 and Profilin. *Nat. Cell Biol.* **4**, 626-631.
- Salmon, E.D., Shaw, S. L., Waters, J., Waterman-Storer, C. M., Maddox, P. S., Yeh, E., Bloom, K.** (1998) A high-resolution multimode digital microscope system. *Methods Cell Biol.* **56**, 185-215.
- Sanchez-Diaz, A., Marchesi, V., Murray, S., Jones, R., Pereira, G., Edmondson, R., Allen, T., Labib, K.** (2008) Inn1 couples contraction of the actomyosin ring to membrane ingression during cytokinesis in budding yeast. *Nat. Cell Biol.* **10**, 395-406.
- Santos, B. and Snyder, M.** (1997) Targeting of chitin synthase 3 to polarized growth sites in yeast requires Chs5p and Myo2p. *J. Cell Biol.* **136**, 95-110.
- Sato, T., del Carmen Ovejero, M., Hou, P., Heegaard, A. M., Kumegawa, M., Foged, N. T., Delaisse, J. M.** (1997) Identification of the membrane-type matrix metalloproteinase MT1-MMP in osteoclasts. *J Cell Sci* **110**, 589-596.
- Sburlati, A. and Cabib, E.** (1986) Chitin synthetase 2, a presumptive participant in septum formation in *Saccharomyces cerevisiae*. *J. Biol. Chem.* **261**, 15147-15152.
- Schilling, K., Opitz, N., Wiesenthal, A., Oess, S., Tikkanen, R., Müller-Esterl, W., Icking, A.** (2006) Translocation of endothelial nitric-oxide synthase involves a ternary complex with caveolin-1 and NOSTRIN. *Mol. Biol. Cell* **17**, 3870-3880.
- Schmidt, M., Bowers, B., Varma, A., Roh, D., Cabib, E.** (2002) In budding yeast, contraction of the actomyosin ring and formation of the primary septum at cytokinesis depend on each other. *J. Cell Sci.* **115**, 293-302.

- Schmidt, M., Varma, A., Drgon, T., Bowers, B., Cabib, E.** (2003) Septins, under Cla4p regulation, and the chitin ring are required for neck integrity in budding yeast. *Mol. Biol. Cell* **14**, 2128-2141.
- Schulz, T.A., Creutz, C. E.** (2004) The tricalbin C2 domains: lipid-binding properties of a novel, synaptotagmin-like yeast protein family. *Biochemistry* **43**, 3987-3995.
- Shaner, N. C., Campbell, R. E., Steinbach, P. A., Giepmans, B. N. G., Palmer, A. E., Tsien, R. Y.** (2004) Improved monomeric red, orange and yellow fluorescent proteins derived from *Discosoma* sp. red fluorescent protein. *Nat. Biotech.* **22**, 1567-1572.
- Shannon, K. B. and Li, R.** (1999) The multiple roles of Cyk1p in the assembly and function of the actomyosin ring in budding yeast. *Mol. Biol. Cell* **10**, 283-296.
- Shannon, K.B., Li, R.** (2000) A myosin light chain mediates the localization of the budding yeast IQGAP-like protein during contractile ring formation. *Curr. Biol.* **10**, 727-730.
- Shao, X., Davletov, B. A., Sutton, R. B., Sudhof, T. C., Rizo, J.** (1996) Bipartite Ca²⁺-binding motif in C2 domains of synaptotagmin and protein kinase C. *Science* **273**, 248-251.
- Sharifmoghadam, M. R. and Valdivieso, M. H.** (2009) The fission yeast SEL1-domain protein Cfh3p: a novel regulator of the glucan synthase Bgs1p whose function is more relevant under stress conditions. *J Biol Chem.*
- Shaw, J. A., Mol, P. C., Bowers, B., Silverman, S. J., Valdivieso, M. H., Duran, A., Cabib, E.** (1991) The function of chitin synthases 2 and 3 in the *Saccharomyces cerevisiae* cell cycle. *J. Cell Biol.* **114**, 111-123.
- Shimada, A., Niwa, H., Tsujita, K., Suetsugu, S., Nitta, K., Hanawa-Suetsugu, K., Akasaka, R., Nishino, Y., Toyama, M., Chen, L., et al.** (2007) Curved EFC/F-BAR-domain dimers are joined end to end into a filament for membrane invagination in endocytosis. *Cell* **129**, 761-772.
- Shuster, C. B. and Burgess, D. R.** (2002) Targeted new membrane addition in the cleavage furrow is a late, separate event in cytokinesis. *PNAS* **99**, 3633-3638.

- Skop, A.R., Liu, H., Yates III, J., Meyer, B. J., Heald, R.** (2004) Dissection of the mammalian midbody proteome reveals conserved cytokinesis mechanisms. *Science* **305**, 61-66.
- Soulard, A., Friant, S., Fitterer, C., Orange, C., Kaneva, G., Mirey, G., Winsor, B.** (2005) The WASP/Las17p-interacting protein Bzz1p functions with Myo5p in an early stage of endocytosis. *Protoplasma* **226**, 89-101.
- Stegmeier, F., and Amon, A.** (2004) Closing mitosis: the functions of the Cdc14 phosphatase and its regulation. *Annu. Rev. Genet.* **38**, 203-232.
- Stetler-Stevenson, W. G.** (1999) Matrix metalloproteinases in angiogenesis: a moving target for therapeutic intervention. *J. Clin. Invest.* **103**, 1237-1241.
- Stevens, R.C., and Davis, T. N.** (1998) Mlc1p is a light chain for the unconventional myosin Myo2p in *Saccharomyces cerevisiae*. *J. Cell Biol.* **142**, 711-722.
- Strickland, L.I., and Burgess, D. R.** (2004) Pathways for membrane trafficking during cytokinesis. *Trends Cell Biol.* **14**, 115-118.
- Sung, M.-K., Huh, W.-K.** (2007) Bimolecular fluorescence complementation analysis system for in vivo detection of protein-protein interaction in *Saccharomyces cerevisiae*. *Yeast* **24**, 767-775.
- Szafer-Glusman, E., Giansanti, M. G., Nishihama, R., Bolival, B., Pringle, J. R., Gatti, M., Fuller, M. T.** (2008) A role for very-long-chain fatty acids in furrow ingression during cytokinesis in *Drosophila* spermatocytes. *Curr. Biol.* **18**, 1426-1431.
- Tarricone, C., Xiao, B., Justin, N., Walker, P. A., Rittinger, K., Gamblin, S. J., Smerdon, S. J.** (2001) The structural basis of Arfaptin-mediated cross-talk between Rac and Arf signaling pathways. *Nature* **411**, 215-219.
- Tomlin, G.C., Hamilton, G. E., Gardner, D. C., Walmsley, R. M., Stateva, L. I., Oliver, S. G.** (2000) Suppression of sorbitol dependence in a strain bearing a mutation in the SRB1/PSA1/VIG9 gene encoding GDP-mannose pyrophosphorylase by PDE2 overexpression suggests a role for the Ras/cAMP signal-transduction pathway in the control of yeast cell-wall biogenesis. *Microbiology.* **146**, 2133-2146.

- Tong, A.H., Drees, B., Nardelli, G., Bader, G. D., Brannetti, B., Castagnoli, L., Evangelista, M., Ferracuti, S., Nelson, B., Paoluzi, S., Quondam, M., Zucconi, A., Hogue, C. W., Fields, S., Boone, C., Cesareni, G.** (2002) A combined experimental and computational strategy to define protein interaction networks for peptide recognition modules. *Science* **295**, 321-324.
- Tong, A.H., Evangelista, M., Parsons, A. B., Xu, H., Bader, G. D., Page, N., Robinson, M., Raghbizadeh, S., Hogue, C. W., Bussey, H., Andrews, B., Tyers, M., Boone, C.** (2001) Systematic genetic analysis with ordered arrays of yeast deletion mutants. *Science* **294**, 2364-2368.
- Tong Z., Gao X.D., Howell A.S., Bose I., Lew D.J., Bi E.** (2007) Adjacent positioning of cellular structures enabled by a Cdc42 GTPase-activating protein-mediated zone of inhibition. *J. Cell Biol.* **179**, 1375-1384.
- Trautwein, M., Schindler, C., Gauss, R., Dengjel, J., Hartmann, E., Spang, A.** (2006) Arf1p, Chs5p and the ChAPs are required for export of specialized cargo from the Golgi. *EMBO J.* **25**, 943-954.
- Trilla, J. A., Duran, A., Roncero, C.** (1999) Chs7p, a new protein involved in the control of protein export from the endoplasmic reticulum that is specifically engaged in the regulation of chitin synthesis in *Saccharomyces cerevisiae*. *J. Cell Biol.* **145**, 1153-1163.
- Tsujita, K., Suetsugu, S., Sasaki, N., Furutani, M., Oikawa, T., Takenawa, T.** (2006) Coordination between the actin cytoskeleton and membrane deformation by a novel membrane tubulation domain of PCH proteins is involved in endocytosis. *J. Cell Biol.* **172**, 269-279.
- Valdivia, R. H. and Schekman, R.** (2003) The yeasts Rho1p and Pkc1p regulate the transport of chitin synthase III (Chs3p) for internal stores to the plasma membrane. *PNAS* **100**, 10287-10292.
- Vallen, E.A., Caviston, J., Bi, E.** (2000). Roles of Hof1p, Bni1p, Bnr1p, and Myo1p in cytokinesis in *Saccharomyces cerevisiae*. *Mol. Biol. Cell* **11**, 593-611.

- Vaduva, G., Martin, N. C., Hopper, A. K.** (1997) Actin-binding verprolin is a polarity development protein required for the morphogenesis and function of the yeast actin cytoskeleton. *J Cell Biol.* **139**, 1821-1833.
- VerPlank, L., and Li, R.** (2005) Cell cycle-regulated trafficking of Chs2 controls actomyosin ring stability during cytokinesis. *Mol. Biol. Cell* **16**, 2529-2543.
- Versele, M. and Thorner, J.** (2005) Some assembly required: yeast septins provide the instruction manual. *Trends Cell Biol.* **15**, 414-424.
- Vrabiou, A. M. and Mitchison, T. J.** (2006) Structural insights into yeast septin organization from polarized fluorescence microscopy. *Nature* **443**, 466-469.
- Wagner, W., Bielli, P., Wacha, S., Ragnini-Wilson, A.** (2002) Mlc1p promotes septum closure during cytokinesis via the IQ motifs of the vesicle motor Myo2p. *EMBO J.* **21**, 6397-6408.
- Wang, C., Hamamoto, S., Orci, L., Schekman, R.** (2006) Exomer: a coat complex for transport of select membrane proteins from the trans-Golgi network to the plasma membrane in yeast. *J. Cell Biol.* **174**, 973-983.
- Warit, S., Zhang, N., Short, A., Walmsley, R. M., Oliver, S. G., Stateva, L. I.** (2000) Glycosylation deficiency phenotypes resulting from depletion of GDP-mannose pyrophosphorylase in two yeast species. *Mol. Microbiol.* **36**, 1156-1166.
- Watts, F., Shiels, G., Orr, E.** (1987) The yeast MYO1 gene encoding a myosin-like protein required for cell division. *EMBO J.* **6**, 3499-3505.
- Wessel, G.M., Berg, L., Adelson, D. L., Cannon, G., McClay, D. R.** (1998) A molecular analysis of hyalin—a substrate for cell adhesion in the hyaline layer of the sea urchin embryo. *Dev Biol.* **193**, 115-126.
- Yeong, F. M.** (2005) Severing all ties between mother and daughter: cell separation in budding yeast. *Mol. Microbiol.* **55**, 1325-1331.
- Yoshida, S., Kono, K., Lowery, D. M., Bartolini, S., Yaffe, M. B., Ohya, Y., Pellman, D.** (2006) Polo-like kinase Cdc5 controls the local activation of Rho1 to promote cytokinesis. *Science* **313**, 108-111.

- Zhang, G., Kashimshetty, R., Ng, K. E., Tan, H. B., Yeong, F. M.** (2006) Exit from mitosis triggers Chs2p transport from the endoplasmic reticulum to mother-daughter neck via the secretory pathway in budding yeast. *J. Cell Biol.* **174**, 207-220.
- Zhang, N., Gardner, D. C., Oliver, S. G., Stateva, L. I.** (1999) Down-regulation of the expression of PKC1 and SRB1/PSA1/VIG9, two genes involved in cell wall integrity in *Saccharomyces cerevisiae*, causes flocculation. *Microbiology.* **145**, 309-316.
- Zhu, G., Chen, J., Liu, J., Brunzelle, J. S., Huang, B., Wakeham, N., Terzyan, S., Li, X., Rao, Z., Li, G., and Zhang, X. C.** (2007) Structure of the APPL1 BAR-PH domain and characterization of its interaction with Rab5. *EMBO J.* **26**, 3484-3493.
- Ziman, M., Chuang, J. S., Schekman, R. W.** (1996). Chs1p and Chs3p, two proteins involved in chitin synthesis, populate a compartment of the *Saccharomyces cerevisiae* endocytic pathway. *Mol. Biol. Cell* **7**, 1909-1919.